Function of the Upstream Activating Factor in Chromatin Structure Organization and Transcriptional Regulation at the Yeast Ribosomal DNA

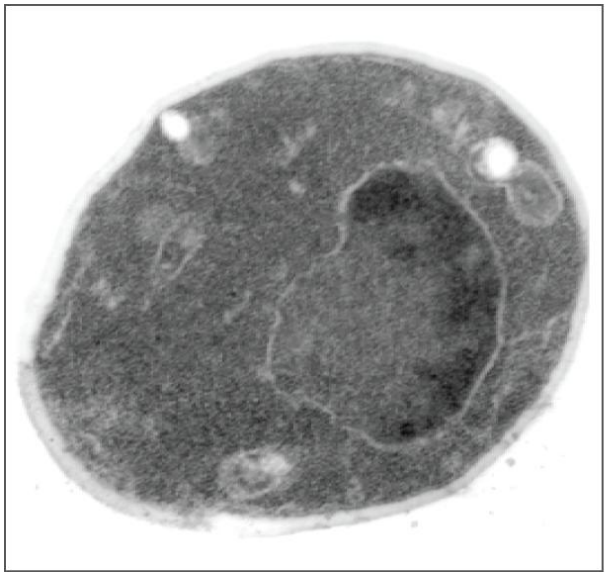

Dissertation

zur Erlangung des Doktorgrades der Naturwissenschaften (Dr. rer. nat.)
der naturwissenschaftlichen Fakultät III – Biologie und vorklinische Medizin -
der Universität Regensburg

vorgelegt von

Hannah Götze

aus Aresing

Dezember 2009

Electron micrographs on the cover visualize ultrastructure of S. cerevisiae and Miller chromatin spreads of actively transcribed ribosomal RNA genes (Isabelle Léger-Silvestre)

Promotionsgesuch eingereicht am: 02. Dezember 2009

Die Arbeit wurde angeleitet von: Prof. Dr. Herbert Tschochner

Prüfungsausschuss:

Vorsitzender:	Prof. Dr. Reinhard Wirth
1. Prüfer:	Prof. Dr. Herbert Tschochner
2. Prüfer:	Prof. Dr. Michael Thomm
3. Prüfer:	Prof. Dr. Reinhard Sterner

Die vorliegende Arbeit wurde in der Zeit von November 2006 bis Dezember 2009 am Lehrstuhl Biochemie III des Institutes für Biochemie, Genetik und Mikrobiologie der Naturwissenschaftlichen Fakultät III der Universität zu Regensburg unter Anleitung von Dr. Joachim Griesenbeck im Labor von Prof. Dr. Herbert Tschochner angefertigt.

Ich erkläre hiermit, dass ich diese Arbeit selbst verfasst und keine anderen als die angegebenen Quellen und Hilfsmittel verwendet habe.
Diese Arbeit war bisher noch nicht Bestandteil eines Prüfungsverfahrens.
Andere Promotionsversuche wurden nicht unternommen.

Regensburg, den 02. Dezember 2009

Hannah Götze

Table of Contents

1 Introduction

1.1 Chromatin structure in eukaryotes

In eukaryotes the DNA in the nucleus is organized on different chromosomes. Each chromosome consists of a linear DNA molecule associated with proteins that are required for compacting the DNA in order to fit in the limited volume of the cells' nucleus. The complex of DNA and protein is called chromatin. The major components of chromatin are DNA and histone proteins. In addition, a variety of nonhistone proteins are involved in establishing chromatin structures. Besides its function in the packaging of DNA, chromatin provides a possible level of control for gene expression, replication and other fundamental cellular processes. Therefore chromatin structure must be highly dynamic, to permit the access of regulatory factors to the DNA (Elgin and Weintraub, 1975; Elgin, 1990).

1.1.1 Basic and higher-order chromatin structures

The basic unit of chromatin is the nucleosome, which is composed of 147 base pairs (bp) of DNA wrapped around a histone octamer of two molecules of each of the core histones H2A, H2B, H3 and H4 (Kornberg and Lorch, 1999b; Luger, 2003). The nucleosomes are separated by a region of linker DNA, which can vary in length from a few base pairs up to about 80 bp (Olins and Olins, 1974). In higher eukaryotes, the average nucleosomal repeat length is about 200 nucleotide pairs. Under these conditions, the nucleosomal linker DNA is bound by a specific protein, the linker histone H1, being responsible for chromatin condensation to the 10 nm nucleosomal filaments and the 30 nm fibers. H1 is larger than the core histones and is less well conserved (Kasinsky et al., 2001; Ausió, 2000). Whereas core histones in *S. cerevisiae* (hereafter called yeast) are similar in sequence and structure to other eukaryotic core histones, the sequence of the putative H1 homolog, designated HHO1, is less conserved (Ushinsky et al., 1997; Patterton et al., 1998). Hho1 is less abundant than core histones and appears to bind only to specific

regions within the yeast genome (Freidkin and Katcoff, 2001). Accordingly, the linker DNA in yeast is shorter than in other eukaryotes (Bash and Lohr, 2001).

Nucleosome positions and structure can be modified by several mechanisms. Chromatin remodeling complexes use the energy of ATP hydrolysis to destabilize histone-DNA interactions (Clapier and Cairns, 2009; Aalfs and Kingston, 2000; Kornberg and Lorch, 1999a). Furthermore, the N-terminal tails of the core histones can be modified enzymatically, thereby performing multiple functions in regulating chromatin structure (Cheung et al., 2000). The histone tails are subject to several types of covalent modifications including acetylation and methylation of lysine residues or phosphorylation of serines amongst many others (Li et al., 2007). These modifications influence higher-order chromatin structures and provide a contact surface for other proteins. Thus, chromatin remodeling as well as histone tail modifications render chromatin a highly dynamic structure with the capacity to regulate multiple cellular processes.

1.1.2 Chromatin and transcription

Two types of chromatin can be distinguished when interphase nuclei of higher eukaryotic cells are investigated by electron microscopy: a highly condensed form, called hetero-chromatin, and a less condensed population, called euchromatin. Euchromatin is composed of the chromosomal 30 nm fibers described before. In contrast, heterochromatin includes additional proteins and represents more compact levels of organization. Euchromatin replicates early in the cell cycle and generally represents genomic regions that are transcriptionally active. Thus, most of the genes coding for proteins are packaged in this form of chromatin (Grewal and Elgin, 2002; Bassett et al., 2009). In euchromatin, nucleosome arrays display an irregular pattern and are interspersed with nucleosome free sites that are hypersensitive to nucleases. The sensitivity to nucleases correlates with histone hyperacetylation, which is linked to activated transcription and generated by histone acetyltransferases (HATs) (Richards and Elgin, 2002; Rice and Allis, 2001). Initiation of gene transcription is regulated by the presence of nucleosomes in the promoter region. Positioning of nucleosomes over key promoter elements can repress transcription by RNA polymerase II (Pol II) *in vitro* (Kornberg et al., 1999b; Lorch et al., 1992). Therefore, HATs and chromatin remodeling

complexes have been suggested to act synergistically in establishing a local chromatin structure allowing for transcription initiation (Fry and Peterson, 2001). As packaging DNA in chromatin has been shown to inhibit transcription *in vitro*, several models have been proposed to explain the mechanism of transcripton elongation through a nucleosomal template. The histone octamers might be detached from active genes during transcription, or they might also be slid out of the way of transcribing polymerase molecules. Another possibility would be an unfolding of nucleosomes with only a portion of the histones remaining associated with the DNA (Workman, 2006; Adams and Workman, 1993). Some of these models suggest the existence of mechanisms for the (partial) eviction of histone molecules in front of elongating polymerases and their subsequent replacement. To fulfill this task, auxiliary factors are involved in facilitating the elongation of polymerases. The FACT complex is a chromatin remodeling complex that enhances transcription elongation through nucleosomes. The complex is capable to re-dispose an H2A/H2B dimer *in vitro* thereby destabilizing nucleosomes during polymerase passage followed by re-constitution of the octamer (Orphanides et al., 1998, 1999; Orphanides and Reinberg, 2000).

1.1.3 Heterochromatin

In contrast to active chromatin, heterochromatic domains are assembled in arrays of regularly spaced nucleosomes, replicating late in cell cycle. Heterochromatic DNA is in general inaccessible to DNA binding factors and thus transcriptionally silent. Heterochromatin formation is observed at repetitive DNA sequences, which seems to be involved in the maintenance of genome stability by inhibiting recombination between homologous repeats (Grewal and Moazed, 2003). Hypoacetylation of histone lysine residues, H3 methylation at lysine 9 and cytosine methylation at CpG residues are characteristic features of heterochromatic regions (Hennig, 1999; Richards et al., 2002). It has been also demonstrated that specific proteins are enriched in heterochromatin (Grewal and Jia, 2007). Thus, the factors that are required for heterochromatin assembly are either histone- or DNA-modifying enzymes or factors that specifically bind to (modified) histones or DNA. In *S. cerevisiae* the SIR (silent information regulator) genes are required for nucleation and spreading of silent chromatin (Hoppe et al., 2002; Carmen

et al., 2002; Gasser and Cockell, 2001). Although the cytological detection of heterochromatic regions in yeast is impossible, similar silencing phenomena were discovered in three different kinds of chromosomal loci: the silent mating-type loci, the telomeric regions and the rDNA locus (Richards et al., 2002; Moazed, 2001) (see also below). Specialized boundary elements mark the borders between active and silenced regions and separate chromatin domains with distinct histone-modification patterns (Noma K et al., 2001; West et al., 2002; Labrador and Corces, 2002). In addition to histone modifications the nucleosome composition contributes to the maintenance of chromatin states. For example the histone variant H2A.Z in *S. cerevisiae* is enriched in euchromatic regions surrounding silent loci and appears to play a role in preventing the spread of heterochromatin (Meneghini et al., 2003).

1.2 Chromatin structure of the yeast ribosomal DNA (rDNA)

The yeast ribosomal RNA (rRNA) genes are an ideal model system to study the interplay between transcription and chromatin structure (Dammann et al., 1993).

In a rapidly growing yeast cell 60% of total transcripts are rRNA (Warner et al., 1999), which are synthesized by a specialized RNA polymerase, RNA polymerase I (Pol I). Pol I is responsible for transcription of a 35S rRNA precursor which is processed into the mature 18S, 5.8S and 25S rRNA species. Besides RNA Pol I, ribosome synthesis is dependent on the activities of RNA polymerase II (Pol II) transcribing the genes for ribosomal proteins, and RNA polymerase III (Pol III), which is required for transcription of the 5S rRNA. In addition about 100 small nucleolar RNAs (snoRNAs) and more than 150 trans-acting factors (Kressler et al., 1999; Venema and Tollervey, 1999; Fatica and Tollervey, 2002) participate in assembly and maturation of the ribosome. This complex and energy consuming process requires mechanisms for efficient coordination of the single steps. Synthesis and processing of rRNAs as well as ribosome subunit assembly take place in the largest sub-nuclear structure, the nucleolus (Fig. 1-1).

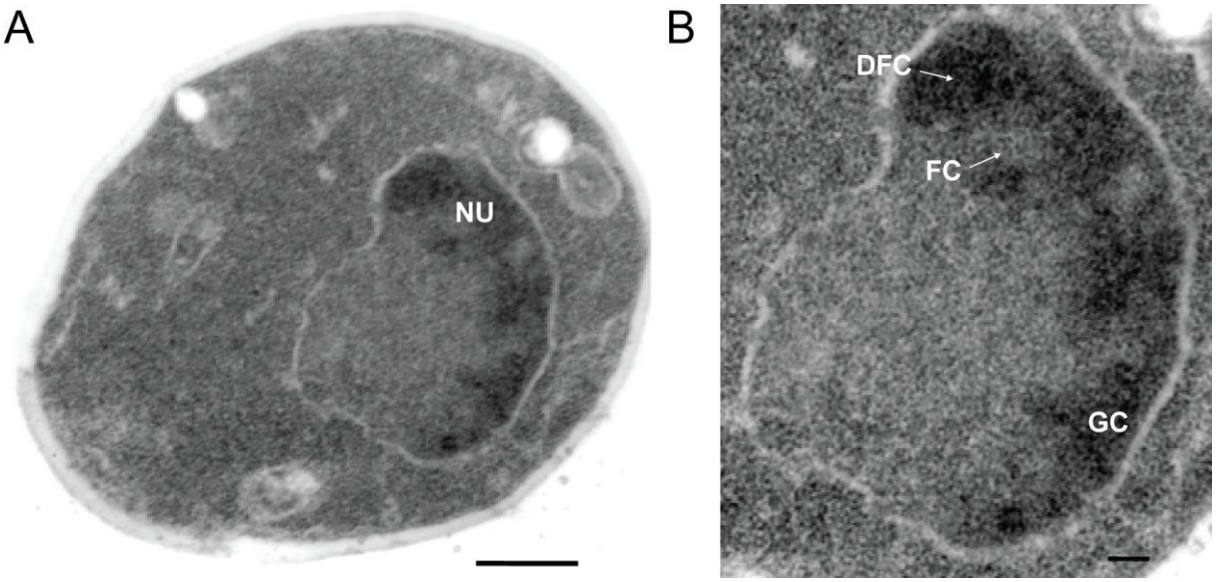

Fig. 1-1 Ultrastructure of yeast cells
After chemical fixation of yeast cells thin sections were prepared for electron microscopy according to the method of Isabelle Léger-Silvestre (Léger-Silvestre et al., 1999). (A) Morphology of the whole cell. The two lipid layers of the plasma membrane are distinct. In the nucleus, one region of low electron density and a large electron-dense area referred to as the nucleolus (NU) are detected. The nucleolus is in close contact with the nuclear envelope. The bar represents 500 nm. (B) Morphology of the nucleolus. In the nucleolus, three distinct morphological compartments are identified: electron-lucid zones resembling fibrillar centres (FC) are detected near the nuclear envelope and contain the rDNA. These electron-lucid zones are surrounded by a dense fibrillar component (DFC) extending as a network throughout the nucleolar volume and containing the Pol I transcription machinery. A granular component (GC) is dispersed throughout the rest of the nucleolus and contains the maturing pre-ribosomes (Léger-Silvestre et al., 1999; Scheer and Hock, 1999). The bar represents 100 nm.

1.2.1 rDNA structure and CIS-elements

In *S. cerevisiae* the rRNA genes are located on the right arm of Chromosome XII and consist of 150-200 transcription units, each with a size of 9.1-kilobase pairs (kb), that are arranged in a tandem array (Petes, 1979) (Fig. 1-2). The rRNA genes make up about 10% of the entire yeast genome, although the number of repeats is dynamic and can vary due to unequal meiotic and mitotic recombination events (Warner, 1989). Each of the repeated rDNA units is composed of the Pol I-transcribed 35S rRNA gene and the gene for 5S rRNA which is transcribed in the opposite direction by Pol III (Philippsen et al., 1978). The presence of the 5S rRNA gene within the rDNA unit in *S. cerevisiae* is different from the situation in other eukaryotes, most of which carry 5S rRNA repeats separately from the nucleolar rRNA repeats (Geiduschek and Kassavetis, 2001; Drouin and de Sá, 1995).

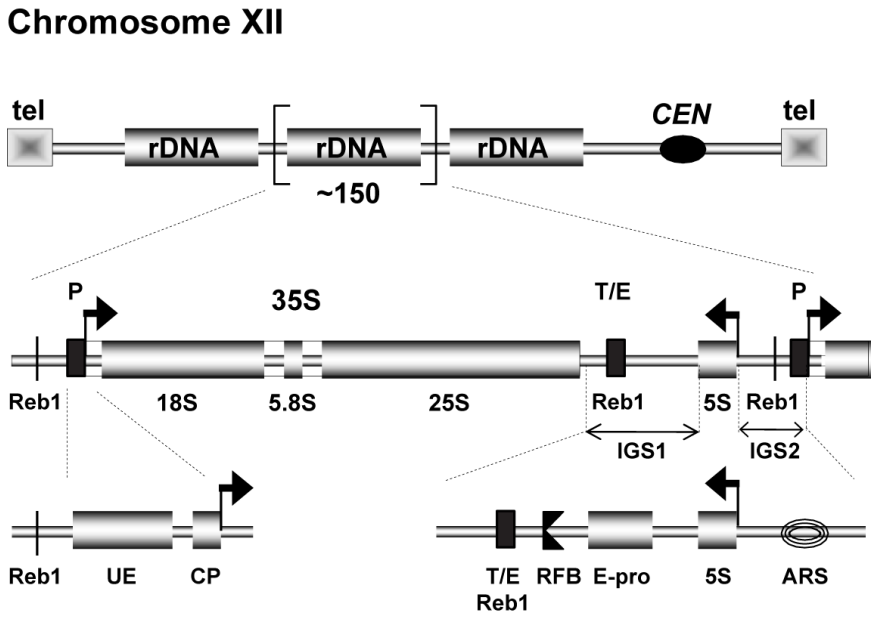

Fig. 1-2 Schematic representation of the rDNA locus in *S. cerevisiae*
The position of the rDNA repeat cluster on chromosome XII with respect to the centromere (CEN) and telomeres (tel) is shown. Each rDNA repeat consists of the Pol I-transcribed 35S rRNA gene (precursor for the 18S, 5.8S and 25S rRNAs), the RNA Pol III-transcribed 5S rRNA gene and two intergenic spacer regions IGS 1 and 2. Arrows mark the transcription start sites and direction. The positions of several DNA elements are indicated. The upstream element (UE) and core promoter (CP) constitute the Pol I promoter (P). Termination occurs at the terminator (T) which is located within a region called the enhancer (E). Binding sites of the Reb1 protein as well as sites of autonomous replication sequence (ARS), bidirectional Pol II promoter E-Pro and replication fork barrier (RFB) are depicted.

The 35S rRNA is transcribed as a precursor that is processed into the mature 18S, 5.8S and 25S rRNAs. Three different elements important for the regulation of rDNA transcription have been identified within the 35S rRNA gene (Kulkens et al., 1991; Musters et al., 1989). The upstream element (UE) and the core promoter (CP) are located on the 5´end of the 35S rDNA within the intergenic spacer region (IGS2). The two elements span about 170 bp and constitute the 35S rDNA promoter. A third element located at the 3´end of the 35S transcription unit and is called the enhancer (ENH). This element has been shown to exhibit a stimulatory effect on RNA synthesis by Pol I in *in vitro* and *in vivo* experiments from Pol I reporter templates (Elion and Warner, 1984, 1986). However, later it was shown that this sequence is dispensable for rDNA transcription in the chromosomal context *in vivo* (Wai et al., 2001).

There are two terminators for 35S rDNA transcription that reside within the ENH region (Reeder et al., 1999). Approximately 90% of all transcripts terminate at a site located 93 nucleotides downstream of the 3' end of mature 25S rRNA. The remaining transcripts terminate at a fail-safe termination site located 250 nucleotides downstream of the 3´end

of the mature 25S rRNA. The terminator at the +93 site contains two elements, one of which is bound by the RNA Pol I enhancer binding protein (Reb1). *In vitro* studies on the mechanism of Pol I termination suggested that the second termination element bound by Reb1 causes Pol I to pause, co-operating with the first, T-rich element to release Pol I (Reeder and Lang, 1997). It appears that the two terminators are not required for efficient rRNA synthesis since the enhancer region has been shown to be dispensable for Pol I transcription (Wai et al., 2001).

Several other cis-regulatory elements that are unrelated to 35S rDNA transcription are located within the IGS1 and IGS2. During s-phase, bidirectional replication is initiated at the ribosomal autonomous sequence (rARS) (Linskens and Huberman, 1988). A replication fork barrier (RFB) site is located near the enhancer element and allows the progression of the replication fork in the direction of 35S rDNA transcription but not in the opposite direction (Brewer et al., 1992; Brewer and Fangman, 1988; Fangman and Brewer, 1992; Kobayashi et al., 1992). The fork blocking protein (Fob1) binds to the RFP and is required for this activity (Kobayashi and Horiuchi, 1996). In addition, the FOB1 gene is required for expansion and contraction of rDNA repeats. The rDNA repeat number can vary and can be adjusted in response to changes in intra- or extracellular conditions. For instance in yeast, the deletion of an essential Pol I subunit results in a decrease in the number of rDNA repeats to about half of the normal number (Kobayashi et al., 1998). These repeat expansion and contraction events require recombination events that are triggered by double strand breaks introduced into the rDNA by FOB1-dependent pausing of the DNA replication machinery at RFB sites (Burkhalter and Sogo, 2004; Kobayashi et al., 1998, 2004). In addition to the RFB, the adjacent region (EXP) has also been shown to be required for repeat expansion (Kobayashi et al., 2001). This region harbors a bidirectional Pol II promoter which drives the transcription of non-coding RNAs (Ganley et al., 2005). Transcription driven by the EXP promoter, E-pro, results in cohesin dissociation from the cohesin associating region (CAR) and is negatively regulated by the Sir2 protein (Kobayashi and Ganley, 2005) (see also below). Cohesin association is suggested to hold sister chromatids in place, preventing unequal recombination and thereby changes in rDNA copy number after the formation of DNA double-strand breaks (Kobayashi et al., 2004). Thus, transcription of E-pro may allow a change in copy number by removing cohesin.

1.2.2 Chromatin structure at the rDNA locus

The 35S rRNA genes coexist in two different chromatin states depending on the transcriptional activity of the gene. In a single cell, only about half of the rDNA repeats is actively transcribed, whereas the other half of the population is transcriptionally inactive (Dammann et al., 1993).

Due to the high copy number of rDNA repeats associated with different chromatin states the analysis of chromatin structure at this locus was difficult using conventional biochemical techniques. Initial experiments using nuclease digestion of rDNA chromatin suggested the presence of nucleosomes along the coding sequence (Lohr, 1983). The classical approach of micrococcal nuclease (MNase) digestion could not reveal the composition of chromatin at individual units. The MNase cuts the DNA within nucleosomal linker regions and at nuclease hypersensitive (HS) sites (Telford and Stewart, 1989). Early studies on rDNA chromatin using this method revealed a digestion pattern that was superimposed on a smear (Conconi, 1987). This result already reflected the heterogeneity in chromatin structure at the rDNA locus. Alternative approaches later allowed the identification of the two different rDNA chromatin states. These approaches included psoralen crosslinking in combination with the use of restriction endonucleases to separate active from inactive chromatin (Conconi et al., 1989; Dammann et al., 1993). Psoralen is a drug which intercalates in double stranded DNA and generates covalent crosslinks between the two DNA strands upon irradiation with UV-A (predominantly 360 nm). Psoralen preferentially intercalates in linker DNA between nucleosomes or in nucleosome-free regions such as promoters, origins of replication or enhancers (Sogo et al., 1986), but does not react with nucleosomal DNA (Hanson et al., 1976). Consequently, nucleosomal and non nucleosomal DNA differ in the degree of psoralen incorporation and can be separated with this method.

Chromatin structure of the rRNA coding regions

Psoralen crosslinking of 35S rDNA chromatin followed by restriction endonuclease digestion and gel electrophoresis revealed a different migration behavior of the corresponding restriction fragments (Fig. 1-3). The slow migrating (s-) band represented

heavily crosslinked DNA and corresponded to actively transcribed, nucleosome-free rDNA. In contrast, the fast migrating (f-) band contained slightly crosslinked DNA and represented the inactive rDNA repeats. This was confirmed by electron micrographs (Fig. 1-3, right panels) suggesting that the f-band DNA was organized in a nucleosomal structure, whereas the s-band DNA appeared to be nucleosome-free (Dammann et al., 1993). Moreover nascent rRNA was found to be crosslinked to the s-band, providing that these DNA fragments originated from actively transcribed genes (Conconi et al., 1989; Dammann et al., 1993).

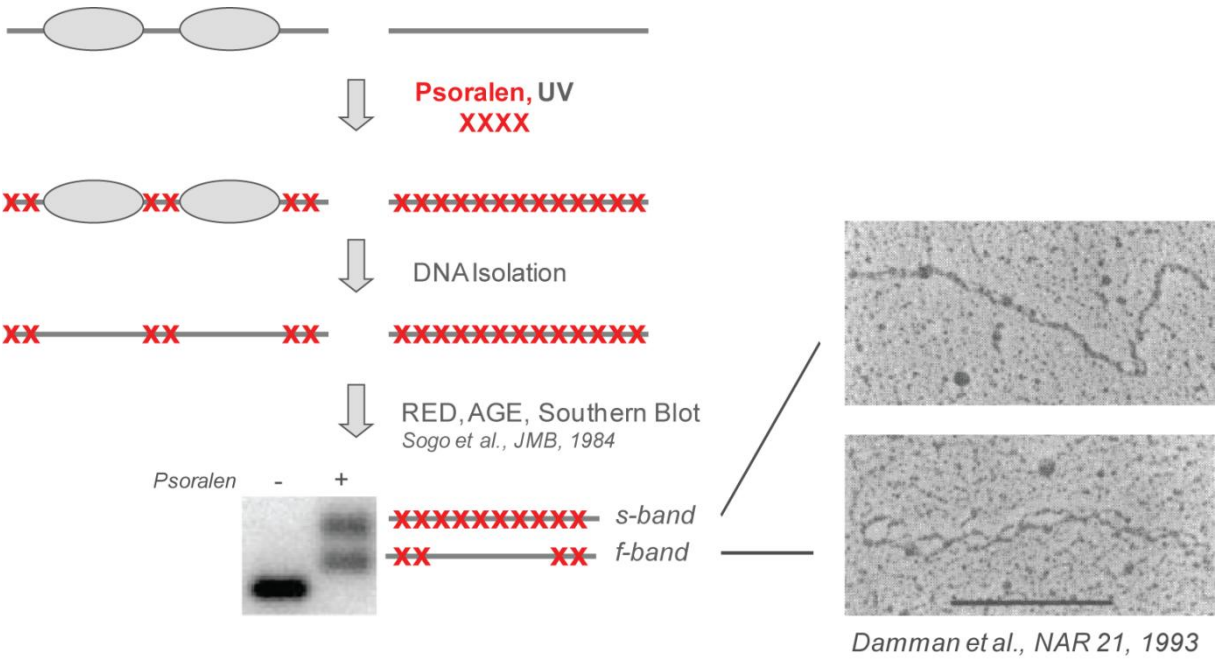

Fig. 1-3 Schematic representation of a psoralen crosslinking experiment
Isolated nuclei are photoreacted with psoralen, which forms a covalent bond between the two DNA strands linking them closely together in the presence of UV light. The nucleosome-free rDNA copies are more accessible to Psoralen than the inactive copies. After DNA isolation and restriction enzyme digest (RED) the fragments are separated by agarose gel electrophoresis (AGE). The two different bands (s-band and f-band) for rDNA chromatin can be visualized in Southern blot analysis (left panels). By purification of the respective DNA from a gel and analyzing the isolated fragments under denaturing conditions in electron microscopy the f-band appears as rows of single-stranded bubbles typical for a nucleosomal organization whereas the s-band shows higher extent of psoralen crosslinking and does not seem to be protected by nucleosomes (Dammann et al., 1993) (right panels).

Contrary to the above results a recent study using chromatin immunoprecipitation (ChIP) suggested that active rDNA repeats exist in a dynamic chromatin structure of unphased nucleosomes (Jones et al., 2007). However, in combining ChEC (Chromatin Endogenous Cleavage) with psoralen analysis our laboratory could demonstrate the specific

association of histone molecules with inactive rDNA whereas actively transcribed rRNA genes were shown to be largely devoid of histone molecules (Merz et al., 2008). Thus, it is still discussed controversially whether or not active rDNA repeats are nucleosome-free.
Electron microscopic analysis of chromatin spreads showed actively transcribed rDNA stretches separated by inactive rDNA repeats, confirming the coexistence of two different rDNA populations (French et al., 2003). This method is called Miller chromatin spreading and allows the visualization of individual rRNA genes and of rDNA chromatin-associated genetic events by electron microscopy (Miller and Beatty, 1969). Actively transcribed rRNA genes can be identified by the nascent rRNA transcripts extending from the DNA backbone (Fig. 1-4, Isabelle Léger-Silvestre).

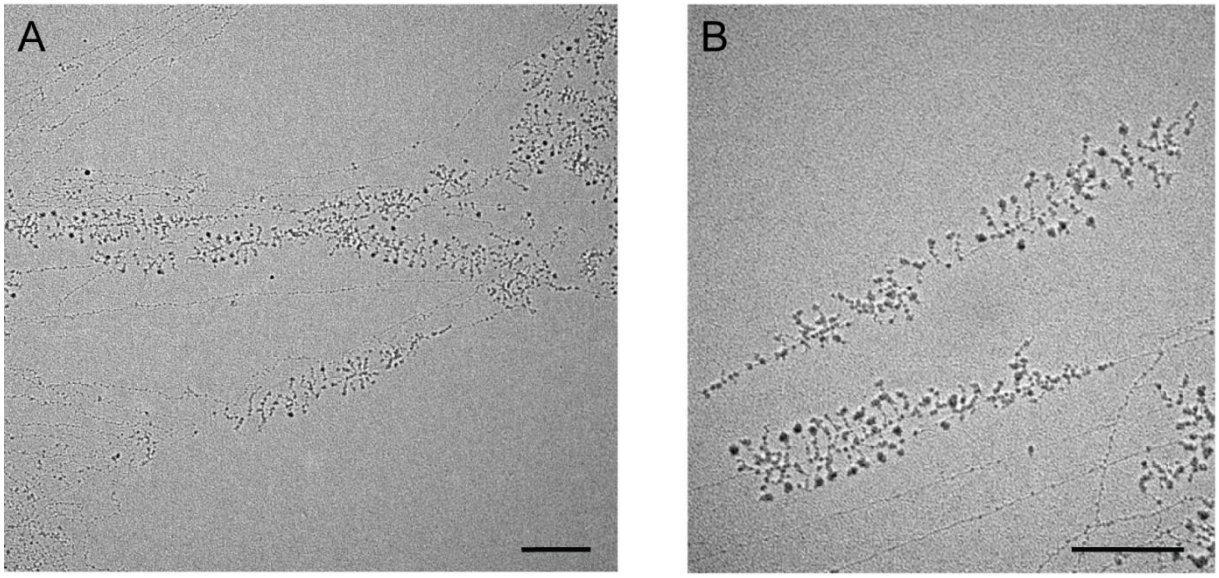

Fig. 1-4 Electron microscopy analysis of Miller chromatin spreads
Overview of chromatin released from a lysed yeast cell by Miller spreading. (A) Low magnification view of a lysed cell. The tandemly repeated and transcriptionally active rRNA genes are especially noticeable in the chromatin mass due to their relatively dark appearance, which is due to multiple nascent RNA transcripts extending from the DNA backbone. (B) Higher-magnification view showing two tandem repeats of active rRNA genes. Bars represent 500 nm (Isabelle Léger-Silvestre).

The nascent transcripts are bound by characteristic “terminal balls” (Osheim et al., 2004). These particles are thought to include U3 small nucleolar RNA (snoRNA) involved in processing of the 35S rRNA precursor (Mougey et al., 1993). The Miller spread method was used to study not only aspects of transcriptional regulation by Pol I (French et al., 2003; Schneider et al., 2006) but also to analyze the structure and co-transcriptional processing of nascent rRNA transcripts (Dragon et al., 2002; Osheim et al., 2004). Thus, it

provides direct insight into Pol I transcription and rRNA processing at the level of individual active genes. In a recent study the 5S rRNA genes transcribed by Pol III located in the intergenic spacer regions at the rDNA locus have been analyzed by this method. Actively transcribed 5S rRNA genes are engaged by one to three polymerases. However, the transcripts are only 132 nucleotides long and therefore are too short to be visualized extending from the gene locus (French et al., 2008).

Chromatin structure of the intergenic spacer regions

Psoralen crosslinking of a fragment containing the entire rDNA IGS regions revealed a nucleosomal organization for the intergenic spacers (Dammann et al., 1993). Again, this was confirmed by ChEC analysis demonstrating that the histone density at the intergenic spacer regions was similar to RNA Pol II-transcribed gene loci (Merz et al., 2008). In addition, studies on rDNA chromatin using MNase digestion revealed the existence of five well-positioned nucleosomes in the IGS2 between the Pol I promoter region and the 5S rRNA gene, with the ARS being located in a nucleosomal linker region. The IGS1 also was suggested to be arranged in nucleosomes, although nucleosomal particles were less well positioned in this sequence context (Vogelauer et al., 1998).

The combination of psoralen crosslinking analysis and electron microscopy allowed the analysis of ribosomal spacer DNA dependent on the transcriptional activity of the rRNA genes. The ribosomal spacers flanking inactive genes showed a regular nucleosomal array typical for inactive bulk chromatin. In contrast, spacers flanking active genes displayed an unusual crosslinking pattern with a broad nucleosome size-distribution intermediate between that expected for mono- and di-nucleosomes (Dammann et al., 1993). In addition, the analysis of rDNA chromatin revealed a structural link between the transcriptional state of a rRNA gene and the 3´flanking enhancer element. While transcriptionally active genes were found to be flanked by non nucleosomal enhancer sequences, inactive genes were followed by enhancers assembled in regularly spaced nucleosomes. It was suggested, that the non nucleosomal enhancer structure downstream of active genes might be related to a function in replication termination with the open enhancer being responsible for the stop of the replication fork (Dammann et al., 1995). Indeed, later studies confirmed that replication initiation occurs only at ARSs

flanked by two active rRNA genes or by an active upstream and an inactive downstream gene (Muller et al., 2000).

There is still very little known about chromatin structure of the 5S rRNA gene. High-resolution mapping of MNase digested yeast chromatin suggested that nucleosomes completely cover the 119 bp of 5S rDNA, thereby occupying multiple alternative positions (Buttinelli et al., 1993). It still remains to be determined, which population of the 5S rRNA genes is packaged in nucleosomes and how this is related to transcription by RNA Pol III. However, a study using Miller chromatin spreading showed that the activity of the 5S rRNA gene is largely independent of the activity of the neighboring 35S rRNA gene and vice versa (French et al., 2008).

1.3 The transcription of ribosomal RNA (rRNA) genes

The transcription of the ribosomal RNA genes by Pol I is an important step in ribosome biogenesis and differs from the transcription of other genes in several aspects. The rRNA genes are arranged in a tandem array and are transcribed by a spezialized polymerase that supports high level of transcription. The identification and characterization of Pol I transcription factors in *S. cerevisiae* was carried out by using genetic approaches that allowed the isolation of mutants defective in rRNA synthesis (Nogi et al., 1991). The method used a system in which the 35S rRNA gene was fused to the GAL7 promoter and transcribed by Pol II. Lethal mutations that affected components specifically involved in rRNA synthesis were suppressed in the presence of galactose. In contrast, these mutant strains were not able to grow on glucose-containing medium. This genetic screen led to the isolation of several mutants defective in rRNA synthesis and resulted in the identification of twelve different genes essential for rRNA transcription.

1.3.1 The mechanism of rRNA gene transcription

Transcription of active rRNA genes by Pol I requires four major transcription factors: upstream activating factor (UAF), core factor (CF), TATA-binding protein (TBP) and Rrn3

(Nomura, 2001). Their arrangement within the ribosomal gene pre-initiation complex (PIC) is shown schematically in Fig. 1-5.

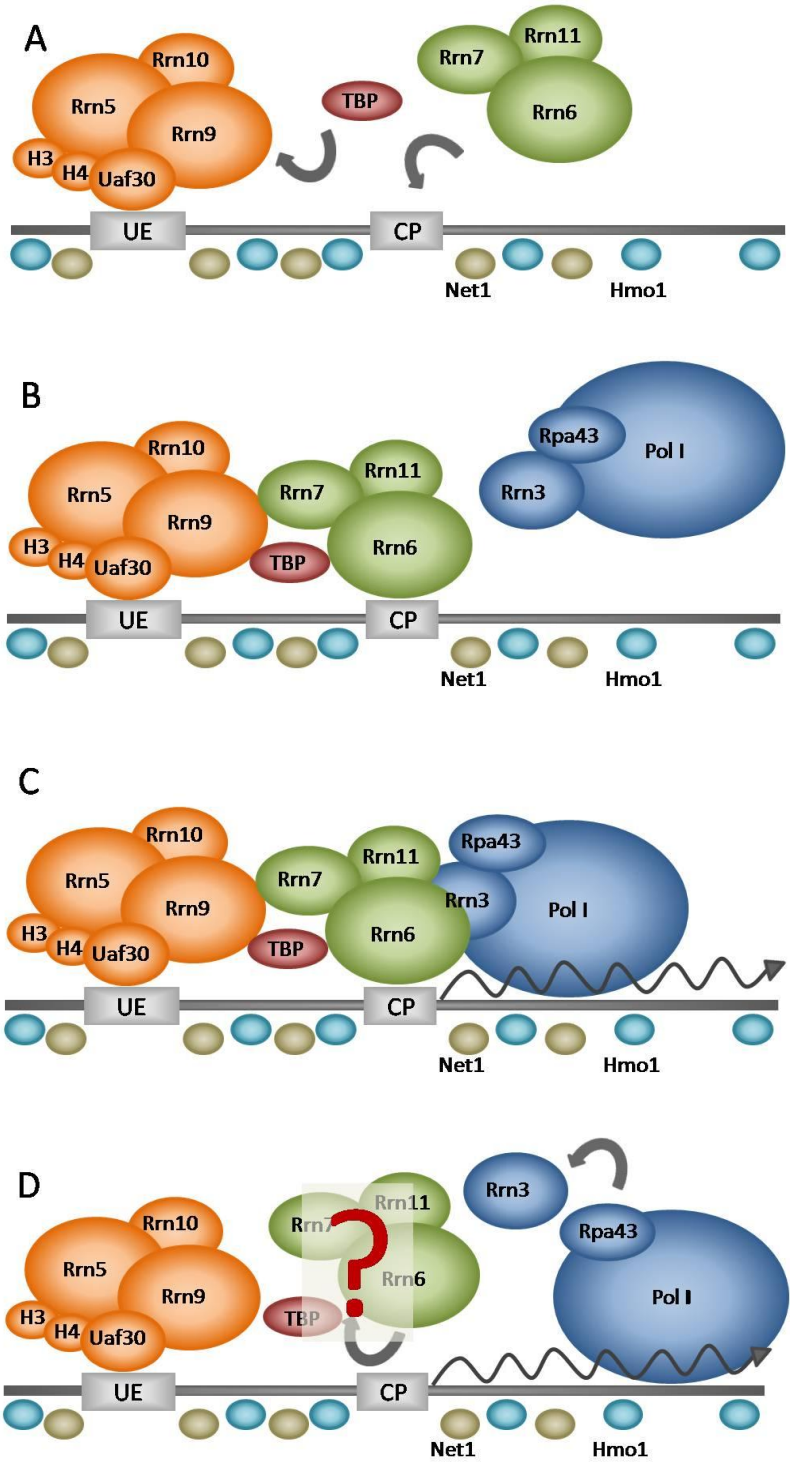

Fig. 1-5
Transcription initiation of ribosomal RNA genes by Pol I
Schematic representation of the assembly of a transcription pre-initiation complex at the rDNA promoter and the initiation cycle.

(A) Initially, UAF binds to the UE which results then with the help of TBP in the recruitment of the CF to the CP.
(B) TBP bridges the two factors by interactions with Rrn9 and Rrn6. Rrn3 interacts directly with the Rpa43 subunit of Pol I, forming an active Pol I-Rrn3 complex.
(C) This active complex is recruited via the Rrn6 subunit of the CF for initiation of trans-cripiton.
(D) After transcription initiation Rrn3 dissociates from the poly-merase. It is still unclear whether TBP and CF remain associated with the rDNA pro-moter region after transcription initiation or if these factors cycle on and off the promoter with each round of transcription

(Nomura, 2001; Aprikian et al., 2001; Peyroche et al., 2000; Moss et al., 2007).

UAF is a multiprotein complex that binds to the upstream element (UE) of the rDNA promoter (Fig. 1-2). The complex consists of the six subunits Rrn5, Rrn9, Rrn10, Uaf30 and the histones H3 and H4 (Keener et al., 1997; Keys et al., 1996; Siddiqi et al., 2001). Uaf30

was demonstrated to be important for UAF recruitment to the UE (Hontz et al., 2009), whereas the functions of the other factors, besides mediating specific protein-protein interactions (Steffan et al., 1996), are still unknown. The histones H3 and H4 are targets for multiple posttranslational modifications (Pazin and Kadonaga, 1997; Li et al., 2007). However, it is not known if they are modified in the context of UAF. The CF contains the three subunits Rrn6, Rrn7 and Rrn11 and interacts with the CP (Keys et al., 1994; Lalo et al., 1996; Lin et al., 1996). TBP bridges the two factors by binding to Rrn9 and Rrn6 (Steffan et al., 1998). Rrn3 interacts directly with Pol I forming an active Pol I-Rrn3 complex (Yamamoto et al., 1996). In addition, Rrn3 binds to the CF subunit Rrn6 suggesting that Rrn3 may act as a bridge between CF and Pol I (Peyroche et al., 2000). For basal transcription *in vitro* CF, Rrn3 and Pol I are sufficient, whereas high levels of transcription in addition require UAF and TBP (Keener et al., 1998). It was concluded, that the ability of UAF to stimulate transcription was mediated by its tight association with the UE resulting in the recruitment of CF with the help of TBP. The formation of this stable pre-initiation complex (PIC) was suggested to be followed by the recruitment of the Pol I-Rrn3 complex (Steffan et al., 1996). An alternative model based on *in vitro* and *in vivo* experiments proposed that Pol I, Rrn3 and CF cycle on and off the UAF bound promoter with each round of transcription and that Pol I is required for stable association of CF with the promoter (Aprikian et al., 2001; Bordi et al., 2001).

After transcription inititation Rrn3 dissociates from the template during or immediately after Pol I has switched from initiation to elongation (Bier et al., 2004).

As mentioned before around 90% of Pol I transcripts are terminated at the Reb1 binding site in the ENH region (Reeder et al., 1997). Pol I molecules reading through this site have been shown to terminate at a fail-safe terminator located just upstream of the RFB (Reeder et al., 1999). Reb1 also binds to a region about 210 bp upstream of the Pol I transcription initiation site (Morrow et al., 1989). Interestingly, both Reb1 recognition sites, but especially the promoter proximal DNA element, contribute to efficient rDNA transcription *in vivo* (Kulkens et al., 1992). A model stated by Kempers-Veenstra *et al.* proposed a function for Reb1 in the structural arrangement of rDNA repeats (Kempers-Veenstra et al., 1986). In this so-called ribomotor model the Pol I transcription unit forms a loop bringing the terminator / ENH element in the proximity of the Pol I promoter. Pol I molecules that have terminated transcription can thus directly be passed to the

promoter. To stabilize such a structure protein factors may be involved, anchoring the rDNA units to the nucleolar matrix. As Reb1 binds to both promoter and enhancer regions of rDNA it was hypothesized to be a potential factor for this stabilizing function. This would be in agreement with the observation that the Reb1 recognition sites contribute to efficient rDNA transcription *in vivo* (Kulkens et al., 1992). However, *in vivo* footprinting analysis revealed that Reb1 binding was not affected by mutations impairing Pol I PIC formation and transcription (Bordi et al., 2001).

Other factors that were shown to be implicated in Pol I transcription termination are the 3' end-processing enzyme Rnt1 and the Rpa12 subunit of Pol I (Prescott et al., 2004).

In addition to the transcription factors mentioned above, several other proteins have been reported to influence rDNA transcription. The Net1 protein is a subunit of the nucleolar RENT complex (regulator of nucleolar silencing and telophase exit) that controls mitotic exit and nucleolar silencing (Shou et al., 1999; Straight et al., 1999). Net1 directly interacts with Pol I and stimulates rRNA synthesis both *in vitro* and *in vivo* (Shou et al., 2001). Another protein involved in rRNA gene transcription is the high-mobility group (HMG) protein Hmo1 which associates throughout the 35S rRNA gene locus in a Pol I-dependent manner and binds to the promoters of most ribosomal protein genes (Kasahara et al., 2007; Hall et al., 2006). Hmo1 has been shown to act synergistically with the Pol I subunit Rpa49. Double mutants of HMO1 and RPA49 were lethal and this lethality was bypassed by Pol II transcription of the *GAL7-35S rDNA* fusion gene, indicating a requirement of this factor for Pol I transcription (Gadal et al., 2002).

1.3.2 The role of UAF in activating RNA polymerase I (Pol I) and suppressing RNA polymerase II (Pol II) transcription of 35S rRNA genes

In all eukaryotes the rRNA genes are transcribed by Pol I. The yeast *S. cerevisiae* has an inherent ability to transcribe rDNA by Pol II but this transcription activity is silenced in normal yeast cells. The first evidence for the existence of a cryptic Pol II promoter in rDNA was reported for respiratory-deficient mitochondrial yeast strains (Conrad-Webb and Butow, 1995). Later studies revealed a role for the transcription factor UAF in silencing of Pol II transcription of rRNA genes (Vu et al., 1999). Deletion of the genes for one of the UAF subunits Rrn5, Rrn9 or Rrn10 allows Pol II transcription of rRNA genes. These

mutants grow extremely slowly and give rise to variants that transcribe chromosomal rDNA by Pol II. The switch to this state (PSW for Polymerase Switch) is accompanied by an expansion of rDNA repeats to levels approximately fivefold higher than found in normal yeast and is inheritable through meiosis and mitosis (Oakes et al., 1999). Electron microscopy analysis determined an average of 1.6 Pol II molecules per rRNA gene in the PSW strains in contrast to about 50 Pol I molecules per active gene in a normal yeast cell. Thus, it seems that the large rDNA array compensates for a very low level of rRNA production from each individual repeat (Hontz et al., 2009). Primer extension analysis revealed multiple start sites for Pol II transcription of rDNA in the PSW strains ranging from -9 to -95 upstream from the normal Pol I initiation site (+1). A major start site was located at position -29. Importantly, deletion of genes that affect recombination within the rDNA repeats, SIR2 and FOB1, increase and decrease the frequency of switching to the PSW state but do not independently lead to Pol II transcription of chromosomal rDNA (Oakes et al., 1999; Vu et al., 1999).

The deletion of the UAF subunit Uaf30 does not completely abolish Pol I transcription but leads to a reduction of rRNA synthesis rate by 70%. Transcription in these mutants is carried out by both polymerases Pol I and Pol II with about 10% of transcripts being produced by Pol II. Thus, in the UAF30 deletion mutant the silencing function of UAF is impaired although the rDNA is still transcribed by Pol I. This was confirmed by the observation that the deletion of UAF30 can result in a PSW phenotype under certain conditions (Siddiqi et al., 2001). The UAF complex can still be purified from a strain missing the Uaf30 subunit and retains an *in vitro* stimulatory effect on Pol I transcription although the activity is reduced about 2-fold. This indicates that the Uaf30 subunit is not important for the assembly of the other subunits to form an active complex. Instead it has been shown to be required for targeting UAF to the UE. Consequently, in the absence of UAF30 only about 13 genes, instead of ~75 genes as in a normal yeast cell become activated. These few active rDNA genes are heavily loaded with about 100 polymerases per repeat, presumably to compensate for the reduced rRNA production. However, in contrast to ~3.750 Pol I molecules being engaged in rRNA transcription in wild-type yeast cells, UAF30 deletion strains only have about 1.300 actively transcribing polymerases in average (Hontz et al., 2008).

In contrast to the deletion of UAF subunits, mutations in subunits of Pol I or other Pol I transcription factors do not independently lead to Pol II transcription of rDNA. Therefore the role of UAF in silencing Pol II transcription of chromosomal rRNA genes is unique. It was suggested that UAF might achieve this function by organizing a Pol I-specific chromatin structure at the rDNA locus that is essential for effective Pol I transcription and responsible for silencing of Pol II transcription (Vu et al., 1999). Other factors might be involved in establishing such a chromatin structure. Thus, the histone deacetylase Rpd3 has been shown to be required for establishing the PSW state. Deletion of the RPD3 gene specifically inhibits Pol II transcription of rRNA genes and leads to an increased silencing of Pol II reporter genes inserted in rDNA (Oakes et al., 2006; Sun and Hampsey, 1999; Smith et al., 1999).

1.4 Silencing of Pol II transcription in rDNA

UAF-dependent suppression of Pol II transcription of rRNA genes was discovered independently from transcriptional silencing of Pol II-dependent genes located within heterochromatic regions in *S. cerevisiae*. This form of transcriptional silencing involves the establishment of a repressive chromatin structure that inhibits transcription. In *S. cerevisiae* this heterochromatin-like silent chromatin has been described to be responsible for transcriptional repression at three different chromosomal loci: the silent mating-type loci (HM), the telomeric regions and the rDNA repeats (for review see Huang, 2002). The SIR (silent information regulator) genes are required for the transcriptional silencing of Pol II reporter genes. In contrast to silencing at HM and telomeres rDNA silencing does not require Sir3 and Sir4. Therefore Sir2 is the only factor essential for silencing at all three silent loci in *S. cerevisiae*. It belongs to a large family of closely related nicotinamide adenine dinucleotide (NAD)-dependent protein deacetylases present in both prokaryotic and eukaryotic species (Dutnall and Pillus, 2001). The histone deacetylase (HDAC) activity of Sir2 is absolutely required for silencing (Imai et al., 2000; Landry et al., 2000; Smith et al., 2000).

1.4.1 Silencing at the silent mating-type loci and telomeric regions

Silencing at the HM loci and at telomeres is important for the maintenance of haploid cell identity and contributes to the retention of telomeric repeats (Rine and Herskowitz, 1987) (Palladino et al., 1993). Silencing at these loci is mediated by the SIR complex containing the Sir2, Sir3 and Sir4 proteins. The SIR complex binds to nucleosomes throughout silent chromatin domains and is recruited to the DNA by proteins associated with chromosome ends or specific regulatory elements called silencers. It has further been shown, that the deacetylase activity of Sir2 is required for the efficient association of the SIR complex with chromatin (Tanny et al., 1999). A stepwise model for spreading of silent chromatin has been proposed (Sperling and Grunstein, 2009; Moazed, 2001). After recruitment of a Sir2/Sir4 complex Sir2 deacetylates H3 and H4 tails, which leads to binding of Sir3 and Sir4 to the modified histone tails, which in turn leads to *de novo* recruitment of a Sir2/Sir4 complex.

1.4.2 Silencing at the rDNA locus

Silencing of Pol II genes in rDNA was discovered by the analysis of retrotransposon TY1 and of reporter genes integrated into rDNA repeats and was demonstrated to be dependent on SIR2 (Smith and Boeke, 1997; Bryk et al., 1997). Sir2 is part of the nucleolar RENT complex which localizes to both the Pol I promoter and to non-transcribed spacer (NTS1) regions within rDNA. Fob1 is required for the association of RENT with the rDNA NTS1 region and for silencing at this location (Huang and Moazed, 2003; Straight et al., 1999). The RENT subunit Net1 mediates silencing by tethering Sir2 to the rDNA and stimulates Pol I transcription both *in vitro* and *in vivo*. As Net1 binds purified Pol I complexes it was suggested, that Pol I is required for recruitment of the RENT complex to promoter and 35S coding regions (Straight et al., 1999; Shou et al., 2001). Net1 is also required for sequestering Cdc14 in the nucleolus until telophase, thereby regulating the exit from mitosis (Shou et al., 1999; Visintin et al., 1999).

Another factor involved in rDNA silencing by a Sir2-independent mechanism is the histone methyltransferase Set1, which is also important for silencing at the HML and telomeric loci (Nislow et al., 1997; Bryk et al., 2002). In addition the SWI/SNF chromatin remodeling

complex that can activate or repress transcription is required for repression of Pol II-dependent transcription in the rDNA. This mechanism is independent of both Sir2 and Set1. The SWI/SNF complex is also involved in silencing at telomeric regions but does not seem to play a role in silencing at the HM loci (Dror and Winston, 2004).

Since Sir2 and its enzymatic activity are required for rDNA silencing, probably (histone) deacetylation is involved in the regulation of the repressive rDNA chromatin structure (Imai et al., 2000; Tanny et al., 1999). Consistent with this it has been shown that the loss of SIR2 leads to an altered sensitivity of rDNA to MNase and *dam* methyltransferase (Fritze et al., 1997), supporting the idea that a Sir2-based silencing mechanism might provoke a repressive rDNA chromatin structure. A mechanism for spreading of such a structure as described for silencing at the HM and telomeric regions (see above) has not been proposed for the rDNA locus. However, it was demonstrated that rDNA silencing is dependent on Pol I activity and spreads unidirectionally in the direction of transcription (Buck et al., 2002).

The repressive structure at the rDNA locus involved in transcriptional silencing also functions in the suppression of mitotic and meiotic recombination between rDNA repeats and in the control of cellular life span (Gottlieb and Esposito, 1989). It has been shown that Sir2 suppresses unequal sister chromatid exchange, as well as intrachromosomal recombination between the repeated array elements (Kobayashi et al., 2004). Increased recombination in the absence of SIR2 leads to the accumulation of extrachromosomal rDNA circles (ERCs) excised from the rDNA array which reduces average life span (Sinclair and Guarente, 1997; Kaeberlein et al., 1999). In contrast, FOB1 (see also above) deletion decreases the recombination rate and the formation of ERCs (Defossez et al., 1999).

Recent work provided insights into the mechanism of Sir2-dependent stabilization of the rDNA array. It was demonstrated that Sir2 inhibits transcription from a previously identified bidirectional Pol II promoter (E-pro) located within IGS1 (Kobayashi et al., 2005). According to these data, a model of rDNA amplification regulation was suggested. In the absence of E-pro transcription cohesin would be associated throughout the IGS keeping rDNA repeats of sister chromatids together and preventing unequal sister chromatid exchange. Instead, transcription of the promoter would lead to disruption of cohesion association and result in instability of the rDNA array (Gartenberg, 2009;

Kobayashi et al., 2005). Thus, Sir2 seems to prevent recombination events via transcriptional control.

1.4.3 Reciprocal Silencing Model

Silencing of Pol II transcription in rDNA is different from silencing at HM loci and telomeric regions as the rDNA locus is a site of active transcription. The paradoxical phenomenon of RNA Pol II silencing within the highly transcribed rDNA region was explained by different models (reviewed in Moazed, 2001). One model proposed that the access of Pol II to the rDNA was generally limited and that silencing of Pol II transcription was independent of Pol I transcription. The second model assumed that silencing of reporter genes occurred only in the transcriptionally inactive rDNA repeats associated with chromatin structures that act repressive on both Pol I and Pol II. In contrast to these two models, more recent data suggested a reciprocal relationship between Pol I and Pol II transcription. First, it was demonstrated that an intact Pol I transcription machinery is required for rDNA silencing because silencing was abolished in strains with deletions in Pol I subunits or in PSW strains carrying deletions in UAF (Buck et al., 2002; Cioci et al., 2003). Furthermore, silencing of Pol II reporter genes was much stronger in a strain with only 25 rDNA copies, all of which are trancriptionally active (French et al., 2003; Cioci et al., 2003). In addition Net1, which is important for rDNA silencing, stimulates Pol I transcription both *in vivo* and *in vitro* (Shou et al., 2001). This confirms a requirement for Pol I in rDNA silencing and supports an alternative model, called the “reciprocal silencing model” (Cioci et al., 2003).

1.4.4 Model for the function of UAF in influencing silencing at the rDNA locus

UAF is a sequence-specific DNA binding complex important for both suppression of Pol II transcription of 35S rDNA and silencing of Pol II reporter genes integrated in rDNA repeats (Vu et al., 1999; Oakes et al., 1999; Siddiqi et al., 2001; Buck et al., 2002; Cioci et al., 2003). Thus it is conceivable, that the two phenomena rely at least in part on similar mechanisms. This is underlined by the observation that the deletion of the histone deacetylase Rpd3 increases silencing of reporter genes (Smith et al., 1999; Sun et al., 1999) and at the same time inhibits Pol II transcription of 35S rRNA genes in PSW strains

(Oakes et al., 2006) (see also above). However, it was demonstrated that the deletion of SIR2 which is important for transcriptional silencing of Pol II reporter genes in rDNA is not required for suppression of Pol II transcription of 35S rRNA genes (Oakes et al., 1999). Therefore a model was proposed in which UAF nucleates a specific chromatin structure at the rDNA promoter region that prevents the access of Pol II to cryptic Pol II promoters for chromosomal rRNA gene transcription (Fig. 1-6). This local structure does not exert an effect on Pol II transcription of reporter genes unless it is spread to other rDNA regions by proteins such as Sir2 or Net1 perhaps together with elongating Pol I (Cioci et al., 2003).

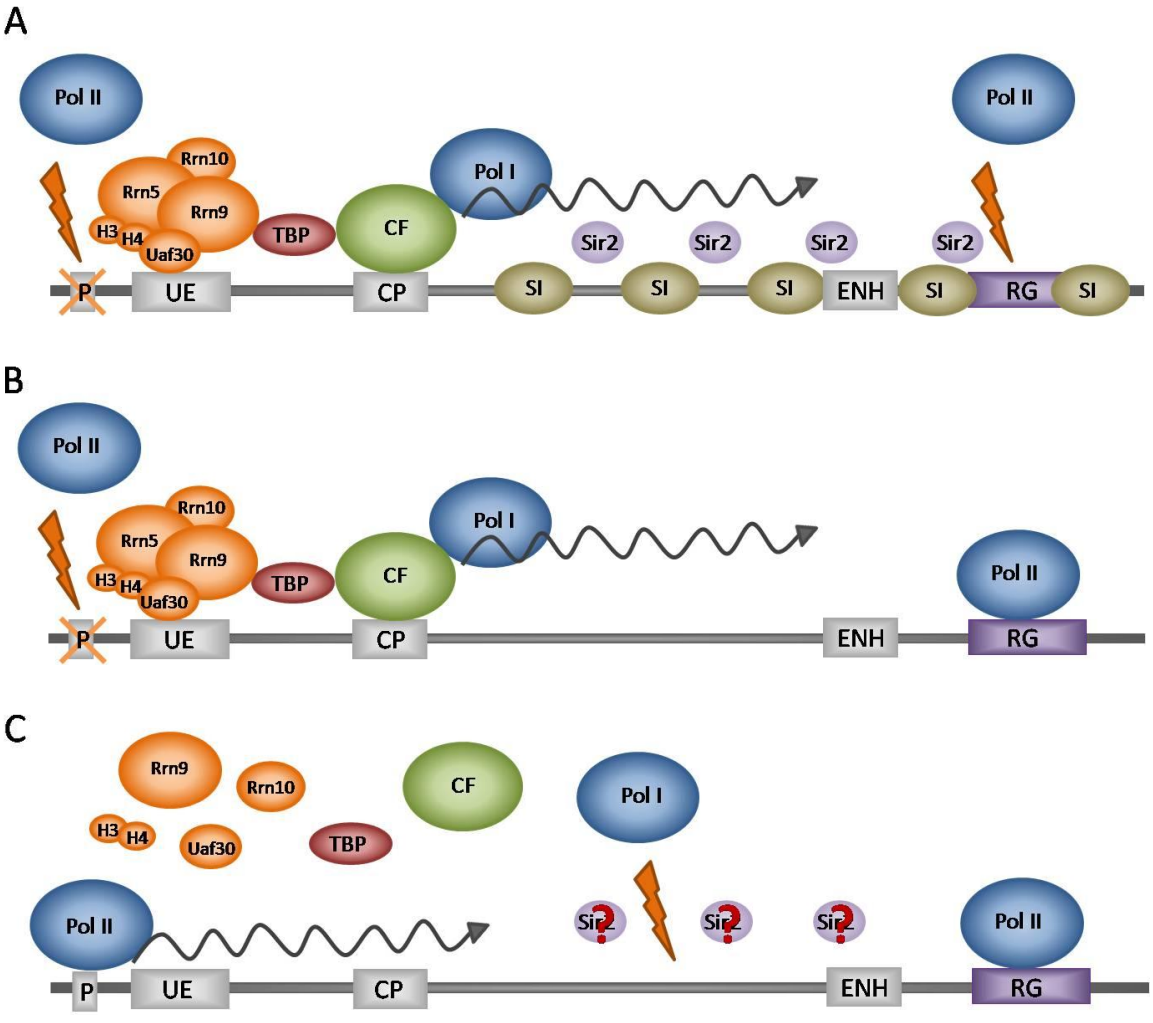

Fig. 1-6 Model for UAF in silencing Pol II transcription at the rDNA locus
(A) UAF mediates a specific promoter structure which limits the access of Pol II to the cryptic Pol II promoter. This chromatin structure required for silencing of Pol II transcription (SI) is spread with the help of other proteins, e.g. Sir2 over the entire rDNA locus resulting in the repression of Pol II transcription of reporter genes (RG) within the NTS region. (B) In the absence of Sir2 only silencing of reporter genes is disrupted as UAF still restricts the access to the cryptic Pol II promoter. (C) In the absence of UAF in the PSW strains suppression of Pol II transcription at the 35S rDNA locus is abolished. In addition the repressive chromatin structure is not spread to the NTS resulting in a loss of silencing of Pol II reporter genes.

Several observations support the idea of a role for UAF in determining chromatin structure at the rDNA locus. The histones H3 and H4 are part of the multiprotein complex and probably contribute to the high affinity of UAF for its binding site (Keener et al., 1997). It is known that H3 and H4 form a tetramer that interacts with DNA and forms a structure similar to a nucleosome (Camerini-Otero et al., 1976; Hayes et al., 1991). However, it is still unknown if H3 and H4 are present in UAF as a tetramer and if UAF might wrap the promoter DNA like a nucleosome. In addition, a portion of the UAF subunit Uaf30 shows structural similarity to a region of BAF60a subunit of human and mouse SWI/SNF chromatin-remodeling complexes. This structural feature also may be related to a function of UAF in organizing chromatin structure (Siddiqi et al., 2001). Thus, it is possible that UAF mediates a special chromatin structure in the promoter region that might then initiate spreading of a chromatin repressive to Pol II transcription along the 35S coding region. Other proteins besides UAF might be involved in spreading of such a structure.

1.5 Objectives

According to the current model, UAF establishes a spezialized rDNA chromatin at the promoter region which is then spread with the help of other factors across the entire rDNA locus. This UAF-mediated chromatin is supposed to determine polymerase specificity and silencing at the rDNA locus (Cioci et al., 2003). The molecular nature of rDNA chromatin, however, remained enigmatic.

The aim of this study was to analyze the influence of UAF on rDNA chromatin structure to provide the molecular basis for the above model. Therefore the chromatin composition at the rDNA locus was analyzed in mutant strains lacking different UAF subunits by exogenous MNase digestion and psoralen crosslinking assays. To define the substructures that account for changes in MNase accessibilities upon deletion of UAF subunits the association of structural rDNA components was investigated using Chromatin Endogenous Cleavage (ChEC) (Merz et al., 2008).

UAF determines polymerase specificity of the 35S rDNA promoter (Vu et al., 1999; Oakes et al., 1999; Siddiqi et al., 2001), and we wanted to elucidate the mechanism of transcription initiation by RNA polymerases other than Pol I in UAF deletion strains. Thus, ChEC was applied to investigate the specific rearrangement of transcription factors and polymerase complexes at the promoter region in diverse mutant backgrounds. Another important role of UAF is silencing of Pol II reporter genes integrated in rDNA (Buck et al., 2002; Cioci et al., 2003). Therefore a special effort was made to define the source of the Pol II silencing defect observed upon UAF deletion.

2 Material and Methods

2.1 Material

2.1.1 Chemicals

All chemicals and solvents used in this work are *pro analysis (p.a.)* and were purchased from the chemicals centre of the University of Regensburg. Water was always purified with an Elgastat Maxima device prior to use.

2.1.2 Buffers and media

If not indicated otherwise, the solvent is H_20. The pH values were measured at room temperature. Percentage is mass per volume (m/v), if not indicated otherwise. pH was adjusted with HCl or NaOH if not indicated otherwise.

LB Medium	Tryptone Yeast Extract NaCl 1M NaOH Agar (for plates) Autoclave	10 g/l 5 g/l 5 g/l 1 ml/l 20 g/l
LB / Amp	Ampicillin in LB Medium (add when medium is <50°C)	50 µg/ml
YPD	Yeast Extract Peptone Glucose Agar (for plates) Autoclave	10 g/l 20 g/l 20 g/l 20 g/l
YPG	Yeast Extract Peptone Galactose Agar (for plates) Autoclave	10 g/l 20 g/l 20 g/l 20 g/l
YPD / Geneticin YPG /Geneticin	Geneticin in YPD /YPG	400 mg/l

IR buffer	Tris-HCl pH 8 EDTA	50 mM 20 mM
IRN buffer	Tris-HCl pH 8 EDTA NaCl	50 mM 20 mM 0.5 M
TBE buffer	Tris Boric acid EDTA	90 mM 90 mM 1 mM
10 x DNA loading buffer	Bromphenol blue Xylen cyanol Glycerine	0.25 % 0.25 % 40 %
TE buffer	Tris-HCl pH 8 EDTA	10 mM 1 mM
20 x SSC	NaCl Tri-sodium citrate dehydrate pH7 with HCl	3 M 0.3 M
Buffer A	Tris-HCl pH 7.4 Spermine Spermidine KCl EDTA	15 mM 0.2 mM 0.5 mM 80 mM 2 mM
Buffer Ag	Buffer A without EDTA EGTA	 0.1 mM
Protease Inhibitors 100x	Benzamidine PMSF Pepstatin A Leupeptin Chymostatin	33 mg/ml 17 mg/ml 137 µg/ml 28.4 µg/ml 200 µg/ml
4 x Upper Tris	Tris SDS Bromphenol blue pH 6.8 with HCl	0.5 M 0.4 %
4 x Lower Tris	Tris SDS pH 8.8 with HCl	1.5 M 0.4 %
10 x Electrophoresis buffer (SDS-PAGE)	Tris Glycin SDS	250 mM 1.9 M 1.0 %

10 x PBS	NaCl	1.37 M
	KCl	27 mM
	$Na_2HPO_4 \cdot 2H_2O$	10 mM
	KH_2PO_4	20 mM
	pH 7.4 with HCl or NaOH	
PBST	PBS	1x
	Tween 20	0.05%
MNase buffer	Tris-HCl pH 8	15 mM
	NaCl	50 mM
	$CaCl_2$	1.4 mM
	EDTA	0.2 mM
	EGTA	0.2 mM
ChIP Lysis buffer	Hepes pH 7.5	50 mM
	NaCl	140 mM
	EDTA	5 mM
	EGTA	5 mM
	Triton X100	1 %
	DOC	0.1 %
ChIP Wash buffer I	Hepes pH 7.5	50 mM
	NaCl	500 mM
	EDTA	2 mM
	Triton X100	1 %
	DOC	0.1 %
ChIP Wash buffer II	Tris-HCl pH 8	10 mM
	LiCl	250 mM
	EDTA	2 mM
	Nonidet P40	0.5 %
	DOC	0.5 %
SORB	LiOAc	100 mM
	Tris/HCl, pH 8	10 mM
	EDTA	1 mM
	Sorbitol	1 M
PEG	LiOAc	100 mM
	Tris/HCl pH 8	10 mM
	EDTA	1 mM
	PEG3350	40%

2.1.3 Nucleic acids

A. Nucleotides

For synthesis of DNA molecules the “desoxynucleotide solution mix” by New England Biolabs was used which contains each of the four desoxynucleotides in 10 mM concentration.

B. Oligonucleotides

Name /Nr.	Sequence	Function	Gene
843	GATGGTACCCATCGTTTCAGATTCCGAGCAATCAGATACAAAGGGCATTTCGTACGCTGCAGGTCGAC	primer to obtain amplicon of pKM9 for genomic integration of MNase-3xHA::KanMX6 / primer to obtain amplicon from pAG37 for deletion of the UAF30 gene	UAF30
844	CTACCGCGGACAACACAAATTTCAACGCCTTGAAATTTTCATGATATCCTTGATATCGATGAATTCGAGCTCG	primer to obtain amplicon of pKM9 for genomic integration of MNase-3xHA::KanMX6	UAF30
935	GATGGTACCAAGAAGAAGAAGGATAAGAAGAAGGACAAATCCAACTCTTCTATTTCGTACGCTGCAGGTCGAC	primer to obtain amplicon of pKM9 for genomic integration of MNase-3xHA::KanMX6	HMO1
936	CTACCGCGGATTTTAGAAAGACAGTAGAGTAATAGTAACGAGTTTGTCCGTCCAATCGATGAATTCGAGCTCG	primer to obtain amplicon of pKM9 for genomic integration of MNase-3xHA::KanMX6	HMO1
941	GATGGTACCGGTACGGGTTCATTTGATGTGTTAGCAAAGGTTCCAAATGCGGCTTCGTACGCTGCAGGTCGAC	primer to obtain amplicon of pKM9 for genomic integration of MNase-3xHA::KanMX6	RPA190
942	CTACCGCGGAAACTAATATTAAATCGTAATAATTATGGGACCTTTTGCCTGCTTATCGATGAATTCGAGCTCG	primer to obtain amplicon of pKM9 for genomic integration of MNase-3xHA::KanMX6	RPA190
1016	GATGGTACCGAAGGTACTAGGGCTGTTACCAAATACTCCTCCTCTACTCAAGCCTCGTACGCTGCAGGTCGAC	primer to obtain amplicon of pKM9 for genomic integration of MNase-3xHA::KanMX6	HTB2
1017	CTACCGCGGTAATAAAAAGAAAACATGACTAAATCACAATACCTAGTGAGTGACATCGATGAATTCGAGCTCG	primer to obtain amplicon of pKM9 for genomic integration of MNase-3xHA::KanMX6	HTB2
1154	GATGGTACCTATGCTTTGAAGAGACAAGGTAGAACCTTATATGGTTTCGGTGGTTCGTACGCTGCAGGTCGAC	primer to obtain amplicon of pKM9 for genomic integration of MNase-3xHA::KanMX6	HHF2
1155	CTACCGCGGGGCATGAAAATAATTTCAAACACCGATTGTTTAACCACCGATTGTATCGATGAATTCGAGCTCG	primer to obtain amplicon of pKM9 for genomic integration of MNase-3xHA::KanMX6	HHF2

1157	GATGGTACCGACTGCATTTCAAGGATCAAAAA TGCCTGTCTGCATAGGATGAATTCGTACGCTGC AGGTCGAC	primer to obtain amplicon of pKM9 for genomic integration of MNase-3xHA::KanMX6	RRN7
1158	CTACCGCGGAGTATGCATAGAAATAGCAATCC AGCGAGAATAATTTAAAAGGAGATCGATGAAT TCGAGCTCG	primer to obtain amplicon of pKM9 for genomic integration of MNase-3xHA::KanMX6	RRN7
1134	GATGGTACCAGAGCTAGTTGATTATTTTAGCTC CAATATTTCAATGAAAACAGAAAATTCGTACGC TGCAGGTCGAC	primer to obtain amplicon of pKM9 for genomic integration of MNase-3xHA::KanMX6	REB1
1135	CTACCGCGGCTATCAAACATTATTGAGTTTTTC GCTTTCACCAATTATATTTTCCGGAAATCGATG AATTCGAGCTCG	primer to obtain amplicon of pKM9 for genomic integration of MNase-3xHA::KanMX6	REB1
1342	GATGGTACCCCAAGCTTTTGAAGCTATATACCC TGTGCTAAGTGAATTTAGAAAAATGTCGTACG CTGCAGGTCGAC	primer to obtain amplicon of pKM9 for genomic integration of MNase-3xHA::KanMX6	SPT15
1343	CTACCGCGGAAATGGAACAAATAGAAAACCTT TTTTTCTTTTCGTCTACTCCTTCCCCAATCGATG AATTCGAGCTCG	primer to obtain amplicon of pKM9 for genomic integration of MNase-3xHA::KanMX6	SPT15
1356	GATGGTACCCTTGTTGCCAAAGAAGTCTGCCA AGGCTACCAAGGCTTCTCAAGAATTATCGTAC GCTGCAGGTCGAC	primer to obtain amplicon of pKM9 for genomic integration of MNase-3xHA::KanMX6	HTA1
1357	CTACCGCGGGGAGAAGCAGTTTAGTTCCTTCC GCCTTCTTTAAAATACCAGAACCGATCATCGAT GAATTCGAGCTCG	primer to obtain amplicon of pKM9 for genomic integration of MNase-3xHA::KanMX6	HTA1
1358	GATGGTACCTATAAATAAAGCATTATTATTGAA AGTGGAAAAAAAGGGAAGTAAGAAATCGTAC GCTGCAGGTCGAC	primer to obtain amplicon of pKM9 for genomic integration of MNase-3xHA::KanMX6	HTZ1
1359	CTACCGCGGATACAGGAGCAGGGAGAATTAC GGGAAATGGGAAAGAAAAACTATTCTTCATCG ATGAATTCGAGCT	primer to obtain amplicon of pKM9 for genomic integration of MNase-3xHA::KanMX6	HTZ1
1492	GATGGTACCCCCCTCCGGCATTATTAAACTAAA CAAGAAGAAGGTCAAACTCTCCACGTCGTACG CTGCAGGTCGA	primer to obtain amplicon of pKM9 for genomic integration of MNase-3xHA::KanMX6	HHO1
1493	CTACCGCGGTTTGATAGTATTGCTATCACCATT GACATTCTCGTTTGGATATTCACTTTATCGATG AATTCGAGCTCG	primer to obtain amplicon of pKM9 for genomic integration of MNase-3xHA::KanMX6	HHO1
1498	GATGGTACCACGAGTTGGACGACTGCCTCATA GAACTGCCTAATGGGAACATATCGTACGCTGC AGGTCGAC	primer to obtain amplicon of pKM9 for genomic integration of MNase-3xHA::KanMX6	RRN9
1499	CTACCGCGGATGAATATTTCTTAATGGAAAAA GGTAAAAAAAAGATTTTCTCATATCGATGAATT CGAGCTCG	primer to obtain amplicon of pKM9 for genomic integration of MNase-3xHA::KanMX6	RRN9
1500	GATGGTACCACGGGTTGGACGAAATGCATTAC AGTGATGAAGACTCAAGTGAGTCGTACGCTGC AGGTCGAC	primer to obtain amplicon of pKM9 for genomic integration of MNase-3xHA::KanMX6	RRN11
1501	CTACCGCGGAAGTTTCCCTAGTTGAAACCAAGT TATTAAAGTTTACTAGTTTGTATCGATGAATTC GAGCTCG	primer to obtain amplicon of pKM9 for genomic integration of MNase-3xHA::KanMX6	RRN11

1509	TTAACAAGTACTAAAGCGTTCGTTGACAGCTTTCTTTGCGTTGCCCGTACGCTGCAGGTCGAC	primer to obtain amplicon from pAG37 for deletion of the UAF30 gene	UAF30
1682	GATGGTACCAAGTTTCTCCAAGAAGATTAATTACGACGCCATTGACGGTTTGTTTAGGTCGTACGCTGCAGGTCGAC	primer to obtain amplicon of pKM9 for genomic integration of MNase-3xHA::KanMX6	BRF1
1683	CTACCGCGGCGTCTTTATTTCCGTTCCCTTTTTCCTTCCTAGGGTTGATTACCTAAACGATCGATGAATTCGAGCTC	primer to obtain amplicon of pKM9 for genomic integration of MNase-3xHA::KanMX6	BRF1
1688	GATGGTACCGCGATGTCTATTTGAAAGTCTCTCAAATGAGGCAGCTTTAAAAGCGAACTCGTACGCTGCAGGTCGAC	primer to obtain amplicon of pKM9 for genomic integration of MNase-3xHA::KanMX6	RPO31
1689	CTACCGCGGGTGGTAGAAAAATAATACAAATGCTATAAAAAAGTTTAAAAACGACTACTATCGATGAATTCGAGCTCG	primer to obtain amplicon of pKM9 for genomic integration of MNase-3xHA::KanMX6	RPO31
1723	GATGGTACCGAAGCCAAGTGGTGGATTTGCATCATTAATAAAAGATTTCAAGAAAAAATCGTACGCTGCAGGTCGA	primer to obtain amplicon of pKM9 for genomic integration of MNase-3xHA::KanMX6	NET1
1724	CTACCGCGGTTTTTTTTACTAGCTTTCTGTGACGTGTATTCTACTGAGACTTTCTGGTAATCGATGAATTCGAGCTCG	primer to obtain amplicon of pKM9 for genomic integration of MNase-3xHA::KanMX6	NET1
1727	GATGGTACCGGATAAGGGCGTGTATGTCGTTACATCAGATGAACATCCCAAAACCCTCTCGTACGCTGCAGGTCGA	primer to obtain amplicon of pKM9 for genomic integration of MNase-3xHA::KanMX6	SIR2
1728	CTACCGCGGTGTAAATTGATATTAATTTGGCACTTTTAAATTATTAAATTGCCTTCTACATCGATGAATTCGAGCTCG	primer to obtain amplicon of pKM9 for genomic integration of MNase-3xHA::KanMX6 / primer to obtain amplicon from pAG37 for deletion of the SIR2 gene	SIR2
1730	TCGGTAGACACATTCAAACCATTTTTCCCTCATCGGCACCATTAAAGCTGGCGTAGCTGCAGGTCGAC	primer to obtain amplicon from pAG37 for deletion of the SIR2 gene	SIR2
1744	GATGGTACCACAGGGTAATGGAGATCAAACAAGAGACTTTGGCACATCAATGGAATTGTCGTACGCTGCAGGTCGA	primer to obtain amplicon of pKM9 for genomic integration of MNase-3xHA::KanMX6	FOB1
1745	CTACCGCGGTTTTTTTTTCACCTATGGTGACTCCTCCTTTCATTCTATCCTACATATTAATCGATGAATTCGAGCTCG	primer to obtain amplicon of pKM9 for genomic integration of MNase-3xHA::KanMX6	FOB1
2009	GATGGTACCTACAAGCGCCGCCGGTGGTATAAGAAAAATAAGTGGCTCCATCAAGAAATCGTACGCTGCAGGTCGC	primer to obtain amplicon of pKM9 for genomic integration of MNase-3xHA::KanMX6	CDC14
2010	CTACCGCGGTAGTAAGTTTTTTTATTATATGATATATATATATATAAAAATGAAATAAAATCGATGAATTCGAGCTCG	primer to obtain amplicon of pKM9 for genomic integration of MNase-3xHA::KanMX6	CDC14
2293	GTTCCGCGGTGCATCTCAAATGGGTAATACTGGATCAGGAGGGTATGATAATGCTTGGTCGTACGCTGCAGGTCGAC	primer to obtain amplicon of pKM9 for genomic integration of MNase-3xHA::KanMX6	RPB3

2294	GTTGGTACCTTTTCGGTTCGTTCACTTGTTTTTTTTCTTCTATTACGCCCACTTGAGAAATCGATGAATTCGAGCTCG	primer to obtain amplicon of pKM9 for genomic integration of MNase-3xHA::KanMX6	RPB3
626	CCATTCCGTGAAACACC	primer to obtain template for Southern probe preparation from genomic DNA	rDNA
627	AAGAAAGAAACCGAAATCTC	primer to obtain template for Southern probe preparation from genomic DNA	rDNA
817	GAGGGACGGTTGAAAGTG	primer to obtain template for Southern probe preparation from genomic DNA	rDNA
818	ATACGCTTCAGAGACCCTAA	primer to obtain template for Southern probe preparation from genomic DNA	rDNA
1161	CAGGTTATGAAGATATGGTGCAA	primer to obtain template for Southern probe preparation from genomic DNA	rDNA
1162	AAAATGGCCTATCGGAATACA	primer to obtain template for Southern probe preparation from genomic DNA	rDNA
1163	TGTTGCTAGATCGCCTGGTA	primer to obtain template for Southern probe preparation from genomic DNA	GAL1
1164	TTTCCGGTGCAAGTTTCTTT	primer to obtain template for Southern probe preparation from genomic DNA	GAL1
1167	TGGATCTAATTTACAGCAGCA	primer to obtain template for Southern probe preparation from genomic DNA	NUP57
1168	CCTGATCCCACTCTTCTTGA	primer to obtain template for Southern probe preparation from genomic DNA	NUP57
2101	GTAGTGCTCTGTGTGCTGCC	primer to obtain template for Southern probe preparation from genomic DNA	HMR
2102	GACGATTAAAAAGATGATCG	primer to obtain template for Southern probe preparation from genomic DNA	HMR
710	TGGAGCAAAGAAATCACCGC	primer used for qPCR amplifying a region in 25S rDNA together with primer 711	rDNA
711	CCGCTGGATTATGGCTGAAC	primer used for qPCR amplifying a region in 25S rDNA together with primer 710	rDNA
920	GCCATATCTACCAGAAAGCACC	primer used for qPCR amplifying a region in 5S rDNA together with primer 921	rDNA
921	GATTGCAGCACCTGAGTTTCG	primer used for qPCR amplifying a region in 5S rDNA together with primer 920	rDNA

969	TCATGGAGTACAAGTGTGAGGA	primer used for qPCR amplifying rDNA promoter region together with primer 970	rDNA
970	TAACGAACGACAAGCCTACTC	primer used for qPCR amplifying rDNA promoter region together with primer 969	rDNA
1502	AACAACGAAACGCCTTCATC	primer used for PCR amplification of the kl URA3 gene from pBS1539 to clone pAG37	kl URA3
1503	AGGGAGCTCTACGACTCACTATAGGG	primer used for PCR amplification of the kl URA3 gene from pBS1539 to clone pAG37	kl URA3

C. DNA size markers

- 2-log-ladder (NEB)
  size of fragments (bp): 10000, 8000, 6000, 5000, 4000, 3000, 2000, 1500, 1200, 1000, 900, 800, 700, 600, 500/517, 400, 300, 200, 100

- XcmI marker generated by double digest of yeast genomic DNA (NOY703) with XcmI and eight other restriction enzymes (see below). The size of the detected fragments depends on the probe.

  XcmI_promoter-probe: 545 (DdeI), 577 (XmnI), 681 (TatI), 802 (HaeIII), 1443 (NdeI), 1992 (SacII), 3434 (DraIII), 4099 (KpnI), 4902 (XcmI)

  XcmI_5S-probe: 535 (HaeIII), 635 (DdeI), 826 (TatI), [1025 (TatI), 1835 (TatI)], 2948 (XmnI), 4236 (XcmI); TatI digestion is incomplete

D. DNA probes for Southern blot detection

All probes have been prepared with the “Rad Prime Labelling System” (Invitrogen)

Name	Synthesis	Gene	Restriction Enzyme	Fragment size
ETS	PCR from genomic DNA using primers 626, 627	rDNA	EcoRI	1.9kb
ETS	PCR from genomic DNA using primers 626, 627	rDNA	SacII, XcmI	2kb
GAL1	PCR from genomic DNA using primers 1163, 1164	GAL1-10	XcmI	6.8kb
GAL1	PCR from genomic DNA using primers 1163, 1164	GAL1-10	EcoRI	1.9kb
IGS2	PCR from genomic DNA using primers 1161, 1162	rDNA	XcmI	4.3kb
NUP57	PCR from genomic DNA using primers 1167, 1168	RPS23A	XcmI	4.2kb
rDNp	PCR from genomic DNA using primers 817, 818	rDNA	XcmI	4.9kb
GIT1	PCR from genomic DNA using primers 2101, 2102	HMR	XcmI	10.7kb

E. Plasmids

Name	Nr.	Cloning	Function	Reference
pBluescript KS (+/-)	1		LacZ T3 and T7 promoter M13 - 20 T7 and SK primer Col E 1 - Origin f1ori (+or -)	Stratagene
pNOY103	186		GAL7-35S rDNA	Nogi et al., 1991
pKM9	643	PCR with primers 839, 840 from pYM1 (V36; 3xHA-Tag) via BbsI, BssHII in BbsI, BssHII from pFA6a-MN-KanMX6 (K456)	(PCR-) template, cloning	Katharina Merz
pKM12	646	PCR with primers 843, 844 from pKM9 via KpnI and SacII in pBluescript KS	genomic C-terminal MNase tagging by recombination, linarisation with KpnI, SacII	Katharina Merz
pKM13	647	PCR with primers 797, 847 from pKM9 cloned in pGEM-TEasy Vector; Orientation: T7	genomic C-terminal MNase tagging by recombination, linarisation with KpnI, SacII	Katharina Merz
pKM14	648	PCR with primers 843, 844 from pKM9 via KpnI and SacII in pBluescript KS	genomic C-terminal MNase tagging by recombination, linarisation with KpnI, SacII	Katharina Merz

pKM15	649	PCR with primers 935, 936 from pKM9 via KpnI and SacII in pBluescript KS	genomic C-terminal MNase tagging by recombination, linarisation with KpnI, SacII	Katharina Merz
pKM18	652	PCR with primers 941, 942 from pKM9 via KpnI and SacII in pBluescript KS	genomic C-terminal MNase tagging by recombination, linarisation with KpnI, SacII	Katharina Merz
pKM20	654	PCR with primers 1016, 1017 from pKM9 via KpnI and SacII in pBluescript KS	genomic C-terminal MNase tagging by recombination, linarisation with KpnI, SacII	Katharina Merz
pAG2-1	825	PCR with primers 1134, 1135 from pKM9 via KpnI and SacII in pBluescript KS	genomic C-terminal MNase tagging by recombination, linarisation with KpnI, SacII	Katharina Merz
pAG5	827	PCR with primers 1342, 1343 from pKM9 via KpnI and SacII in pBluescript KS	genomic C-terminal MNase tagging by recombination, linarisation with KpnI, SacII	Katharina Merz
pAG6	828	PCR with primers 1157, 1158 from pKM9 via KpnI and SacII in pBluescript KS	genomic C-terminal MNase tagging by recombination, linarisation with KpnI, SacII	Katharina Merz
pAG13	834	PCR with primers 1356, 1357 from pKM9 via KpnI and SacII in pBluescript KS	genomic C-terminal MNase tagging by recombination, linarisation with KpnI, SacII	Joachim Griesenbeck
pAG14	835	PCR with primers 1358, 1359 from pKM9 via KpnI and SacII in pBluescript KS	genomic C-terminal MNase tagging by recombination, linarisation with KpnI, SacII	Joachim Griesenbeck
pAG24	839	PCR with primers 1744, 1745 from pKM9 via KpnI and SacII in pBluescript KS	genomic C-terminal MNase tagging by recombination, linarisation with KpnI, SacII	Joachim Griesenbeck
pAG31	899	PCR with primers 1492, 1493 from pKM9 via KpnI and SacII in pBluescript KS	genomic C-terminal MNase tagging by recombination, linarisation with KpnI, SacII	Joachim Griesenbeck
pAG33	901	PCR with primers 1500, 1501 from pKM9 via KpnI and SacII in pBluescript KS	genomic C-terminal MNase tagging by recombination, linarisation with KpnI, SacII	Joachim Griesenbeck
pAG34	902	PCR with primers 1498, 1499 from pKM9 via KpnI and SacII in pBluescript KS	genomic C-terminal MNase tagging by recombination, linarisation with KpnI, SacII	Joachim Griesenbeck
pAG37	937	insertion of a SmaI/SacI restricted PCR fragment obtained from pBS1539 (Puig et al., 2001) using primers 1502 and 1503 into SmaI/SacI restricted pKM9	(PCR-) template for UAF30 and SIR2 knock out	Joachim Griesenbeck
pMW4	983	PCR with primers 1682, 1683 from pKM9 via KpnI and SacII in pBluescript KS	genomic C-terminal MNase tagging by recombination, linarisation with KpnI, SacII	Manuel Wittner
pMW9	988	PCR with primers 1686, 1687 from pKM9 via KpnI and SacII in pBluescript KS	genomic C-terminal MNase tagging by recombination, linarisation with KpnI, SacII	Manuel Wittner
pMW15	1082	PCR with primers 1727, 1728 from pKM9 via KpnI and SacII in pBluescript KS	genomic C-terminal MNase tagging by recombination, linarisation with KpnI, SacII	Manuel Wittner

pMW18	1085	PCR with primers 1723, 1724 from pKM9 via KpnI and SacII in pBluescript KS	genomic C-terminal MNase tagging by recombination, linarisation with KpnI, SacII	Manuel Wittner
CDC14	1140	PCR with primers 2009, 2010 from pKM9 via KpnI and SacII in pBluescript KS	genomic C-terminal MNase tagging by recombination, linarisation with KpnI, SacII	Manuel Wittner

2.1.4 Enzymes and polypeptides

All enzymes were used with the provided buffers.

Go Taq Polymerase	PROMEGA
Herculase	STRATAGENE
T4-DNA-polymerase	NEW ENGLAND BIOLABS
Restriction endonucleases	NEW ENGLAND BIOLABS
T4-DNA-ligase	NEW ENGLAND BIOLABS
Zymolyase T100	Seikagaku Corporation
Prestained protein-marker broad range	NEW ENGLAND BIOLABS

2.1.5 Antibodies

Primary antibodies

3F10 anti-HA	monoclonal rat	(1:5000)	Roche
12CA5 anti-HA	monoclonal mouse	(1:1000)	E. Kremmer
anti-tubulin	monoclonal rat	(1:1000)	Abcam
anti-rpS8	monoclonal rabbit	(1:1000)	G. Dieci
anti-rpa135	monoclonal rabbit	(1:10000)	A. Sentenac

Secondary antibodies

AlexaFluor® 488 goat anti-rat	(1:500)	Molecular Probes
AlexaFluor® 594 goat anti-mouse	(1:500)	Molecular Probes
Goat anti-mouse (peroxidase-conjugated)	(1:3000)	Jackson ImmunoResearch
Goat anti-rabbit (peroxidase-conjugated)	(1:2500)	Jackson ImmunoResearch
Goat anti-rat (peroxidase-conjugated)	(1:2500)	Jackson ImmunoResearch

2.1.6 Organisms

A. Host bacteria

For cloning, the electro-competent *E. coli* strain "XL1BlueMRF" by Stratagene was used. genotype: Δ(mcrA)183, Δ(mcrCB-hsdSMR-mrr)173, endA1, supE44, thi-1, recA1, gyrA96, relA1, lac, λ-, [F´, proAB, lacIqZΔM15, tn10(tetr)].

B. Yeast strains

Creation of UAF30 or SIR2 deletion strains

Plasmid pAG37 (K937) was constructed by insertion of a SmaI / SacI restricted PCR fragment obtained from pBS1539 (Puig et al., 2001) using primers 1502 and 1503 into SmaI / SacI restricted pKM9 (K643) (Merz et al., 2008). To establish UAF30 or SIR2 deletion strains the URA3 gene from *Kluyveromyces lactis* (*kl URA3*) was amplified with primers 843 and 1509, or 1728 and 1730 from plasmid pAG37. The amplified fragment was framed by 50 bp of DNA sequence homologous to the 5' sequence upstream of the ATG, and 50 bp of sequence homologous to the DNA downstream of the stop codon of the UAF30, or SIR2 open reading frame. The amplicon was directly used for transformation.

Strains used in this study

Name /Nr.	Parent	Genotype	Comment	Reference
NOY505		mata; ade2-1; ura3-1; trp1-1; leu2-3,112; his3-11; can1-100		Nogi et al., 1993
NOY558		matα; ade2-1; ura3-1; his3-11; trp1-1; leu2-3,112; can1-100; rrn7::LEU2; pNOY103		Nogi et al., 1991
NOY699		matα; ade2-1; ura3-1; his3-11; trp1-1; leu2-3,112; can1-100; rrn5::LEU2; pNOY103		Nogi et al., 1991
NOY408 -1a		matα; ade2-1; ura3-1; his3-11; trp1-1; leu2-3,112; can1-100; rpa135::LEU2; pNOY103		Nogi et al., 1991
NOY604		matα; ade2-1; ura3-1; his3-11; trp1-1; leu2-3,112; can1-100; rrn3::HIS3; pNOY103		Nogi et al., 1991

NOY703		matα; ade2-1; ura3-1; his3-11; trp1-1; leu2-3,112; can1-100; rrn9::HIS3; pNOY103		Oakes et al., 1999
CG379		ade5; his7-2; leu2-112; trp1-289; ura3-52		Cadwell et al, 1997
YCC95		mat_alpha; ade5; his7-2; leu2-112; trp1-289; ura3-52; rrn3-8		Cadwell et al, 1997
y617	NOY505	mata; ade2-1; ura3-1; trp1-1; leu2-3,112; his3-11; can1-100; HTB2-MNase-3xHA::KanMX6	obtained by transformation with KpnI/SacII restricted pKM20	Katharina Merz
y618	NOY505	mata; ade2-1; ura3-1; trp1-1; leu2-3,112; his3-11; can1-100; UAF30-MNase-3xHA::KanMX6	obtained by transformation with KpnI/SacII restricted pKM12	Katharina Merz
y619	NOY505	mata; ade2-1; ura3-1; trp1-1; leu2-3,112; his3-11; can1-100; RRN10-MNase-3xHA::KanMX6	obtained by transformation with KpnI/SacII restricted pKM13	Katharina Merz
y620	NOY505	mata; ade2-1; ura3-1; trp1-1; leu2-3,112; his3-11; can1-100; HHT1-MNase-3xHA::KanMX6	obtained by transformation with KpnI/SacII restricted pKM14	Katharina Merz
y621	NOY505	mata; ade2-1; ura3-1; trp1-1; leu2-3,112; his3-11; can1-100; HMO1-MNase-3xHA::KanMX6	obtained by transformation with KpnI/SacII restricted pKM15	Katharina Merz
y624	NOY505	mata; ade2-1; ura3-1; trp1-1; leu2-3,112; his3-11; can1-100; RPA190-MNase-3xHA::KanMX6	obtained by transformation with KpnI/SacII restricted pKM18	Katharina Merz
y879	NOY505	mata; ade2-1; ura3-1; trp1-1; leu2-3,112; his3-11; can1-100; HHF2-MNase-3xHA::KanMX6	obtained by transformation with PCR product (1154/1155) from pKM9	Katharina Merz
y881	NOY505	mata; ade2-1; ura3-1; trp1-1; leu2-3,112; his3-11; can1-100; RRN7-MNase-3xHA::KanMX6	obtained by transformation with KpnI/SacII restricted pAG6	Katharina Merz
y890	NOY558	matα; ade2-1; ura3-1; his3-11; trp1-1; leu2-3,112; can1-100; rrn7::LEU2;pNOY103; HMO1-MNase-3xHA::KanMX6	obtained by transformation with KpnI/SacII restricted pKM15	Katharina Merz
y938	YCC95	matα; ade5; his7-2; leu2-112; trp1-289; ura3-52; rrn3-8; RPA190-MNase-3xHA::KanMX6	obtained by transformation with KpnI/SacII restricted pKM18	Ulrike Stöckl
y945	CG379	matα; ade5; his7-2; leu2-112; trp1-289; ura3-52; RPA190-MNase-3xHA::KanMX6	obtained by transformation with KpnI/SacII restricted pKM18	Ulrike Stöckl
y952	NOY505	mata; ade2-1; ura3-1; trp1-1; leu2-3,112; his3-11; can1-100; FOB1-MNase-3xHA::KanMX6	obtained by transformation with KpnI/SacII restricted pAG24	this work
y954	NOY505	mata; ade2-1; ura3-1; trp1-1; leu2-3,112; his3-11; can1-100; HTZ1-MNase-3xHA::KanMX6	obtained by transformation with KpnI/SacII restricted pAG14	this work

y956	NOY505	mata; ade2-1; ura3-1; trp1-1; leu2-3,112; his3-11; can1-100; HTA1-MNase-3xHA::KanMX6	obtained by transformation with KpnI/SacII restricted pAG13	this work
y1109	NOY558	matα; ade2-1; ura3-1; his3-11; trp1-1; leu2-3,112; can1-100; rrn7::LEU2;pNOY103; UAF30-MNase-3xHA::KanMX6	obtained by transformation with KpnI/SacII restricted pKM12	this work
y1120	NOY505	mata; ade2-1; ura3-1; trp1-1; leu2-3,112; his3-11; can1-100; uaf30Δ::kl URA3	obtained by transformation with PCR product (843/1509) from pAG37	this work
y1141	NOY505	mata; ade2-1; ura3-1; trp1-1; leu2-3,112; his3-11; can1-100; RRN11-MNase-3xHA::KanMX6	obtained by transformation with KpnI/SacII restricted pAG33	Maria Hondele
y1143	CG379	matα; ade5; his7-2; leu2-112; trp1-289; ura3-52; RRN11-MNase-3xHA::KanMX6	obtained by transformation with KpnI/SacII restricted pAG33	Maria Hondele
y1144	YCC95	matα; ade5; his7-2; leu2-112; trp1-289; ura3-52; rrn3-8; RRN11-MNase-3xHA::KanMX6	obtained by transformation with KpnI/SacII restricted pAG33	Maria Hondele
y1145	NOY505	mata; ade2-1; ura3-1; trp1-1; leu2-3,112; his3-11; can1-100; HHO1-MNase-3xHA::KanMX6	obtained by transformation with KpnI/SacII restricted pAG31	Maria Hondele
y1148	YCC95	matα; ade5; his7-2; leu2-112; trp1-289; ura3-52; rrn3-8; SPT15-MNase-3xHA::KanMX6	obtained by transformation with KpnI/SacII restricted pAG5	Maria Hondele
y1149	CG379	matα; ade5; his7-2; leu2-112; trp1-289; ura3-52; SPT15-MNase-3xHA::KanMX6	obtained by transformation with KpnI/SacII restricted pAG5	Maria Hondele
y1151	NOY505	mata; ade2-1; ura3-1; trp1-1; leu2-3,112; his3-11; can1-100; RRN9-MNase-3xHA::KanMX6	obtained by transformation with KpnI/SacII restricted pAG34	Maria Hondele
y1171	y617	mata; ade2-1; ura3-1; trp1-1; leu2-3,112; his3-11; can1-100; uaf30Δ::kl URA3; HTB2-MNase-3xHA::Kan MX6	obtained by transformation with PCR product (843/1509) from pAG37	this work
y1172	y890	mata; ade2-1; ura3-1; trp1-1; leu2-3,112; his3-11; can1-100; uaf30Δ::kl URA3; HMO1-MNase-3xHA::Kan MX6	obtained by transformation with PCR product (843/1509) from pAG37	this work
y1174	y624	mata; ade2-1; ura3-1; trp1-1; leu2-3,112; his3-11; can1-100; uaf30Δ::kl URA3; RPA190-MNase-3xHA::Kan MX6	obtained by transformation with PCR product (843/1509) from pAG37	this work
y1175	y879	mata; ade2-1; ura3-1; trp1-1; leu2-3,112; his3-11; can1-100; uaf30Δ::kl URA3; HHF2-MNase-3xHA::Kan MX6	obtained by transformation with PCR product (843/1509) from pAG37	this work

y1177	y952	mata; ade2-1; ura3-1; trp1-1; leu2-3,112; his3-11; can1-100; uaf30Δ::kl URA3; FOB1-MNase-3xHA::Kan MX6	obtained by transformation with PCR product (843/1509) from pAG37	this work
y1184	NOY505	mata; ade2-1; ura3-1; trp1-1; leu2-3,112; his3-11; can1-100; REB1-MNase-3xHA::KanMX6	obtained by transformation with PCR product (1334/1335) from pKM9	this work
y1185	NOY505	mata; ade2-1; ura3-1; trp1-1; leu2-3,112; his3-11; can1-100; SPT15-MNase-3xHA::KanMX6	obtained by transformation with KpnI/SacII restricted pAG5	this work
y1273	NOY505	mata; ade2-1; ura3-1; trp1-1; leu2-3,112; his3-11; can1-100; BRF1-MNase-3xHA::KanMX6	obtained by transformation with KpnI/SacII restricted pMW4	Manuel Wittner
y1294	NOY505	mata; ade2-1; ura3-1; trp1-1; leu2-3,112; his3-11; can1-100; RPO31-MNase-3xHA::KanMX6	obtained by transformation with KpnI/SacII restricted pMW9	Manuel Wittner
y1328	y1184	mata; ade2-1; ura3-1; trp1-1; leu2-3,112; his3-11; can1-100; uaf30Δ::kl URA3; REB1-MNase-3xHA::Kan MX6	obtained by transformation with PCR product (843/1509) from pAG37	this work
y1329	y1185	mata; ade2-1; ura3-1; trp1-1; leu2-3,112; his3-11; can1-100; uaf30Δ::kl URA3; SPT15-MNase-3xHA::Kan MX6	obtained by transformation with PCR product (843/1509) from pAG37	this work
y1330	y1294	mata; ade2-1; ura3-1; trp1-1; leu2-3,112; his3-11; can1-100; uaf30Δ::kl URA3; RPO31-MNase-3xHA::Kan MX6	obtained by transformation with PCR product (843/1509) from pAG37	this work
y1341	y624	mata; ade2-1; ura3-1; trp1-1; leu2-3,112; his3-11; can1-102; sir2Δ::kl URA3; RPA190-MNase-3xHA::Kan MX6	obtained by transformation with PCR product (1728/1730) from pAG37	this work
y1345	y1184	mata; ade2-1; ura3-1; trp1-1; leu2-3,112; his3-11; can1-102; sir2Δ::kl URA3; REB1-MNase-3xHA::Kan MX6	obtained by transformation with PCR product (1728/1730) from pAG37	this work
y1346	y1185	mata; ade2-1; ura3-1; trp1-1; leu2-3,112; his3-11; can1-102; sir2Δ::kl URA3; SPT15-MNase-3xHA::Kan MX6	obtained by transformation with PCR product (1728/1730) from pAG37	this work
y1347	y1294	mata; ade2-1; ura3-1; trp1-1; leu2-3,112; his3-11; can1-102; sir2Δ::kl URA3; RPO31-MNase-3xHA::Kan MX6	obtained by transformation with PCR product (1728/1730) from pAG37	this work
y1356	y618	mata; ade2-1; ura3-1; trp1-1; leu2-3,112; his3-11; can1-102; sir2Δ::kl URA3; UAF30-MNase-3xHA::Kan MX6	obtained by transformation with PCR product (1728/1730) from pAG37	this work

y1357	y619	mata; ade2-1; ura3-1; trp1-1; leu2-3,112; his3-11; can1-102; sir2Δ::kl URA3; RRN10-MNase-3xHA::Kan MX6	obtained by transformation with PCR product (1728/1730) from pAG37	this work
y1358	y621	mata; ade2-1; ura3-1; trp1-1; leu2-3,112; his3-11; can1-102; sir2Δ::kl URA3; HMO1-MNase-3xHA::Kan MX6	obtained by transformation with PCR product (1728/1730) from pAG37	this work
y1450	NOY505	mata; ade2-1; ura3-1; trp1-1; leu2-3,112; his3-11; can1-100; SIR2-MNase-3xHA::KanMX6	obtained by transformation with KpnI/SacII restricted pMW15	Manuel Wittner
y1453	NOY505	mata; ade2-1; ura3-1; trp1-1; leu2-3,112; his3-11; can1-100; NET1-MNase-3xHA::KanMX6	obtained by transformation with KpnI/SacII restricted pMW18	Manuel Wittner
y1560	CG379	matα; ade5; his7-2; leu2-112; trp1-289; ura3-52; RPO31-MNase-3xHA::KanMX6	obtained by transformation with KpnI/SacII restricted pMW9	Manuel Wittner
y1566	YCC95	matα; ade5; his7-2; leu2-112; trp1-289; ura3-52; rrn3-8; RPO31-MNase-3xHA::KanMX6	obtained by transformation with KpnI/SacII restricted pMW9	Manuel Wittner
y1671	NOY505	mata; ade2-1; ura3-1; trp1-1; leu2-3,112; his3-11; can1-100; CDC14-MNase-3xHA::KanMX6	obtained by transformation with KpnI/SacII restricted CDC14	Manuel Wittner
y1674	NOY699	matα; ade2-1; ura3-1; his3-11; trp1-1; leu2-3,112; can1-100; rrn5::LEU2; pNOY103; SIR2-MNase-3xHA::KanMX6	obtained by transformation with KpnI/SacII restricted pMW15	this work
y1676	NOY699	matα; ade2-1; ura3-1; his3-11; trp1-1; leu2-3,112; can1-100; rrn5::LEU2; pNOY103; HMO1-MNase-3xHA::KanMX6	obtained by transformation with KpnI/SacII restricted pKM15	this work
y1679	NOY699	matα; ade2-1; ura3-1; his3-11; trp1-1; leu2-3,112; can1-100; rrn5::LEU2; pNOY103; HTB2-MNase-3xHA::KanMX6	obtained by transformation with KpnI/SacII restricted pKM20	this work
y1681	NOY505	mata; ade2-1; ura3-1; trp1-1; leu2-3,112; his3-11; can1-100; RBP3-MNase-3xHA::KanMX6	obtained by transformation with PCR product (2293/2294) from pKM9	this work
y1688	y1681	mata; ade2-1; ura3-1; trp1-1; leu2-3,112; his3-11; can1-100; uaf30Δ::kl URA3; RPB3-MNase-3xHA::Kan MX6	obtained by transformation with PCR product (843/1509) from pAG37	this work
y1689	y1453	mata; ade2-1; ura3-1; trp1-1; leu2-3,112; his3-11; can1-100; uaf30Δ::kl URA3; NET1-MNase-3xHA::Kan MX6	obtained by transformation with PCR product (843/1509) from pAG37	this work
y1690	y1145	mata; ade2-1; ura3-1; trp1-1; leu2-3,112; his3-11; can1-100; uaf30Δ::kl URA3; HHO1-MNase-3xHA::Kan MX6	obtained by transformation with PCR product (843/1509) from pAG37	this work

y1691	y1450	mata; ade2-1; ura3-1; trp1-1; leu2-3,112; his3-11; can1-100; uaf30Δ::kl URA3; SIR2-MNase-3xHA::Kan MX6	obtained by transformation with PCR product (843/1509) from pAG37	this work
y1692	y1151	mata; ade2-1; ura3-1; trp1-1; leu2-3,112; his3-11; can1-100; uaf30Δ::kl URA3; RRN9-MNase-3xHA::Kan MX6	obtained by transformation with PCR product (843/1509) from pAG37	this work
y1694	y1273	mata; ade2-1; ura3-1; trp1-1; leu2-3,112; his3-11; can1-100; uaf30Δ::kl URA3; BRF1-MNase-3xHA::Kan MX6	obtained by transformation with PCR product (843/1509) from pAG37	this work
y1695	y954	mata; ade2-1; ura3-1; trp1-1; leu2-3,112; his3-11; can1-100; uaf30Δ::kl URA3; HTZ1-MNase-3xHA::Kan MX6	obtained by transformation with PCR product (843/1509) from pAG37	this work
y1696	y1671	mata; ade2-1; ura3-1; trp1-1; leu2-3,112; his3-11; can1-100; uaf30Δ::kl URA3; CDC14-MNase-3xHA::Kan MX6	obtained by transformation with PCR product (843/1509) from pAG37	this work
y1705	YCC95	matα; ade5; his7-2; leu2-112; trp1-289; ura3-52; rrn3-8; SIR2-MNase-3xHA::KanMX6	obtained by transformation with KpnI/SacII restricted pMW15	this work
y1706	YCC95	matα; ade5; his7-2; leu2-112; trp1-289; ura3-52; rrn3-8; CDC14-MNase-3xHA::KanMX6	obtained by transformation with KpnI/SacII restricted 1140	this work
y1707	YCC95	matα; ade5; his7-2; leu2-112; trp1-289; ura3-52; rrn3-8; NET1-MNase-3xHA::KanMX6	obtained by transformation with KpnI/SacII restricted pMW18	this work
y1708	YCC95	matα; ade5; his7-2; leu2-112; trp1-289; ura3-52; rrn3-8; RPB3-MNase-3xHA::KanMX6	obtained by transformation with PCR product (2293/2294) from pKM9	this work
y1710	CG379	matα; ade5; his7-2; leu2-112; trp1-289; ura3-52; SIR2-MNase-3xHA::KanMX6	obtained by transformation with KpnI/SacII restricted pMW15	this work
y1711	CG379	matα; ade5; his7-2; leu2-112; trp1-289; ura3-52; CDC14-MNase-3xHA::KanMX6	obtained by transformation with KpnI/SacII restricted CDC14	this work
y1712	CG379	matα; ade5; his7-2; leu2-112; trp1-289; ura3-52; NET1-MNase-3xHA::KanMX6	obtained by transformation with KpnI/SacII restricted pMW18	this work
y1713	CG379	matα; ade5; his7-2; leu2-112; trp1-289; ura3-52; RPB3-MNase-3xHA::KanMX6	obtained by transformation with PCR product (2293/2294) from pKM9	this work
y1716	CG379	matα; ade5; his7-2; leu2-112; trp1-289; ura3-52; BRF1-MNase-3xHA::KanMX6	obtained by transformation with KpnI/SacII restricted pMW4	this work

y1926	NOY408-1a	matα; ade2-1; ura3-1; his3-11; trp1-1; leu2-3,112; can1-100; rpa135::LEU2; pNOY103; RRN7-MNase-3xHA::KanMX6	obtained by crossing NOY408_1a and y881	this work
y1927	NOY408-1a	matα; ade2-1; ura3-1; his3-11; trp1-1; leu2-3,112; can1-100; rpa135::LEU2; pNOY103; UAF30-MNase-3xHA::KanMX6	obtained by crossing NOY408_1a and y618	this work
y1928	NOY604	matα; ade2-1; ura3-1; his3-11; trp1-1; leu2-3,112; can1-100; rrn3::HIS3; pNOY103; RRN7-MNase-3xHA::KanMX6	obtained by crossing NOY604_1a and y881	this work
y1929	NOY604	matα; ade2-1; ura3-1; his3-11; trp1-1; leu2-3,112; can1-100; rrn3::HIS3; pNOY103; UAF30-MNase-3xHA::KanMX6	obtained by crossing NOY604_1a and y618	this work

2.1.7 Apparatus

Name	Supplier
Agarose gel UV imaging system GelMax	INTAS
BAS cassette 2040	Fuji
BAS-III imaging plate	Fuji
Branson Sonifier 250	Branson
DNA cross-linking system Fluo-Link tFL20.M	Vilber Loumat
Electroporation device Micropulser™	Biorad
Hybridization tubes	Bachofer, Rettberg
Microcentrifuge Biofuge fresco	Heraeus
Microcentrifuge Biofuge pico	Heraeus
Mini hybridization ofen	MWG biotech
Rotor Gene RG-3000	Corbett Research
Sub-cell® Gt Agarose Gel Electrophoresis System	Biorad
Phospho imager FLA5000	Fujifilm
Table centrifuge Ct412	Jouan
Thermocycler PCRSprint	Hybaid
Thermocycler PCRSprint	Biorad
UV/Visible-spectrophotometer	Amersham Biosciences
Vibrax VXR basic	IKA

2.1.8 Consumables

Name	Supplier
Filter paper 3MM	Whatman
Gene pulser cuvettes	BioRad
Glass beads (0.75-1 mm)	Roth
Immobilon-P transfer membrane	Millipore
Multiwell plates (24 wells)	Nunc
Positive TM membrane	Qbiogene

2.2 Methods

2.2.1 Enzymatic manipulation of DNA

A. Polymerase chain reaction (PCR)

PCR was performed in 50 µl reactions. Each reaction contained the DNA to be amplified, 0.25 mM desoxynucleotides, 20 pmol of each the forward and the reverse primer, PCR buffer to a final concentration 1x with 1.5 mM $MgCl_2$ and 2.5 U GoTaq polymerase. The components were mixed in a 0.2 or 0.5 ml reaction tube.

Semi-hotstart was performed to eliminate primer-dimers, mispriming and secondary structure of the primer molecules. The reaction tubes were placed into the PCR machine block when the temperature had reached 80°C. DNA was initially denatured by heating the samples 3 minutes to 95°C. Amplification was performed in 30 cycles. Each cycle consisted of denaturation of double-stranded DNA (45 seconds at 94°C), annealing of primers to matching DNA sequences (30 seconds at 3°C below melting temperature of the primers) and amplification (1 min per 1 kb at 72°C). When all cycles were complete, amplification was continued for 10 minutes at 72°C. Temperature was then lowered to 4°C for storage.

B. Sequence specific restriction endonucleases

Restriction enzyme digestion was performed in buffer and temperature conditions as indicated by NEB. ChEC samples were digested in 20-30 µl reactions overnight. Control digestions for cloning were performed in 50 µl reactions with 1 µl of restriction enzyme per

1 µg of DNA. Total glycerol concentration (present in restriction enzyme storage buffer) should not exceed 5%.

C. Unspecific restriction endonucleases (MNase)

The prepared nuclei (see 2.2.5) were resuspended in 500 µl MNase buffer on ice and washed twice (13000 rpm, 2 min, 4°C). Then the pellet was resuspended in MNase buffer to a volume of 1 ml. The suspension was dispersed to five microreaction tubes equally (200 µl each tube), the aliquots were prewarmed at 37°C for 2 min and then incubated with 0, 0.05, 0.15, 0.3 or 1 Units (U) MNase for nuclei and 0, 0.125, 0.375, 0.75 or 2.5 mU MNase for genomic DNA (50 A_{260}U/µl MNase: 500 U MNase (SIGMA) in 850 µl MNase buffer (20 mM Tris-HCl pH 8, 1 mM $CaCl_2$)). After 20 min digestion at 37°C the reaction was stopped by adding 200 µl of IRN buffer. RNA was digested with 2 µl RNAseA (20 mg/ml) for 1h at 37°C. Afterwards, SDS (final concentration 0.5%) was added together with 4 µl of proteinase K (20 mg/ml stock) and incubated for 1 h at 56°C. The formaldehyde crosslink was reversed by incubation at 65°C overnight or for at least 8 h. DNA was isolated by phenol-chloroform extraction, precipitated with ethanol and resuspended in 50 µl TE buffer.

D. DNA Ligation

In order to clone DNA sequences into vectors, quantity of purified DNA fragments digested with restriction endonuclease(s) was measured by UV spectrometry (see 2.2.3A). A three-time excess of insert DNA compared to the vector DNA fragment was incubated in a 20 µl ligase reaction (400 U T4 DNA ligase NEB, 50 mM Tris-HCl, 10 mM $MgCl_2$, 1 mM ATP, 10 mM Dithiothreitol, 25 µg/ml BSA) for 1 h at room temperature or overnight at 16°C. One µl of ligation reaction was used for *E. coli* transformation (see 2.2.11B).

2.2.2 Purification of nucleic acids

A. Plasmid Isolation

Plasmid DNA was isolated from *E. coli* cultures with kits. Pelleted cells were lysed with a buffer containing NaOH and SDS. Genomic DNA and proteins were precipitated when the alkaline lysate was neutralized with KOAc. The supernatant which still contained the

plasmids was transferred to an anion exchange column which bound the DNA under low salt conditions. Remaining RNA and proteins were washed away. Then, plasmid DNA was eluted with high salt buffers, desalted by isopropanol precipitation and resuspended in TE or water. Minipreps (up to 4 ml of *E. coli* culture) were prepared with the Invitrogen PureLink Quick Plasmid miniprep kit. Midipreps (50 ml of *E. coli* culture, yield up to 100 µg of DNA) were prepared with the Invitrogen PureLink Quick Plasmid midiprep kit. Preparation was performed as indicated in the manual.

B. Isolation of genomic DNA from yeast

A culture of yeast cells was grown overnight in 5 ml YPD. Cells were spun down and resuspended in 500 µl H_2O. Cells were spun down again and resuspended in 500 µl 1 M sorbitol, 0.1 M EDTA. 3 µl of 2% zymolyase (10 mM TrisCl pH 8, 5% glucose, 2% zymolyase) were added and incubated for 60 minutes at 37°C. Spheroblasts were spun down at 5000 rpm for 5 minutes (table-top centrifuge). After addition of 500 µl IR buffer and 50 µl 10% SDS, the samples were vortexed until lysis was complete (about 1 minute at full speed). Samples were incubated for 30 minutes at 65°C. For precipitation of nucleic acids, 200 µl of 5 M KOAc was added and samples were kept on ice for 20 minutes. Samples were spun down at 13000 rpm for 20 minutes at 4°C, the supernatant was transferred to a new microtube. 1.5 µl of RNAseA (100 mg/ml) were added and samples were incubated at room temperature overnight. After addition of 750 µl 2-propanol, DNA was precipitated at room temperature for 5 minutes and pelleted (13000 rpm, 5 minutes in table-top centrifuge). The pellet was washed once with ice-cold 70% EtOH and spun again (13000 rpm, 5 minutes in table-top centrifuge). The supernatant was discarded and the DNA pellet air-dried to eliminate remnants of ethanol. The dry pellet was resuspended in 50 µl TE buffer.

C. Phenol Extraction

DNA from watery samples with lysed cells was extracted by phenol-chloroform. About one volume of Phenol-chloroform-isoamyl alcohol (25:24:1) was added to the sample. Samples were vortexed until the solution was milky. Samples were centrifuged for at least 5 minutes at room temperature. An aliquot of the upper aqueous phase was transferred to a new reaction tube. The white layer of denatured protein in between the upper aqueous and the lower phenol phase should not be disturbed.

D. Ethanol precipitation

If samples did not yet contain at least 0.25 M salt (e.g. 0.5x IRN buffer is sufficient), an equal volume of IRN was added to the sample. DNA was precipitated by addition of 2.5 new volumes of 100% ethanol; to precipitate small amounts of DNA, glycogen (5 µl of 20 mg/ml) was supplemented. Samples were frozen (-20°C) for at least 1 hour, DNA was pelleted at full speed for 20 minutes at 4°C. To eliminate salt, the pellet was washed with ice-cold 70% ethanol. The supernatant was discarded, the pellet air-dried and resuspended in TE or water.

E. Purification of PCR products

The "QIAquick PCR purification Kit" by Qiagen is a fast and easy method to purify enzymatically treated DNA samples (e.g. PCR products, ligation reactions). DNA above an exclusion size (depending on experimental conditions) was bound to a silicate gel column while smaller DNA molecules (primers), salts, nucleotides, enzymes and glycerol were removed. DNA was eluted with 2 mM or 10 mM Tris-Cl, pH 8.

2.2.3 Quantitative and qualitative analysis of nucleic acids

A. UV spectrometry

Concentration of pure DNA samples was measured by nanodrop UV spectrometry at 260 nm wavelength. The concentration [c] of DNA was calculated with the formula:

c [µg/ml] = OD_{260}* 1/sample-volume * 50 µg/ml

To determine contamination with proteins and RNA, absorbance was concomitantly measured at 280 nm. The ratio of OD_{260}/OD_{280} of pure DNA is between 1.8 and 2.0.

B. Agarose gel electrophoresis

0.7 to 2.0% agarose 1x TBE gels were casted in a horizontal gel chamber. 1x TBE was also used as a running buffer. Electrophoresis was performed at 3 to 5 volts per cm. ChEC and MNase gels were 1 cm high, 15 cm broad and 20 cm long. They were run at 100 V in a BioRad gel apparatus.

C. Southern Blot, hybridization and detection of radioactive probes

a. Southern blot

By Southern blot, the DNA was transferred from an agarose gel to a positively charged nylon membrane (Positive^{TM} Membrane, Qbiogen). For denaturation of double-stranded DNA, the gel was incubated twice for 15 minutes in 0.5 M NaOH, 1.5 M NaCl on a shaker. Subsequently, the gel was incubated twice for 15 minutes in transfer buffer (1 M NH_4OAc). The DNA was transferred upwards with capillary flow of transfer buffer through a blotting pile. The pile consisted of from bottom to top: a bridge of 2 thin Whatman papers placed over a reservoir of 1 M NH_4OAc (Whatman 3MM, Whatman, 17*34cm) framed with parafilm to prevent bypass of the capillary flow, the gel (upside down), the membrane (Positive^{TM} Membrane, Qbiogen), three thin Whatman papers (15*20cm) and recycling paper towels (about 5 cm). All layers apart from the recycling paper towels were soaked with 1 M NH_4OAc. The pile was covered with a glass or plastic plate. A weight (about 0.5 kg) assured that the capillary transfer was not interrupted. It is important that no air bubbles remain between the membrane and the gel. Blotting was performed overnight or for at least 6 h (1% gel). Afterwards, the DNA was crosslinked to the membrane (0.3J/cm^2). In this step, thymine bases are covalently bound to the amino groups of the membrane. The membrane can be dried and stored at room temperature.

b. Hybridization

Up to four blots can be stacked into one hybridization tube, separated by meshes. Membranes were prehybridized for 1 h at hybridization temperature (65°C) with hybridization buffer (0.5 M sodium phosphate buffer pH 7.2, 7% SDS). The buffer used for prehybridization was discarded and new prewarmed hybridization buffer (15 ml) was poured into the tube. The probe was mixed with 150 µl salmon sperm DNA (stock: 10 mg/ml -> end concentration 100 µg/ml), boiled at 95°C for five minutes and pipetted into the tube. Hybridization occured overnight at hybridization temperature with the tubes rotating in a hybridization oven. The blots should be covered with liquid, stick to the wall of the tube and not roll. After hybridization, the hybridization buffer containing the probe can be stored at -20°C and reused. First, blots were rinsed once with 30 ml 3x SSC, 0.1% SDS. Blots were

washed at hybridization temperature while rotating the tube in the hybridization oven. Three washing buffers with decreasing salt- and rising SDS-concentration were used in the following order:

Wash 1: 0.3x SSC, 0.1% SDS
Wash 2: 0.1x SSC, 0.1% SDS
Wash 3: 0.1x SSC, 1.5% SDS

Each wash step was repeated twice for 15 min. Afterwards the blots were dried and stored at room temperature.

c. Detection of radioactive probes

A Fuji phosphor-imaging plate (IP) was erased with the “eraser” (Raytest). The blot was put into a Fuji cassette. The IP was taken out of the erase in the dark and put onto the blot (white side of the IP onto the blot). The time of exposure depended on the radioactive signal. IPs were scanned with 100 µM resolution in a phosphor imager (FLA5000 by Fujifilm).

d. Quantification of Southern Blots with *MultiGauge*

For quantitative analysis of Southern blot signals the profile quantitation module of the *MultiGauge 3.0* (Fujifilm) software was used. The signal intensities over the entire length of the respective lane of the Southern blot were recorded. The data were transferred to Excel (Microsoft) for data refinement and graphical representation.

D. Quantitative real-time PCR (qPCR)

qPCR was used to measure the amount of a specific DNA fragment with high accuracy. The amount of DNA present at the end of each single PCR cycle was detected by measuring the fluorescence of SYBR-Green (Roche). SYBR-Green is a dye that shows fluorescence when bound to DNA double helices, but not in solution (excitation at 509 nm, emission at 526 nm). Therefore, the intensity of the fluorescence signal allows direct measurement of the actual amount of DNA present in a sample.

qPCR reactions were performed in 0.1 ml or in 0.2 ml tubes, the reaction volume was 20 µl. The reaction contained 4 µl of DNA sample and 16 µl of master mix. The master mix contained 4 pmol of each the forward and the reverse primer, 0.25 µl of a 1:400000 SYBR-Green stock solution in DMSO, 0.4 U HotStarTaq-polymerase (Qiagen) and premix. Premix consisted of $MgCl_2$ (to adjust a final concentration of 2.5 mM in the qPCR reaction), dNTPs (final concentration 0.2 mM in the qPCR reaction), 10x PCR buffer (Qiagen; 1x final concentration in the qPCR reaction). SYBR-Green was thawed in the dark.
qPCR was performed in a Rotor-Gene RG3000 system (Qiagen). SYBR-Green was excited at 480 nm, fluorescence was recorded at 510 nm. Data were evaluated by analyzing the data with the comparative quantitation module of the RotorGene analysis software.

2.2.4 Formaldehyde crosslink (FA-X)

A culture of yeast cells (300 ml YPD) was cultivated overnight and then crosslinked in exponential growth (final OD_{600} = 0.5). Formaldehyde was added to a final concentration of 1% and cells were fixed for 15 minutes at growth temperature while shaking. If cells were temperature-shifted before crosslink, cell density at the time of harvest should nevertheless be the same. Crosslink was quenched with glycine (final concentration 125 mM) for at least five minutes at room temperature. Cells were harvested (4000 rpm, 10 min at 4°C in CONTRON A6.9 rotor) and resuspended in 5-6 ml water. Cells were separated to aliquots; the number of aliquots was calculated by multiplying the final OD with 10 and rounding down. Aliquots were transferred to microreaction tubes, pelleted (full speed, 1 min at 4°C in table-top centrifuge, discard supernatant), frozen in liquid nitrogen and stored at -80°C.

2.2.5 Preparation of nuclei

All steps were performed on ice. Cells were resuspended in 0.5 ml ChEC buffer A + Protease Inhibitors (1x PIs) and pelleted (13000 rpm, 2 min at 4°C in table-top centrifuge). The wash was repeated three times. Cells were resuspended in 350 µl buffer A + PIs. Cells were broken with glass beads (0.75-1 mm diameter, ROTH, stored at -20°C; add so many glass beads that they are just covered with cell suspension) for 10 minutes at full speed in the Vibrax (in cold room). The reaction tube was pierced at the bottom and top with a hot needle and placed in

a 15 ml falcon tube. After centrifugation (2000 rpm, 2 min at 4°C in a table centrifuge (JOUAN)) the glass beads remained in the reaction tube, which was discarded. The cell lysate was transferred into a microreaction tube and centrifuged again (13000 rpm, 2 min at 4°C in table-top centrifuge). The supernatant was discarded. The lysate pellet (containing intact nuclei) was resuspended in 0.5 ml buffer A + PIs. One additional wash step with 0.5 ml A + PIs was applied. The supernatant was carefully removed (buffer A contains 2 mM EDTA to repress MNase activity).

2.2.6 Chromatin Endogenous Cleavage (ChEC)

For ChEC, at least one protein must be fused to MNase. Nuclei of formaldehyde-crosslinked cells were prepared as described above and then resuspended in an appropriate volume of buffer Ag + PIs (450 to 500 µl, 20 – 50 µl more than required for the time course). Buffer Ag contains 0.1 mM EGTA, thus MNase is not repressed any more. Samples were incubated at 30°C, shaking at 750 rpm. One or two 0 min (untreated) aliquots of the well-mixed sample were taken (80 µl) and the samples were incubated for two more minutes before the MNase digestion reaction was started. MNase digestion was started with $CaCl_2$ (0.1 M stock, 2 µl per 100 µl reaction volume, final concentration 2mM). Aliquots were taken at appropriate time points. For low abundance proteins or single-cutters, the time course 3', 10', 30', 60' was used. For high-abundance proteins, shorter time points were obligatory. The digestion reaction was immediately stopped by pipetting the aliquot into 100 µl IRN buffer. Before taking an aliquot, samples should be mixed at higher rotation rates as nuclei sediment. Stopped aliquots can be kept at room temperature. When the time course was complete, 100 µl IRN was added to the 0 min aliquots. RNA in the samples was digested with 2 µl RNAseA (20 mg/ml) for 1 h at 37°C. Afterwards, SDS (final concentration 0.5%) was added together with 2 µl of proteinase K (20 mg/ml stock) and incubated for 1 h at 56°C. The formaldehyde crosslink was reversed by incubation at 65°C overnight or for at least 8 h. DNA was isolated by phenol-chloroform extraction, precipitated with ethanol and resuspended in 50 µl TE buffer.

2.2.7 Psoralen treatment

Psoralen crosslinking was performed on nuclei. Nuclei were suspended in 1 ml buffer Ag/IRN (1:1). 200 µl of this suspension were incubated with Psoralen and another 200 µl were treated with Ethanol as a control. The remaining nuclei were pelleted, frozen in liquid nitrogen and stored at -80°C. All samples were pipetted into the wells of a 24 tissue culture plate (for suspension cells). To each sample 10 µl of trimethylpsoralen (TMP, 0.2 mg/ml in ethanol) or ethanol was added, mixed and stored on ice in the dark for 5 minutes. Then, samples were irradiated with long-wavelength UV light (288 nm) for 5 minutes. The addition of psoralen and irradiation was repeated four times in total. Tissue plates were kept on a metal plate on ice during the irradiation. During irradiation it was important to remove the plastic cover of the 24 well plates. Then, samples were transferred to reaction tubes and subjected to further DNA workup. For this the RNA was digested with 2 µl RNAseA (20 mg/ml) for 1 h at 37°C. Afterwards, SDS (final concentration 0.5%) was added together with 2 µl of proteinase K (20 mg/ml stock) and incubated for 1 h at 56°C. The formaldehyde crosslink was reversed by incubation at 65°C overnight or for at least 8 h. DNA was isolated by phenol-chloroform extraction, precipitated with ethanol and resuspended in 50 µl TE buffer.

2.2.8 Digestion and separation of DNA fragments

DNA was digested with restriction enzymes in a 20-30 µl reaction. For good blot quality, about 10-15 µl of DNA should be digested. The restriction enzyme XcmI can cleave cryptic recognition sites if present in excess, so the amount of this enzyme should be well-controlled (0.5 µl of XcmI per sample). Gels (15 cm*20 cm) were casted with 250 ml of agarose TBE solution (with SYBR® Safe) and run in a BioRad gel electrophoresis apparatus. For normal ChEC experiments or exogenous MNase digestion assays, DNA was separated at 100 V in a 1% agarose gel for 6 h. Psoralen-treated samples were separated in a 1% agarose gel (without SYBR® Safe) at 100 V; the gel was run until the bromophenolblue band had just migrated out of the gel. Before blotting, psoralen gels were de-crosslinked on the gel viewer (254 nm). Gels were irradiated twice on each side for 2 min.

2.2.9 Chromatin ImmunoPrecipitation (ChIP)

ChIP was performed mainly as described (Hecht and Grunstein, 1999) in three independent experiments for each protein. Formaldehyde fixed cells from 50 ml of an exponentially growing yeast culture were washed (1 min, 13000 rpm, 4°C) with 1 ml of cold ChIP lysis buffer and suspended in 400 µl of ChIP lysis buffer. EGTA and EDTA in the buffer suppress MNase activity. Glass beads (∅ 0.75-1.0 mm, Roth) were added and cells were disrupted on a VXR basic IKA Vibrax orbital shaker for 45 min with 2000-2200 rpm at 4°C. DNA was sonicated in a volume of 1 ml ChIP lysis buffer using a Branson Sonifier 250 to obtain an average DNA fragment size of 500-1000 bp. Cell debris was removed by centrifugation (20 min, 13000 rpm, 4°C). The chromatin extracts were split into three aliquots. 40 µl of each aliquot served as an input control. 250 µl of each aliquot were incubated for 90 min at 4°C with 1 µg of a monoclonal α-HA antibody (3F10, Roche). Then the lysates were incubated for 90 min at 4°C with 50 µl of Protein G sepharose (Amersham) to enrich the MNase-HA_3-tagged proteins bound by the antibody. After immunoprecipitation, the beads were washed three times with ChIP lysis buffer, twice with ChIP washing buffer I and twice with ChIP washing buffer II followed by a final washing step with TE buffer. 250 µl of buffer IRN were added to the beads (IPs) and to the input samples. DNA was isolated as described for ChEC experiments (see 2.2.6). Both, input and IP DNA were resuspended in 50 µl of TE buffer.
Relative DNA amounts present in input and IP DNA were determined by quantitative PCR using a RotorGene 3000 system (Corbett Life Science) and the comparative analysis software module. Primer pairs used for amplification are listed in 2.1.3B. Input DNA was diluted 1:1000, and IP DNA was diluted 1:200 prior to analysis. Retention of specific DNA-fragments was calculated as the fraction of the total input DNA. The mean values and error bars were derived from three independent ChIP experiments analyzed in triplicate quantitative PCR reactions.

2.2.10 ImmunoFluorescence Microscopy (IFM)

A. Preparation of cells

A culture of yeast cells (5 ml YPD) was crosslinked in exponential growth (final OD_{600} = 0.5). Formaldehyde was added to a final concentration of 4% and cells were fixed for 1 h at

growth temperature while shaking. Spheroblasting of cells was done in 0.1 M potassium phosphate buffer pH 7.5 for 45 min at 30°C using 50 µg/ml zymolyase T100. Fixed spheroblasts were put on poly-L-lysine treated 3-well diagnostic slides (Menzel-Glaeser), blocked with 2% BSA in 1xTBS/0.1%NP40.

B. Immunodetection of proteins

Cells on the slides were treated with the following antibodies in 1xTBS/0.1%BSA: rat anti-tubulin in a dilution of 1:1000 and mouse anti-HA in a dilution of 1:1000. For fluorescence detection the secondary antibodies Alexa Fluor 488 goat anti-rat and Alexa Fluor 594 goat anti-mouse were used in dilutions of 1:500 in 1xTBS/0.1%BSA. DNA–staining was achieved by subsequent treatment with 1 µg/ml DAPI in Moviol-solution (0.1 g/ml Moviol (Hoechst) in 25% Glycerin/0.1 M Tris pH 8.5).
Images were captured with an AxioCam MR CCD camera mounted on an Axiovert 200M Zeiss microscope and processed with Axiovision V 4.7.1.0 and Adobe Photoshop.

2.2.11 Manipulation of *Escherichia coli*

A. Preparation of electrocompetent bacteria

An overnight culture of *E. coli* XL1-Blue in SOB medium (OD_{600} approx. 3) was diluted 1:100 in SOB prewarmed to 37°C; this culture was grown with vigorous aeration at 300 rpm and 37°C for about 3 h, until the OD_{600} reached a value between 0.4 and 0.6. Then, the culture was chilled on ice for 15 min before being centrifuged for 10 min at 1000 rpm and 4°C in a GS3 rotor. Centrifugation was repeated after resuspension of the pellet in 400 ml ice-cold, sterile water and, after that, in 200 ml ice-cold, sterile water. The washed pellet was resuspended in 10 ml cold, sterile 10% (v/v) glycerol, transferred to a Falcon tube, and centrifuged at 2000 rpm and 4°C for 10 min. After resuspension of the pellet in 1.5 ml cold, sterile 10% (v/v) glycerol (about $1–3 \cdot 10^{10}$ cells/ml) 50–100 µl aliquots were stored at –80°C.

B. Transformation by electroporation

The required number of aliquots plus a background control aliquot was thawed on ice and pipetted into a chilled 0.2 cm electroporation cuvette. About 1 ng of a plasmid miniprep or up to 3 µl of a ligation sample were pipetted into the cell drop. Pulsing was performed with

programme EC2 in a micropulser. Immediately after the pulse, 1 ml 37°C LB medium was added and the sample was transferred in a microreaction tube following an incubation step for 30-60 min at 37°C. 100 µl of the supernatant was plated on LB-Amp. The residual cells were spun down for one minute at 5000 rpm in a microfuge. About 800 µl were discarded and the pellet was resuspended in the remaining supernatant, plated onto LB-Amp and incubated overnight at 37°C.

C. Liquid culture

A single colony was picked from a plate or a piece of frozen culture was scratched from the glycerol stock. Cells were transferred into a sterile tube containing 5 ml of LB-Amp (50 µg/ml ampicilline). The culture was incubated at 37°C overnight.

2.2.12 Manipulation of *Saccharomyces cerevisae*

A. Preparation of competent yeast cells

50 ml of an exponentially growing yeast culture was pelleted (2000 rpm, 5 min at room temperature). The pellet was washed at room temperature with 25 ml autoclaved H_2O, then with 5 ml SORB. The pellet was resuspended in 500 µl SORB, transferred to a reaction tube and repelleted. The supernatant was completely removed, the pellet then resuspended in 360 µl SORB. 40 µl of salmon sperm DNA (Invitrogen) was boiled at 95°C for 5 minutes and added to the cell suspension. After mixing, 50 µl aliquots were transferred to fresh reaction tubes and placed at -80°C for storage.

B. Transformation of competent yeast cells

The required number of competent cell aliquots plus a background control was thawed on ice. DNA (2 µg per transformation in about 1 µg/µl concentration) was added to the cells, the sample was mixed. 6 volumes of PEG were added; samples were mixed thoroughly and incubated at room temperature for about 30 minutes. 1/9 of total volume (cells plus DNA plus PEG) of pure, sterile DMSO was added, samples were mixed and heat-shocked at 42°C for about 15 minutes. Temperature-sensitive cells (YCC95) were not heat-shocked at 30°C. Cells were pelleted (2000 rpm, 2 minutes at room temperature in table-top centrifuge), the supernatant completely removed and the pellet resuspended in 1 ml appropriate rich

medium (without antibiotics). Cells were grown at appropriate temperature (30°C for wild-type cells, 24°C for YCC95) for about 2 to 3 hours. After that, cells were pelleted, 9/10 of the supernatant was discarded. The cell pellet was resuspended in the remaining supernatant and plated on selective agar plates. When cells were selected for resistance to Geneticin they were replica-plated to identify positive clones.

C. Liquid culture

Yeast cultures were inoculated with a single colony from plates or with a piece of frozen culture ice from a -80°C glycerol stock. Cultures were grown in the respective medium at optimal growth temperature (24°C for YCC95, 30°C for all others). Precultures were grown in sterile plastic tubes (10 ml tube volume, 4 ml maximal culture volume). Other cultures were grown in glass flasks; the culture volume should not exceed 1/3 of the flask volume.

D. Permanent culture in glycerol

2 ml of a freshly stationary yeast culture were mixed with 1 ml of sterile 50% glycerol and separated to two aliquots. Cells were frozen on dry ice and stored at -80°C.

E. Establishment of MNase fusion strains

For each target gene, a PCR was performed with overhang primers. The primers are composed of a 5’ sequence complementary to the target gene (50 bp immediately before or after the stop codon) and 3’ sequence complementary to pKM9 (S3 and S2 adapter, priming before and after the MNase-HA-KanMX cassette). The PCR was performed with a proofreading enzyme (Herculase); the PCR product was cloned into pBluescript and sequenced. After verification of sequence correctness, the plasmid was prepared with the Midi-prep kit. The insert was excised with restriction enzyme digestion and transformed into competent yeast cells. The KanMX marker was used for selection on Geneticin plates; initial plates wer replica-plated. To screen for positive clones, colonies were stroked out, protein was isolated (denaturing protein isolation) and checked for HA signals of correct size (molecular weight of the protein factor plus 22 kDa for the tag) by Western blot.

2.2.13 Protein-biochemical methods

A. Denaturing protein extraction of yeast cells

About 1 ml (or less, depends on abundance of the desired protein) of an overnight yeast liquid culture was spun down. Cells were resuspended in 1 ml ice-cold water. Samples were chilled on ice and supplemented with 150 µl of pre-treatment solution (1.85 M NaOH, 1M β-mercapto-ethanol) for 15 minutes on ice. Proteins were precipitated with 150 µl 55% trichloro acetic acid for 10 minutes on ice and pelleted (13000 rpm, 10 minutes at 4°C in table-top centrifuge). The supernatant was discarded and the pellet resuspended in 30-50 µl HU-buffer (5% SDS, 200 mM Tris pH 6.8, 1 mM EDTA, 2.13 mM β-mercapto-ethanol, 8 M urea, bromophenolblue; store at -20°C). If colour turns yellow, the pH of the suspension is too acidic and must be neutralized with ammonia gas until the colour turns (dark) blue again. Proteins were denatured for 10 minutes at 65°C while shaking. Insoluble cell particles were pelleted (13000 rpm, 1 min at room temperature). An adequate volume of the supernatant was analyzed by Western blot.

B. SDS-Polyacrylamide gel electrophoresis

Proteins were separated according to molecular weight by vertical, discontinuous SDS-PAGE according to Laemmli (1970). The discontinuous system consisted of a lower separating gel and an upper stacking gel:

separating gel	6%	8%	10%	12.5%	14.5%
H_2O	5.5 ml	4.82 ml	4.2 ml	3.3 ml	2.68 ml
4x Lower Tris	2.5 ml	2.5 ml	2.5 ml	2.5 ml	2.5 ml
30% Acrylamide (AA) + 0.8% Bis-AA	2.0 ml	2.68 ml	3.3 ml	4.2 ml	4.82 ml
10% SDS	100 µl				
TEMED	5 µl				
25% APS	50 µl				

stacking gel	6%	4%
H_2O	2.75 ml	3.05
4x Upper Tris	1.25 ml	1.25
30% AA + 0.8% bAA	1.00 ml	0.65
10% SDS	50 µl	
TEMED	5 µl	
25% APS	25 µl	

Pre-stained marker (NEB) was used as a molecular weight marker. The bands were stained blue so they were visible in the gel and on the membrane. Gels were run at 140 V for 1.5 h or until the bromophenolblue band reached the lower border of the gel.

C. Western blot

After SDS-PAGE, the proteins were associated with SDS and therefore negatively charged. They were blotted by semi-dry transfer from the gel to a PVDF-membrane by the electric current (BIORAD semi-dry transfer apparatus). Three layers of thin Whatman paper were soaked in blotting buffer (25 mM Tris, 190 mM glycine, 20% methanol, pH 8.3) and piled on the lower electrode (anode) of the semi-transfer device. The membrane (Immobilon PSQ 0.2 µm, Millipore) was first soaked in methanol, then in blotting buffer. It was put onto the pile of Whatman papers, air bubbles were carefully removed as they prevent the flow of the electric current. The membrane must be kept wet (with blotting buffer) all the time. The gel apparatus was disassembled, the gel was transferred onto the membrane. Air bubbles were removed and the gel was covered with three more layers of soaked Whatman paper. The blot was run at 24 V for 1.5 h. After blotting, the marker bands should be marked with a pen.

D. Ponceau staining

Western blots can be stained with Ponceau (0.5% Ponceau in 1% acetic acid) to control if all proteins were transferred properly. Staining was performed for one to three minutes at room temperature in a tray. Afterwards, the membrane was washed with water.

E. Detection of proteins by chemiluminescence

The membrane was blocked with blocking solution (5% milk powder in 1x PBST) to prevent unspecific binding of the antibody. Blocking was performed in a tray for 1 h at room temperature or overnight at 4°C while shaking. The membrane was wrapped into a 50 ml falcon tube containing the first antibody dilution (appropriate dilution in 1x PBST with 5% milk powder, 3 ml for large membrane) and rotated at room temperature for 1 h. After three five-minute washes with 1x PBST in a tray, the membrane was wrapped into a 50 ml falcon tube with the second antibody (appropriate dilution in 1x PBST with 5% milk powder, 3 ml for large membrane) and rotated at room temperature for half an hour. The membrane was washed three times for five minutes with 1x PBST. The secondary antibody was coupled to

horseradish peroxidase (POD) which catalyzes the oxidation of diacylhydrazides via an activated intermediate that decays to the ground state by emission of light in the visible range. The membrane was put between the two sheets of a thin plastic bag (ROTH) and covered with a liquid film of reaction substrates (BM chemiluminescence blotting substrate (POD), ROCHE). The position of the PSM bands was marked with a fluorescent pen. Detection followed immediately after addition of the substrate in a LAS-3000 fluorescence reader (FUJIFILM).

F. Quantification of Western blots with Multi Gauge

For quantitative analysis of Western blot signals the profile quantitation module of the *MultiGauge 3.0* (Fujifilm) software was used. After background subtraction signal intensities of the individual peaks were obtained by computing the integral of the peak area.

3 Results

3.1 UAF influences long-range chromatin structure at the RNA polymerase I-transcribed 35S coding region of the rDNA locus

To investigate the influence of UAF on rDNA chromatin structure *in vivo* the accessibility of Micrococcal nuclease (MNase) to the rDNA was analyzed in different UAF deletion strains. In addition, the effect of deletions in other Pol I transcription factors or of Pol I subunits on rDNA chromatin structure was examined. In these mutant strains Pol I transcription is strongly reduced or even completely abolished. To exclude that the observed effects on chromatin structure were caused by altered Pol I transcription, the establishment of alternative rDNA chromatin structures after disruption of Pol I transcription was also analyzed.

Nuclei are isolated from formaldehyde-crosslinked yeast cells and the chromatin is digested with rising amounts of MNase. This enzyme introduces DNA double-strand breaks in chromatin at nucleosomal linker regions and at nuclease hypersensitive (HS) sites (Telford et al., 1989). After DNA isolation, the DNA is digested with the restriction enzyme XcmI that cuts the rDNA within the IGS2 and the 25S rRNA gene resulting in two fragments (Fig. 3-1). The fragments are separated in a 1% agarose gel and transferred onto a nylon membrane by Southern blotting. Using the indirect end-labeling technique the rDNA fragments produced by the MNase cleavage activity can be directly visualized. By hybridization of the membranes with probe rDNp a 4.9 kb fragment encompassing the rDNA promoter and 35S coding region is detected. With probe IGS2 a 4.3 kb fragment of IGS1 and IGS2 flanking the 5S rRNA gene is visualized (Fig. 3-1).

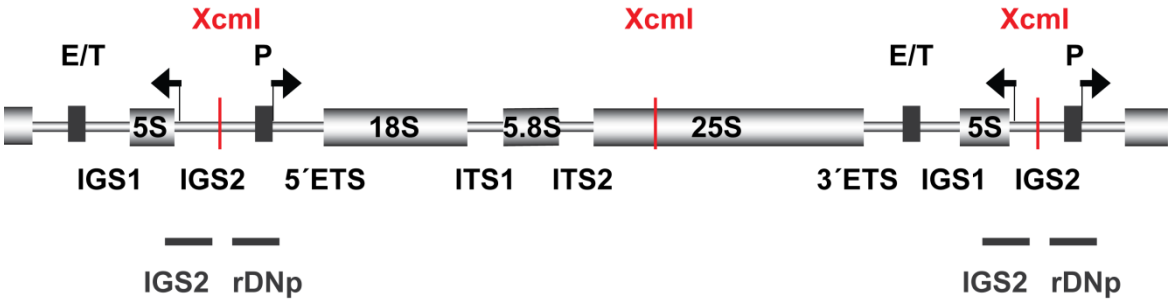

Fig. 3-1 The rDNA locus including XcmI restriction sites and probes used for indirect end-labeling
Schematic representation of the yeast rDNA locus including promoter (P) and enhancer/terminator (E/T) elements as well as the intergenic spacer regions (IGS), the external transcribed spacers (ETS) and the internal transcribed spacers (ITS). The XcmI restriction sites are depicted in red, Southern probes used for indirect end-labeling analysis are indicated below as grey bars.

3.1.1 The wild-type strain NOY505 displays MNase pattern similar to naked DNA

First, the rDNA chromatin structure was analyzed in a wild-type strain and compared to non-crosslinked rDNA to confirm and extend initial experiments performed by Katharina Merz during her PhD thesis (Merz, 2007).

The 35S rRNA genes in a wild-type yeast cell coexist in two different chromatin states depending on the transcriptional activity of the gene. Actively transcribed rDNA repeats are nucleosome-free whereas the inactive copies are assembled into nucleosomes. This heterogeneity in chromatin structure is reflected in the different MNase accessibilities of the two rDNA populations.

The MNase cleavage pattern of rDNA from a wild-type strain (NOY505) was analyzed in comparison to naked DNA (nDNA) digested with rising amounts of the enzyme (Fig. 3-2). DNA was isolated and investigated by Southern blotting. The results obtained by hybridizing the blots with probe rDNp detecting the rDNA promoter region or probe IGS2 visualizing the 5S rRNA gene and the 3´end of the 35S rRNA gene are reported in Figure 3-2A. A profile analysis of the digestion pattern is shown in Figure 3-2B.

The MNase cleavage pattern within the 35S rRNA coding region of the wild-type strain was similar to that observed for naked rDNA after treatment with MNase (Fig. 3-2A, left panel, compare lanes 1-5 with 6-10; see Fig. 3-2B, upper panel for a profile analysis of lanes 4 and 9 in Fig. 3-2A). This is consistent with the interpretation that in a wild-type yeast cell a large fraction of the rDNA is devoid of histone molecules (Merz et al., 2008), whereas the remainder is assembled into randomly positioned nucleosomes.

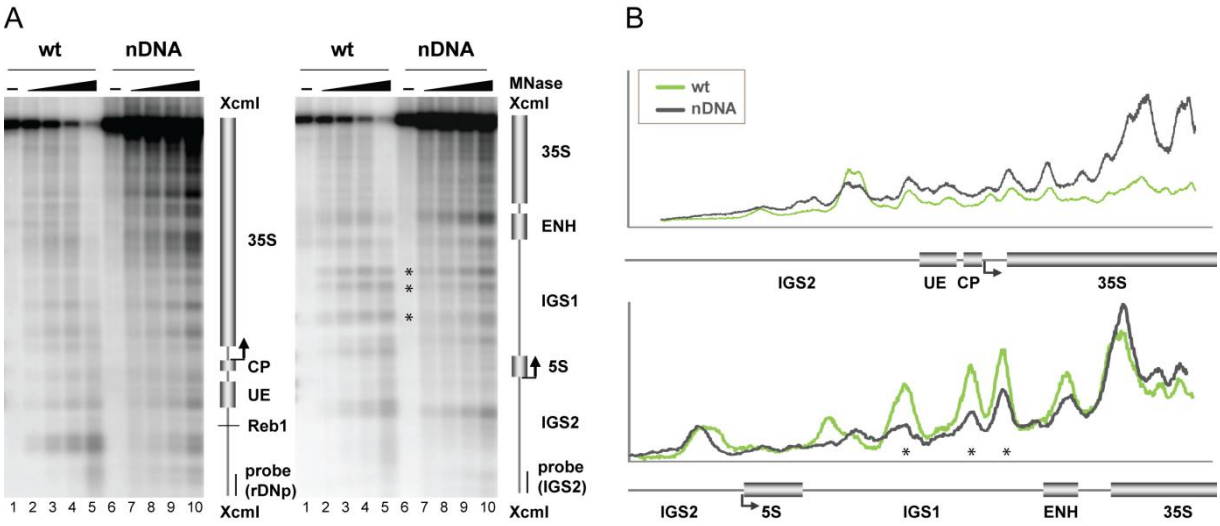

Fig. 3-2 MNase digestion pattern of crosslinked DNA is similar to naked DNA
(A) Wild-type yeast cells (NOY505, wt) were cultured to exponential phase in YPD at 30°C before formaldehyde crosslinking and preparation of nuclei. Isolated nuclei or purified yeast genomic DNA (nDNA) were treated with MNase. Isolated nuclei were incubated for 20 min at 37°C in the absence (-) or presence of 0.05, 0.15. 0.3, 1 units (U) of MNase. Yeast genomic DNA was incubated for 20 min at 37°C in the absence (-) or presence of 0.125, 0.375, 0.75, 2.5 mU MNase. DNA was isolated, digested with XcmI, separated in a 1% agarose gel, and analyzed in a Southern blot by indirect end-labeling with probe rDNp visualizing a 4.9-kb fragment of promoter and coding region of the 35S rRNA gene or with probe IGS2 detecting a 4.3-kb fragment of IGS1 and IGS2 flanking the 5S rRNA gene and the 3´end of the 35S rRNA gene. Data were collected using a FLA-5000 imaging system (FujiFilm). Cartoons of the genomic regions including important features as described in the legend of Fig. 1-2, as well as the positions of the probes used for indirect end-labeling are depicted on the right. (B) Profiles of DNA-fragment patterns obtained after digestion with 0.3 units MNase for nuclei and 0.75 mU MNase for nDNA. FLA-5000 data presented in (A) were analyzed with the MultiGauge software (FujiFilm). The signal intensity in the respective lanes was plotted against the distance of migration in the gel. Signal intensities of MNase profiles compared in one graph were normalized to the leftmost peak. Cartoons of the genomic regions including important features as described in the legend of Fig. 1-2 are indicated below the graphs.

For the intergenic spacer regions differences in MNase accessibility were observed (Fig. 3-2A, right panel, compare lanes 1-5 with 6-10; see Fig. 3-2B, lower panel, for a profile analysis of lanes 4 and 9 in Fig. 3-2B). The protection against the enzymatic cuts was altered within IGS1 in the wild-type strain compared to naked rDNA, resulting in a more distinct band pattern for the crosslinked rDNA (Figs. 3-2A and 3-2B, asterisk). Psoralen crosslinking analysis showed that the ribosomal spacer regions are in principle organized in nucleosomal structures (Dammann et al., 1993). Later studies revealed the existence of five well-positioned nucleosomes within IGS1, and implicated a nucleosomal arrangement for IGS2 (Vogelauer et al., 1998). Thus nucleomal protection might explain the differences between the digestion pattern of IGS2 chromatin in the wild-type strain and the naked rDNA.

3.1.2 The carbon source does not influence MNase accessibility in the 35S coding region

The yeast strains analyzed in this study were originally isolated as mutants defective in the transcription of 35S rRNA genes by RNA polymerase I. The strains carry a multicopy plasmid, pNOY103, containing the 35S rDNA under the control of the GAL7 promoter which is transcribed by RNA polymerase II. Therefore growth of the mutant strains NOY558 (*rrn7Δ*), NOY408-1a (*rpa135Δ*) and NOY604 (*rrn3Δ*) depends on the presence of galactose in the medium. The strain NOY699 (*rrn5Δ*) is a PSW strain transcribing chromosomal rDNA by RNA polymerase II and can grow in the absence of galactose. The strains NOY505 (wt) and yR47 (*uaf30Δ*) can also be grown in glucose medium.

Earlier studies demonstrated that the MNase accessibility within the IGS2 region of rDNA differed with respect to growth conditions (Vogelauer et al., 1998). To test the influence of the carbon source on the rDNA chromatin structure within the transcribed region, the strain NOY505 was cultured in YPD and YPG. Exponentially growing cells from each culture were crosslinked with formaldehyde, nuclei were prepared and the DNA was digested with rising amounts of MNase. The cleavage pattern for the GAL gene locus and rDNA ORF and IGS regions were analyzed in Southern Blot (Fig. 3-3).

Hybridization of the blot with the GAL1 probe revealed a nucleosomal digestion pattern in YPD for the *GAL1*, *GAL10*, and *GAL7* genes being repressed and presumably fully assembled into nucleosomes under these growth conditions (Fig. 3-3, left panel, lanes 1-5). Upon transcriptional activation in galactose the GAL gene locus displayed an altered MNase pattern (Fig. 3-3, left panel, lanes 6-10). This is in good agreement with ealier observations (Lohr, 1984; Lohr and Hopper, 1985). In contrast, the rDNA promoter as well as the 5S and IGS regions did not show any differences in MNase accessibility with respect to the different carbon sources (Fig. 3-3, middle and right panels, compare lanes 1-5 with 6-10).

Although the carbon source did not influence the MNase accessibility in this experiment, for the following analyses all strains were grown in galactose medium to ascertain the comparability of the results.

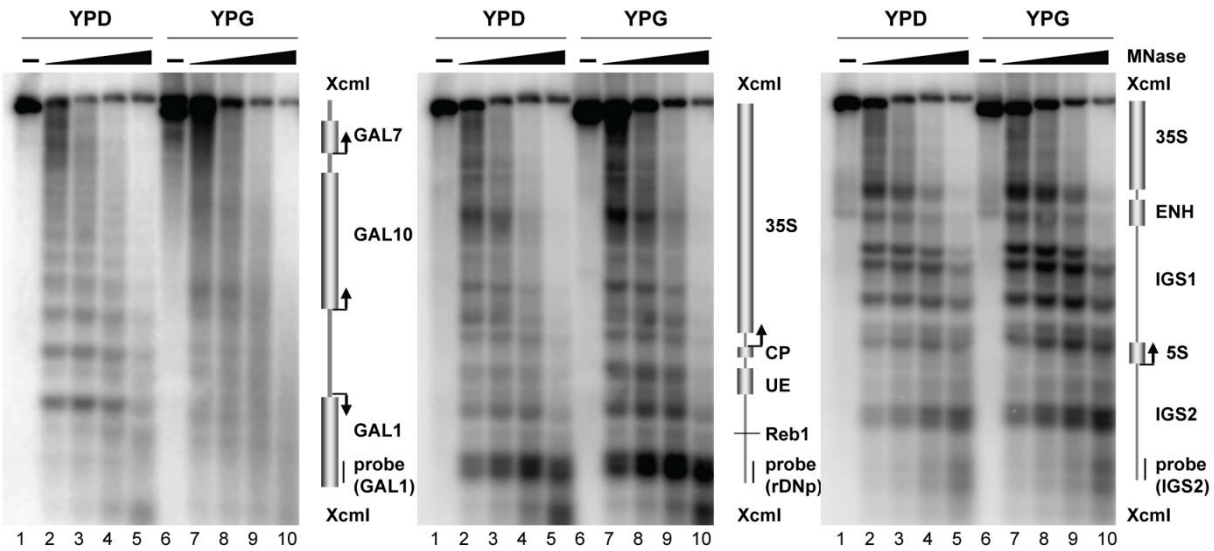

Fig. 3-3 MNase digestion of rDNA chromatin in YPD and YPG
Wild-type yeast (NOY505) were cultured to exponential phase in YPD or YPG at 30°C. After formaldehyde cross-linking, isolated nuclei were incubated for 20 min at 37°C in the absence (-) or presence of 0.25, 0.5, 1, 2 units of MNase. DNA was isolated, digested with XcmI, separated in 1% agarose gel, and analyzed in a Southern blot by indirect end-labeling with probes visualizing either a 6.8-kb fragment containing the *GAL* gene locus (GAL1), a 4.9-kb fragment of promoter and coding region of the 35S rRNA gene (rDNp), or a 4.3-kb fragment of IGS1 and IGS2 flanking the 5S rRNA gene and the 3´end of the 35S rRNA gene (IGS2). Data were collected using a FLA-5000 imaging system (FujiFilm). Cartoons of the genomic regions including important features as described in the legend of Fig. 1-2, as well as the probes used for indirect end-labeling are depicted on the right.

3.1.3 Deletion of UAF subunits or components of the basal Pol I transcription machinery leads to drastic changes in chromatin structure at the 35S rDNA locus

In order to examine if there are detectable changes in rDNA chromatin structure when UAF complex formation is impaired, the MNase accessibility of 35S rDNA chromatin from two different UAF deletion strains was analyzed in comparison to the reference wild-type strain. The *rrn5Δ* strain is a PSW strain using RNA polymerase II for transcription of chromosomal rDNA (Oakes et al., 1999; Vu et al., 1999). In the mutant strain lacking the Uaf30 subunit of UAF (*uaf30Δ)* both polymerases Pol I and Pol II have been demonstrated to transcribe the rDNA (Siddiqi et al., 2001).

Nuclei from formaldehyde-crosslinked yeast cells were prepared and incubated with rising amounts of MNase. DNA was isolated and investigated by Southern blotting. The results obtained by hybridizing the blots with a probe detecting the rDNA promoter region are reported in Figure 3-4A. A profile analysis of the digestion pattern is shown in Figure 3-4B.

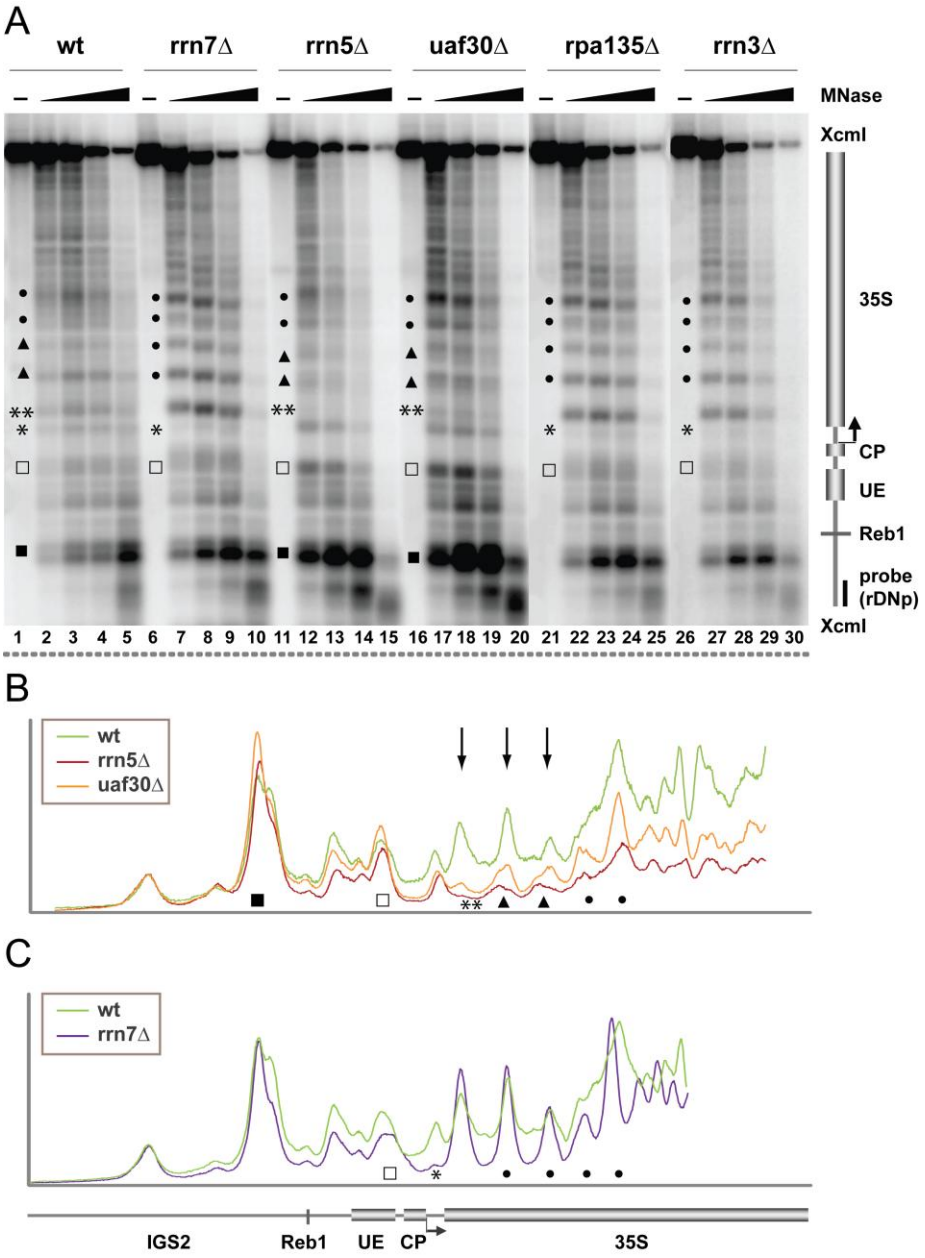

Fig. 3-4 UAF influences long-range chromatin structure at the RNA Pol I-transcribed 35S coding region of the rDNA locus

(A) Wild-type yeast (NOY505, wt), or mutant (NOY408-1a, NOY558, NOY604, NOY699, y1120) strains deleted in the genes indicated above the respective lanes were cultured to exponential phase in YPG at 30°C. After formaldehyde crosslinking, isolated nuclei were incubated for 20 min at 37°C in the absence (-) or presence of 0.05, 0.15, 0.3 and 1 units of MNase. DNA was isolated, digested with XcmI, separated in a 1% agarose gel, and analyzed in a Southern blot by indirect end-labeling with probe rDNp visualizing a 4.9-kb fragment of promoter and coding region of the 35S rRNA gene. Data were collected using a FLA-5000 imaging system (FujiFilm). Different symbols highlight changes in MNase accessibility and are referred to in the text. A cartoon of the genomic region including important features as described in the legend of Fig. 1-2, as well as the probe used for indirect end-labeling are depicted on the right. (B-C) Profiles of DNA-fragment patterns obtained after digestion with 0.3 Units MNase of the samples indicated in the legend of each graph. FLA-5000 data presented in (A) were analyzed with the MultiGauge software (FujiFilm). The signal intensity in the respective lanes was plotted against the distance of migration in the gel. Signal intensities of MNase profiles compared in one graph were normalized to the leftmost peak. Different symbols highlight changes in MNase accessibility as described above (A). A cartoon of the genomic region including important features as described in the legend of Fig. 1-2 is indicated below the graphs.

Significant differences in chromatin digestion profiles for the 35S transcribed region of the rDNA locus were observed in the mutant strains (Fig. 3-4A, compare lanes 1-5 with 11-20; see Fig 3-4B for a profile analysis of lanes 4, 14 and 19 in Fig. 3-4A). The deletion of either UAF subunit lead to a decrease in protection against MNase digestion around the Reb1 binding site upstream of the promoter (Figs. 3-4A and 3-4B, black squares) and within the upstream element (Figs. 3-4A and 3-4B, blank squares). This suggests that UAF limits the access of the MNase to these regions in the wild-type strain. The structural changes observed for the promoter region extended to the 35S coding region, revealing a more regular and distinct cleavage pattern in rDNA of the UAF deletion mutants compared to the MNase cleavage pattern in 35S rDNA of the wild-type strain. Whereas some 35S rDNA regions were more protected in the *uaf* deletion strains (Figs. 3-4A and 3-4B, double asterisk), others became more susceptible to the enzymatic cleavages (Figs. 3-4A and 3-4B, black dots). For two cleavage sites a clear shift towards the rDNA promoter region was detected (Figs. 3-4A and 3-4B, black triangles).

The observed alterations in MNase accessibility were more pronounced in the *rrn5Δ* strain. In this PSW strain rRNA genes are exclusively transcribed by Pol II (Vu et al., 1999). The digestion pattern of the *uaf30Δ* mutant showed some reminiscent of 35S rDNA digestion pattern in the wild-type (Fig. 3-4B, arrows). This is consistent with a heterogeneous population of Pol I- and Pol II-transcribed rDNA chromatin states in this strain (Siddiqi et al., 2001).

To examine how the deletion of other PIC components influences rDNA chromatin structure, MNase profiles were analyzed for three other strains that carry mutations in essential CF or Pol I subunit genes. In the strains NOY558, lacking the Rrn7 subunit of the CF complex, NOY408-1a, lacking the Rpa135 subunit of the RNA polymerase I and NOY604, lacking Rrn3, the Pol I transcription of chromosomal rDNA is abolished. As already described above, these mutants are only viable in the presence of galactose because the rDNA locus is transcribed from a multicopy plasmid containing the 35S rDNA under the control of the GAL7 promoter (Nogi et al., 1991).

The rDNA accessibility for MNase was nearly identical in all three mutant strains but different from rDNA accessibility for MNase in the wild-type strain, or in the UAF deletion mutants (Fig. 3-4A, compare lanes 6-10 and 21-30 with lanes 1-5 and 11-20; see Fig. 3-4C for a profile analysis of lanes 4 and 9 in Fig. 3-4A). The strong loss of protection at the Reb1

binding site and within the upstream element observed for the UAF mutant strains was not detectable in strains with deletions in CF or Pol I subunits. The UAF complex is still bound to the promoter in these mutants ((Bordi et al., 2001), and Fig. 3-19) suggesting that this interaction is important for maintenance of promoter architecture and for the restricted access of the enzyme to these regions. A broad smear was observed at the transcription initiation site in the *rrn7Δ*, *rrn3Δ*, and *rpa135Δ* strains, whereas a more distinct cut occurred at the same rDNA position in the wild-type strain and UAF deletion mutants (Figs. 3-4A and 3-4C, blank squares, asterisk). The chromatin within the 35S open reading frame showed a clear regularly spaced pattern in the strains deficient in Pol I transcription (Figs. 3-4A and 3-4C, black dots). This could indicate protection by translationally phased nucleosomes in the *rrn7Δ*, *rrn3Δ*, and *rpa135Δ* strains.

As a control, the same blots were hybridized with probe IGS2 detecting the 5S rDNA and intergenic spacer regions (Fig. 3-5). No significant differences in MNase digestion profiles were detected for any of the strains within the main part of this region (Fig. 3-5A, compare lanes 1-5 with 6-30; see Fig. 3-5B for a profile analysis of lanes 4, 9, 14 and 19 in Fig. 3-5A). The same result has already been reported for MNase accessibilities within IGS2 in the *rrn7Δ* and *rrn5Δ* strains (Vogelauer et al., 1998). Accordingly, only slight changes in MNase digestion patterns were detected upstream of the 5S rRNA gene and within the rDNA enhancer region. Within the IGS2 the MNase accessibility in the mutant strains was diminished at one specific site compared to the wild-type strain (Fig. 3-5A, compare lanes 1-5 with 6-30, black squares; see see Fig. 3-5B for a profile analysis of lanes 4, 9, 14 and 19 in Fig. 3-5A). In addition, a slight band shift and alteration in signal intensity is detected particularly in the UAF deletion strains within the rDNA enhancer region (Fig. 3-5A, compare lanes 1-5 with 6-30, black triangles; see see Fig. 3-5B for a profile analysis of lanes 4, 9, 14 and 19 in Fig. 3-5A). Thus, the observed differences in the accessibility of rDNA chromatin in the respective genetic backgrounds are largely confined to the Pol I-transcribed region. The 35S rDNA displays characteristic differences in MNase accessibilities, depending on the presence of UAF and correlating with the transcriptional state of 35S rRNA genes.

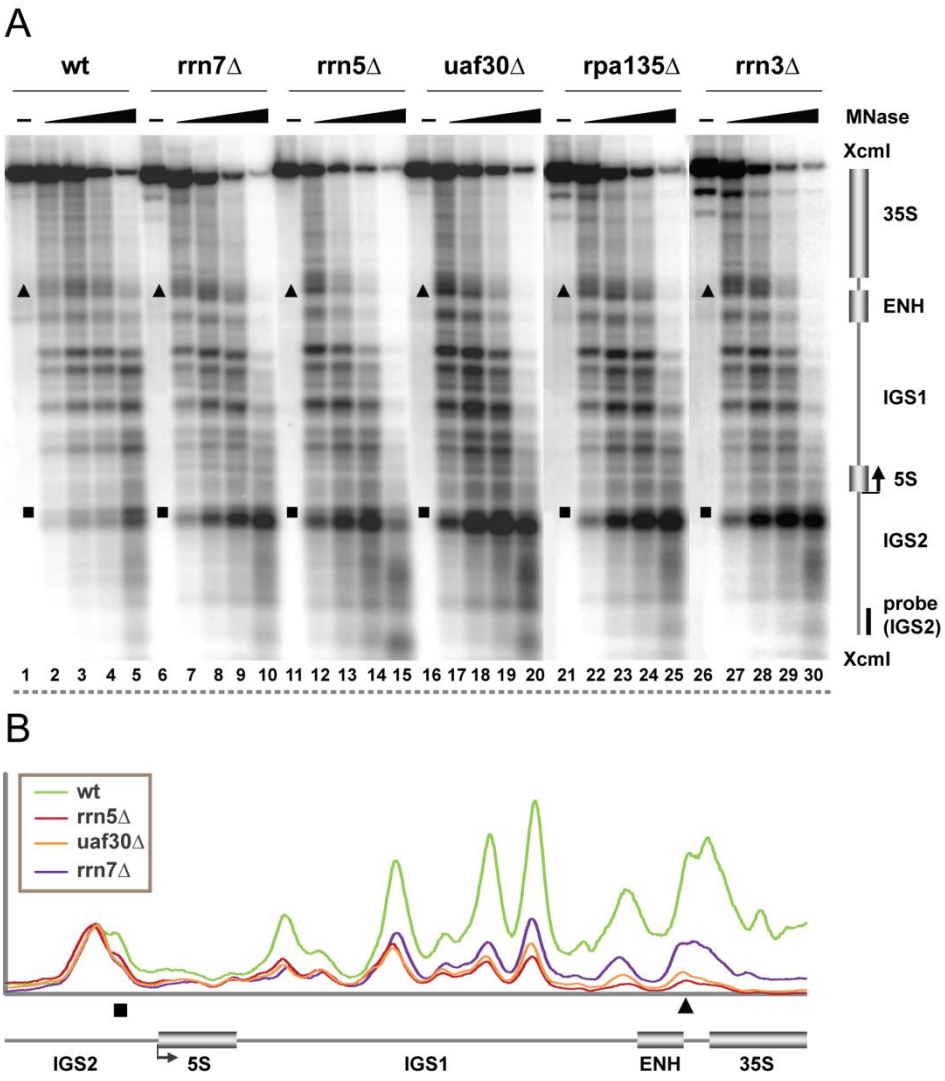

Fig. 3-5 Chromatin structure at the IGS is not affected in any of the mutant strains
(A) The identical membranes as in Fig. 3-4A were analyzed in Southern blot with probe IGS2 visualizing a 4.3-kb fragment of IGS1 and IGS2 flanking the 5S rRNA gene and the 3´end of the 35S rRNA gene. Data were collected using a FLA-5000 imaging system (FujiFilm). Symbols highlight changes in MNase accessibility and are referred to in the text. A cartoon of the genomic region including important features as described in the legend of Fig. 1-2, as well as the probe used for indirect end-labeling is depicted on the right. (B) Profiles of DNA-fragment patterns obtained after digestion with 0.3 Units MNase of the samples indicated in the legend of each graph. FLA-5000 data presented in (A) were analyzed as described in the legend to Fig. 3-4.

3.1.4 Inhibition of Pol I transcription does not alter MNase accessibility of the 35S rDNA

The transcription of rDNA by Pol I is strongly impaired or even completely abolished in the mutant strains analyzed above. To investigate, whether the disruption of RNA polymerase I transcription at the rDNA locus already is sufficient to establish alternative rDNA chromatin structures, MNase digestion patterns of a strain carrying a temperature-sensitive allele of the Pol I-specific transcription initiation factor Rrn3 (*rrn3-ts*) and the isogenic wild-type strain

(*RRN3*) were compared (Fig. 3-6 and PhD thesis Katharina Merz). The *rrn3-ts* strain supports rDNA transcription at 24°C while incubation at 37°C leads to transcriptional shutdown and dissociation of Pol I from the rRNA gene (Cadwell et al., 1997). UAF and CF remain bound to the rDNA promoter region after the temperature shift (Fig. 3-18 and PhD thesis Katharina Merz). Cells were grown at 24°C overnight. The RRN3 wild-type strain was incubated for 2 hours at 37°C before formaldehyde crosslinking. The *rrn3-ts* strain was split into two aliquots. Half of the culture was treated with formaldehyde, harvested and stored, whereas the other half was incubated for another 2 hours at 37°C before formaldehyde crosslinking. After preparation of nuclei and MNase digestion DNA was isolated and analyzed in Southern blot as described above. The results obtained by hybridizing the blots with probes detecting the rDNA promoter and IGS regions are reported in Figure 3-6A. Profile analyses of the digestion patterns are shown in Figure 3-6B.

There were no significant differences in 35S rDNA cleavage pattern detectable when comparing the results obtained for the *rrn3-ts* strain cultured at 24°C or 37°C with results obtained for the *RRN3* wild-type strain cultured at 37°C (Fig. 3-6A, upper panel, compare lanes 6-15 with 1-5, see Fig. 3-6B, upper panel, for a profile analysis of lanes 4, 9 and 14 in Fig. 3-6A). Hybridization of the same membrane with probe IGS2 detecting the 5S and intergenic spacer regions also did not reveal any differences in MNase digestion profiles for the different strains (Figs. 3-6A and 3-6B, lower panels).

Thus, the rDNA chromatin state established when 35S rRNA genes are actively transcribed by Pol I seems to remain stable even after Pol I has left the locus (Fig. 3-22). Consequently, the absence of Pol I is not sufficient for a reorganization of rDNA chromatin and additional cellular mechanisms might be required to alter rDNA chromatin structure. Accordingly, the changes in MNase accessibility observed for the *uaf* deletion strains are not a direct consequence of impaired Pol I transcription.

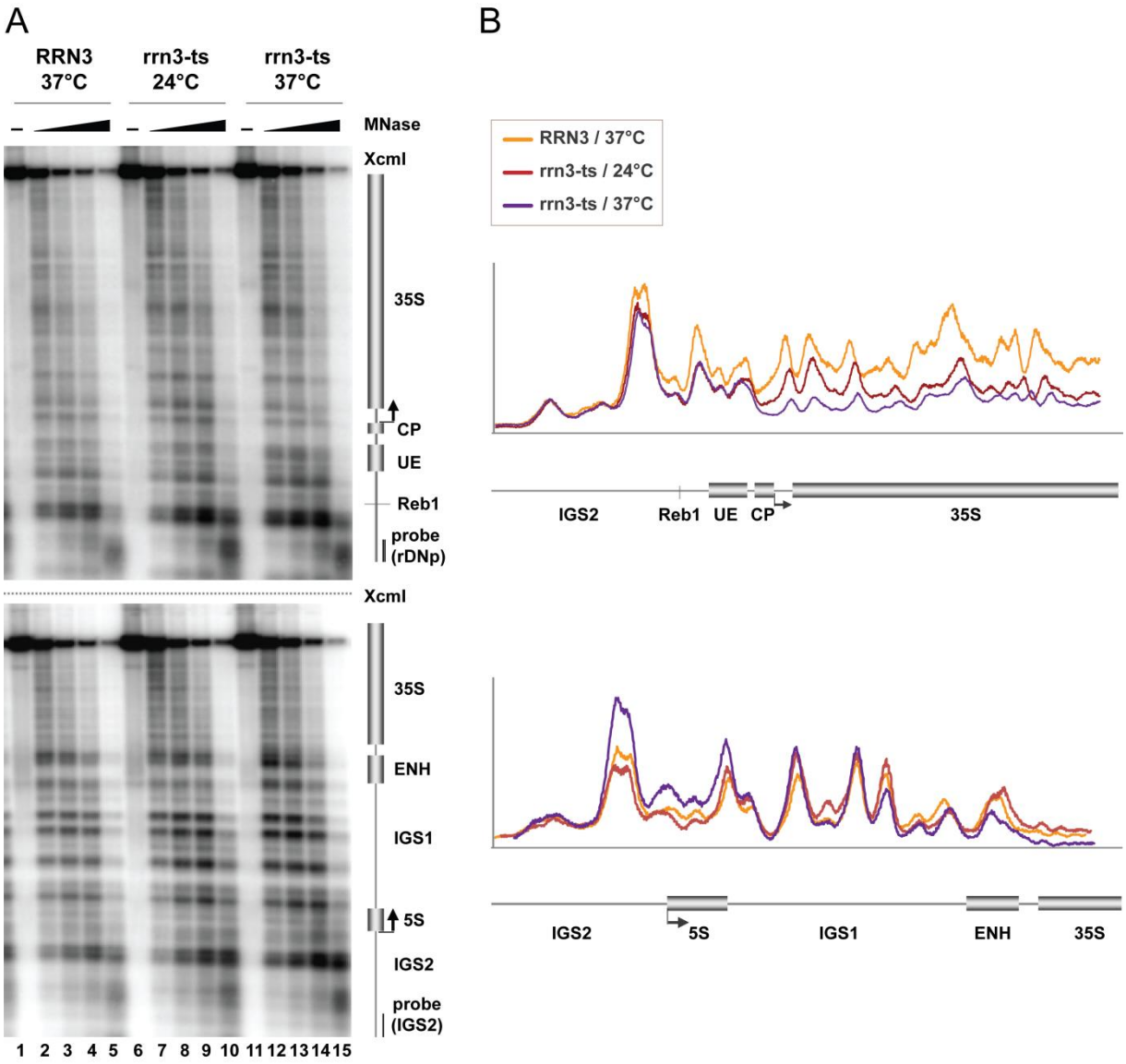

Fig. 3-6 Pol I shutdown is not sufficient to establish an alternative rDNA chromatin structure

(A) Yeast cells carrying a wild-type RRN3 locus (CG379), or a temperature sensitive allele rrn3-ts (Ycc95) were cultured at 24°C in YPD. Cells were split and either fixed with formaldehyde or further incubated in YPD at 37°C for another 120 minutes before formaldehyde crosslinking. Isolated nuclei were incubated for 20 min at 37°C in the absence (-) or presence of 0.05, 0.15, 0.3 and 1 units of MNase. DNA was purified and analyzed as described in the legend to Fig. 3-4 (upper panel). In addition the membrane was analyzed in Southern blot with probe IGS2 visualizing a 4.3-kb fragment of IGS1 and IGS2 flanking the 5S rRNA gene and the 3´end of the 35S rRNA gene (lower panel). Cartoons of the genomic regions including important features as described in the legend of Fig. 1-2, as well as the probes used for indirect end-labeling are depicted on the right (B) Profiles of DNA-fragment patterns obtained after digestion with 0.3 Units MNase of the samples indicated in the legend of each graph. FLA-5000 data presented in (A) were analyzed with the MultiGauge software (FujiFilm). The signal intensity in the respective lanes was plotted against the distance of migration in the gel. Signal intensities of MNase profiles compared in one graph were normalized to the leftmost peak. A cartoon of the genomic region is indicated below the graphs.

3.2 Establishment and characterization of a yeast strain library expressing MNase fusion proteins in UAF30 wild-type and *uaf30Δ* strains

As outlined above, chromatin structure at the Pol I-transcribed rDNA locus is strongly dependent on the presence of UAF at the rDNA promoter region. To gain more insight into the organization of rDNA chromatin with respect to UAF binding, the association of a large set of rDNA chromatin components or factors involved in Pol I transcritpion was analyzed in UAF deletion mutants by Chromatin Endogenous Cleavage (ChEC) (Schmid et al., 2004). In order to apply this technique, genomic loci of the set of selected genes were manipulated to express the respective factors as fusion proteins with a C-terminal micrococcal nuclease (MNase). A schematic overview of a ChEC experiment is presented in Figure 3-7.

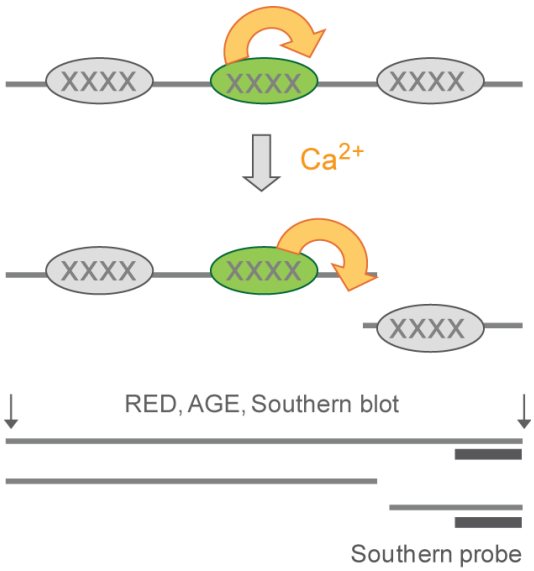

Fig. 3-7
Schematic representation of a ChEC experiment
Exponentially growing yeast cells expressing a MNase fusion protein (MNase in orange) are treated with formaldehyde, crosslinking the proteins to the DNA (crosses). Nuclei are prepared and the MNase is activated by the addition of calcium. The DNA is cut in the proximity of the binding site of the MNase fusion protein. The reaction is stopped by the addition of EDTA. DNA is isolated and linearized with restriction enzymes (RED, arrows). After agarose gel electrophoresis (AGE), the DNA is transferred to a nylon membrane by Southern blotting. For Southern blot analysis a probe is chosen binding directly upstream of the restriction site. Cleavage events mediated by the MNase fusion proteins are detected by indirect end-labeling (probes are indicated as grey bars).

The ChEC method allows the precise localization of specific factors at the DNA (Schmid *et al.*, 2004). A prerequisite for ChEC is a low intracellular Ca^{2+} concentration (in yeast cells and nuclei: 50-200 nM), as MNase activity is strictly dependent on the presence of calcium ions (Telford and Stewart, 1989 and references therein). The cells expressing the MNase fusion proteins are treated with formaldehyde, crosslinking the proteins to their respective DNA binding sites. Nuclei are isolated and calcium is added to a final concentration of 2 mM, which activates the endonuclease activity of the fusion protein. The MNase cuts the DNA in the proximity of the protein binding site (at maximum 100-200 bp from binding site). The reaction is stopped by the addition of the calcium chelating reagent EDTA, the DNA is

isolated and linearized with restriction enzymes. The restriction fragments are separated by agarose gel electrophoresis. The DNA is transferred to a nylon membrane and indirect end-labeling analysis allows the precise localization of cleavage sites mediated by the MNase fusion proteins (see also Fig. 3-1).

Besides the MNase, a 3xHA tag is fused to the protein. This allows to control the correct expression of the protein by Western blot analysis, as well as to verify subcellular localization by ImmunoFluorescence Microscopy (IFM). In addition strain identity was confirmed by PCR-based genotyping after each ChEC experiment.

The chromatin structure of the *uaf30Δ* closely resembles those of a full PSW strain (Figs. 3-4A and 3-4B; Fig. 3-13). This strain displayed a relatively mild growth defect (doubling time of 210 min in YPD), when compared to the PSW strains (doubling time of 7 h in YPD). Furthermore, the copy number of rDNA repeats was increased at most by a factor of 1.5 in all of the *uaf30Δ* strains analyzed in this study, compared to a 2- to 4-fold increase in repeat copy number in the PSW strains. In addition, MNase tagging of proteins in the PSW strains often failed while the UAF30 knockout could be established in all the MNase strains without difficulties. Therefore most of the subsequent analyses were performed in the *uaf30Δ* mutant.

3.2.1 Expression of histone MNase fusion proteins in the UAF30 deletion strain

Since we wanted to compare and interprete cleavage efficiencies of MNase fusion proteins in different genetic backgrounds it was important to analyze the expression levels of the different MNase tagged factors in the *uaf30Δ* strain compared to expression levels in the respective UAF30 wild-type strain. As mentioned above, this is possible due to the 3xHA tag at the C-terminus of the fusion proteins.

First, the expression of the MNase fusion proteins of the histones H2B, H4, and H2A was monitored in both wild-type and *uaf30Δ* strains. Proteins were extracted from one OD cells of each strain and the same volumina were separated by SDS-PAGE in a 10% acrylamide gel. After blotting to a PVDF membrane the MNase fusion proteins were detected by Western blot analysis using an antibody directed against the HA-eptiope. Antibodies directed against the Pol I subunit Rpa135 and against the ribosomal protein rpS8 served as a loading control.

Signal intensities obtained from all three antibodies were determined with the MultiGauge software (FujiFilm) and results are shown in Fig. 3-8.

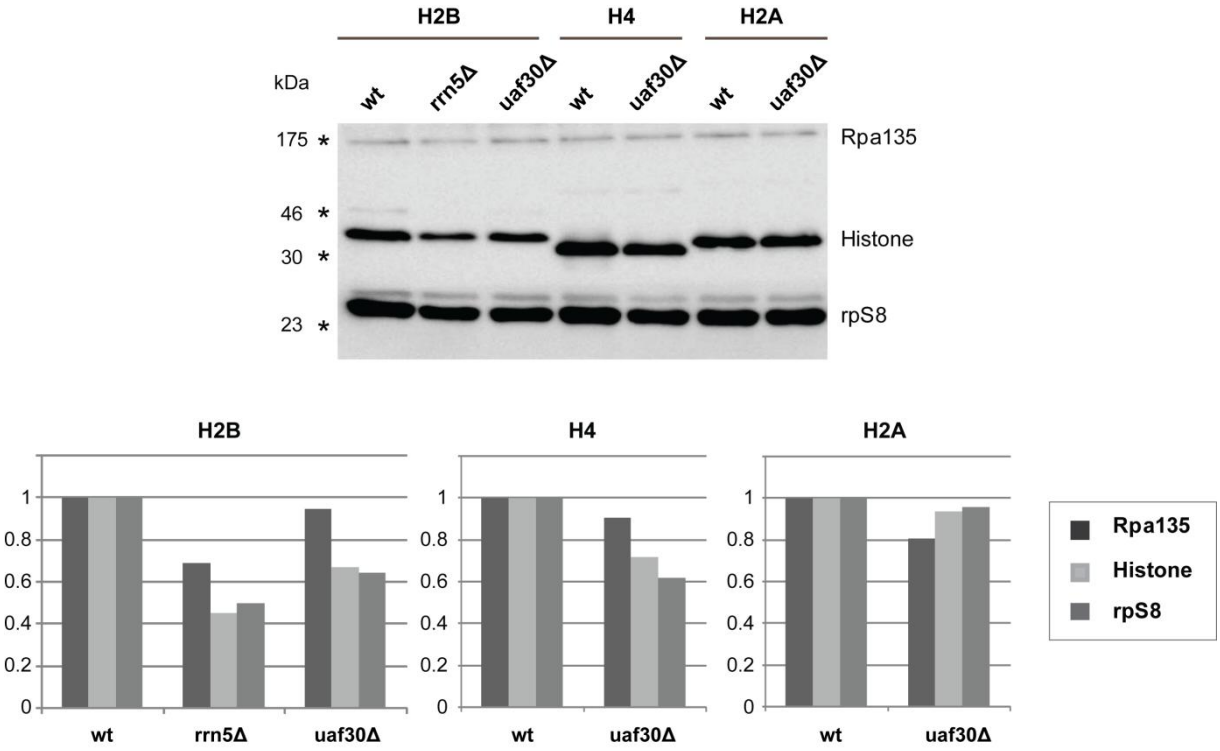

Fig. 3-8 Expression of histones H2B, H4 and H2A in UAF mutant strains
Yeast strains (y617, y879, y956, y1171, y1175, y1326, y1679) expressing histones H2B, H4 or H2A as fusion proteins with a C-terminal MNase-3xHA-tag and carrying a wild-type UAF30 and RRN5 locus (wt), or a complete deletion of one of the genes were cultured to exponential phase in YPD at 30°C. Proteins were extracted from one OD cells, extracts were separated by SDS-PAGE in a 10% acrylamide gel and transferred to a PVDF membrane. Signal intensities after Western blot analyis using antibodies 3F10 α-HA, α-rpa135 or α-rpS8 were determined with the MultiGauge software (FujiFilm), normalized to the signal in the respective wild-type strain and depicted in the diagrams below.

Immunodetection with the α-HA antibody revealed proper expression of histones H2A, H2B and H4 fused to MNase in the wild-type and *uaf30Δ* strain, for H2B-MNase also in the *rrn5Δ* strain. Also the expression of the Pol I subunit Rpa135 and the rpS8 protein could be verified in the different genetic backgrounds. Intriguingly, the detected signal intensities for all the analyzed proteins were lower in the UAF30 or RRN5 deletion mutants compared to the wild-type strains (Fig. 3-8, see graphs below for quantitation of the signal intensities in the mutant strains relative to the respective wild-type strains). Since the protein load was adjusted to OD values this might reflect differences in cell size in UAF30 and *uaf30Δ* strains (see below). Histone H2B and H4 expression levels seemed to be lower in *uaf30Δ* strains (and *rrn5Δ* cells in case of H2B) when normalizing the signals to Rpa135. Normalizing to rpS8

suggested instead that histone fusion protein levels are similar in both wild-type and mutant strains.

3.2.2 Analysis of MNase fusion protein expression in the UAF30 deletion strain

To control the proper expression of other MNase-tagged rDNA associated factors analyzed in this study Western blot analysis was performed with wild-type and UAF30 deletion strains expressing MNase fusion proteins of Rrn7, Fob1, Sir2, Cdc14, Brf1, Rrn9, Rpb3, Reb1, Net1, Rpo31 and Rpa190. An antibody directed against tubulin served as a loading control (Fig. 3-9).

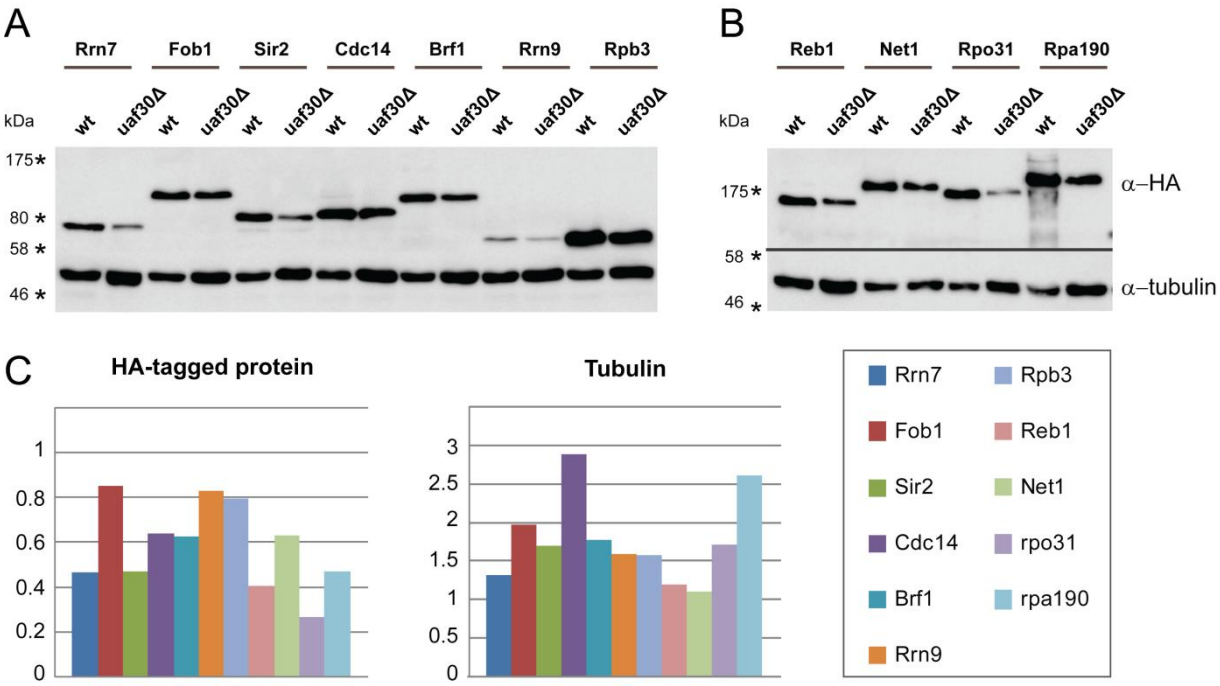

Fig. 3-9 MNase fusion protein expression in wild-type and UAF30 deletion strains
(A-B) Yeast strains (y624, y881, y952, y1121, y1151, y1174, y1177, y1184, y1273, y1294, y1328, y1330, y1450, y1453, y1671, y1681, y1688, y1689, y1691, y1692, y1694, y1696) expressing the protein indicated above each lane with a C-terminal MNase-3xHA-tag and carrying a wild type UAF30 locus, or a complete deletion of the gene were cultured to exponential phase in YPD at 30°C. Proteins were extracted from one OD cells, extracts were separated by SDS-PAGE in a 10% (A) or 8% (B) acrylamide gel and transferred to a PVDF membrane. (C) Signal intensities after Western blot analysis using antibodies 3F10 α-HA or α-tubulin were determined with the MultiGauge software (FujiFilm) and normalized to the signal in the respective wild-type strain. The signal for the wild-type strain was set to 1 and the ratios of protein or tubulin levels were depicted in the diagrams. Note the different scales as the signals for the protein levels in the UAF30 deletion mutant were lower, whereas tubulin levels were higher compared to signal intensities in the respective wild-type strains.

Western blot analysis using the α-HA antibody confirmed the correct expression of all MNase fusion proteins in both *uaf30Δ* and wild-type strains. Similar to the results obtained for the histone fusion proteins the detected signal intensity for the HA-tag was overall lower in the UAF30 deletion mutant compared to the wild-type strain (Fig. 3-9C, left panel). As outlined above this might reflect differences in cell size in UAF30 and *uaf30Δ* strains since the protein load was adjusted to OD values. Interestingly, immunodetection with the α-tubulin antibody revealed elevated signals in the *uaf30Δ* mutants compared to the wild-type strains (Fig. 3-9C, right panel).

We conclude that expression of the same MNase fusion proteins was similar in the different genetic backgrounds analyzed (at most a 3-fold difference was observed). However, because of the lack of a *bona fide* reference protein a strict comparative quantification of expression levels was not possible.

3.2.3 Immunofluorescence microscopy analysis of UAF30 deletion strain

Tubulin is a component of microtubules that serve as structural components within cells and are involved in many cellular processes including mitosis, cytokinesis, and vesicular transport (Hawkins et al., 2009). Alterations in tubulin levels might be an indication for differences in cell morphology in the UAF30 deletion mutant.

To analyze the cell morphology and the tubulin expression in the UAF30 deletion strains, IFM analysis was performed with an α-tubulin antibody (Fig. 3-10). To detect subcellular compartments antibodies raised against the HA-tagged rDNA associated nucleolar protein Fob1, and DAPI staining of the DNA for visualization of the nucleus were applied. Additionally, the tubulin signal (Fig. 3-10, green) and the staining for Fob1 (Fig. 3-10, red) were overlaid for better visualization of subcellular distribution (Fig. 3-10, merge). Whole yeast cells morphology was visualized by differential contrast (Fig. 3-10, DIC).

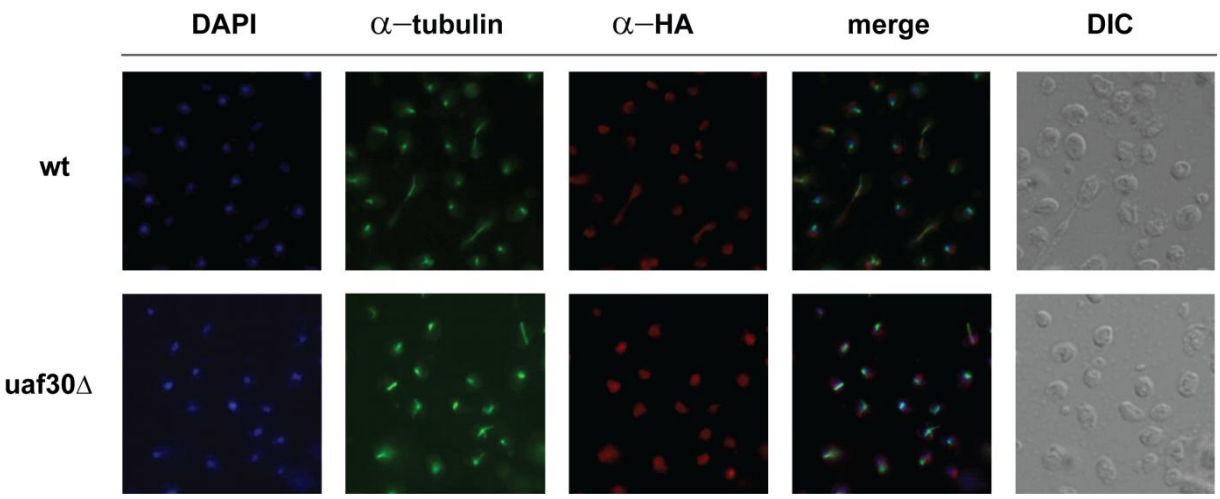

Fig. 3-10 Subcellular localization of tubulin in UAF30 deletion and wild-type strains expressing Fob1-MNase

The localization of tubulin was analyzed in yeast strains (y952, y1177) expressing FOB1 as a fusion protein with a C-terminal MNase and carrying a wild-type UAF30 locus, or a complete deletion of the gene by fluorescence microscopy using antibodies 12CA5 α-HA or α-tubulin and secondary antibodies Alexa Fluor 488 goat α-rat and Alexa Fluor 594 goat α-mouse. Nucleolar structures were visualized by the anti-HA antibody detecting Fob1, yeast nuclei were stained with DAPI. Additionally, the tubulin signal (green) and the staining for Fob1 (red) were overlaid for better visualisation of subcellular distribution (merge). Whole yeast cells morphology was visualized by differential contrast (DIC).

As expected in the wild-type background a typical nucleolar signal was detected for Fob1-HA in the nuclear border region (Fig. 3-10, see merge for co-localization of Fob1-HA and DAPI staining). In the UAF30 deletion mutant Fob1 also showed a nucleolar distribution, but the signal seemed to be more diffuse.

The staining for tubulin in the wild-type strain revealed a punctual signal in proximity of the nucleus for most of the cells. This signal represents the spindle pole body (SPB) which is the origin of microtubules and is embedded in the nuclear membrane (Brinkley et al., 1985). In some of the wild-type cells the mitotic spindle apparatus was visible as a bar bisecting the nucleus, detecting cells in the state of mitosis. In the UAF30 mutant strain the tubulin signal seemed to be stronger and not as sharp and punctual as observed for the UAF wild-type strain. Importantly, the wild-type and UAF30 deletion strain also differed slightly in cell size. Thus, the different protein levels observed for the different strain backgrounds could be due to the fact that the protein load was adjusted to the OD and not to the cell number. The cell morphology is disturbed in UAF30 deletion strains. However, the molecular basis for this phenomenon had not been determined.

3.3 Association of structural rDNA components in UAF30 deletion strains

Comparative analysis of MNase accessibility of the 35S rRNA coding region in wild-type and mutant strains demonstrated that proper rDNA chromatin structure depends on the presence of UAF. To investigate whether the observed changes in MNase digestion patterns for the UAF mutant strains are reflected by alterations in the association of factors bound to the rDNA locus, ChEC experiments were performed with structural rDNA components like histone proteins and the HMG box protein Hmo1.

3.3.1 Association of histones H2B, HHO1 and HTZ1 with the rDNA locus changes upon deletion of UAF30

To analyze histone association in this genetic background, ChEC was performed with wild-type and *uaf30Δ* strains expressing the core histone H2B, the yeast linker histone Hho1 and the histone variant H2A.Z (Htz1) as MNase fusion proteins. Cleavage of the fusion proteins was monitored in Southern blot analysis with a probe detecting the rDNA promoter region (Fig. 3-11A). Profiles for each factor are depicted in Fig. 3-11B.

The cleavage patterns produced by H2B-MNase expressed in wild-type and *uaf30Δ* strains were similar to those obtained in rDNA from wild-type and *uaf30Δ* strains after incubation with exogenously added MNase (Fig. 3-11A, compare lanes 1-5 with Fig. 3-4A lanes 1-5 and Fig. 3-11A, compare lanes 6-10 with Fig. 3-4A lanes 16-20). The region in proximity to the Reb1 binding site and the upstream element became more susceptible to digestion of the MNase fusion protein upon deletion of UAF30 (Figs. 3-11A and 3-11B, upper panel, black and blank squares), wheras other areas got more protected to the enzymatic cuts (Figs. 3-11A and 3-11B, upper panel, asterisk). The digestion profiles of the 35S coding region showed a more distinct cleavage pattern in comparison to the wild-type strain (Figs. 3-11A and 3-11B, upper panel, black dots). The slight effects in accessibility to the enzymatic cuts observed for H2B-MNase were even more pronounced in profiles for the strains expressing the yeast linker histone Hho1 and the histone variant Htz1 as MNase fusion proteins (Fig. 3-11A, lanes 11-30 and Fig. 3-11B, middle and lower panels).

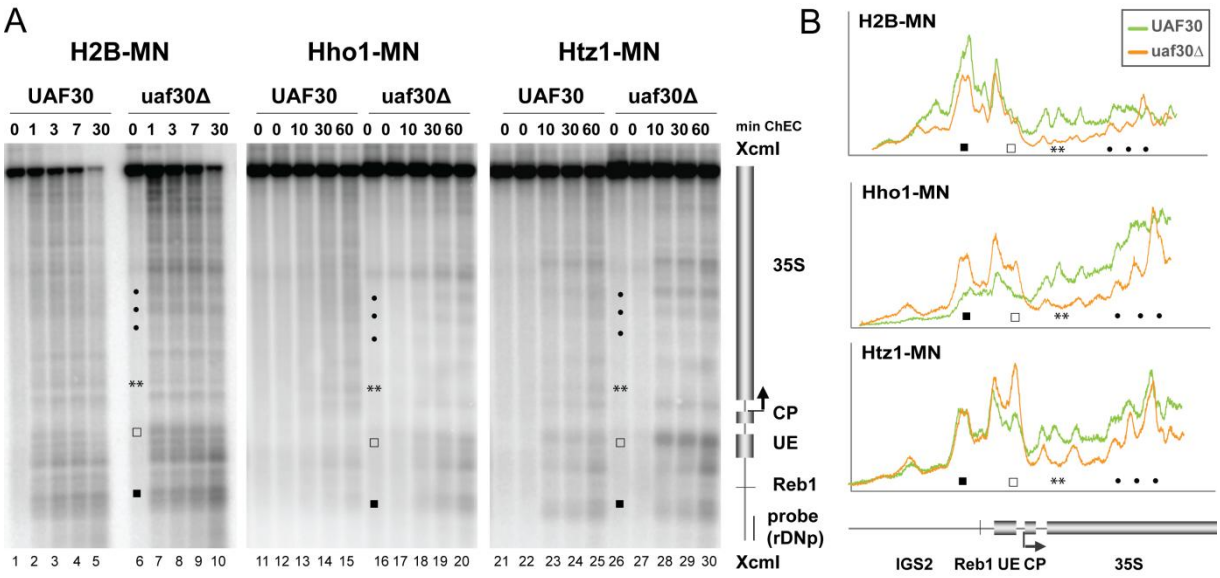

Fig. 3-11 Reorganization of structural rDNA components in the *uaf30Δ* strain
(A) Yeast strains (y617, y954, y1145, y1171, y1690, y1695) expressing the genes indicated above each panel as fusion proteins with a C-terminal MNase and carrying a wild-type UAF30 locus, or a complete deletion of the gene were cultured to exponential phase in YPD at 30°C. After formaldehyde crosslinking, isolated nuclei were subjected to ChEC for the times indicated above each lane. DNA was isolated and analyzed as described in the legend to Figure 3-4A. Different symbols highlight changes in MNase accessibility as described in the legend to Fig. 3-4A. (B) Profiles of DNA-fragment patterns obtained after 30 minutes (H2B-MNase expressing strains) or 60 minutes (other strains) ChEC of the fusion protein indicated in the legend of each graph. FLA-5000 data presented in (A) were analyzed with the MultiGauge software (FujiFilm). The signal intensity in the respective lanes was plotted against the distance of migration in the gel. Signal intensities of MNase profiles compared in one graph were normalized to the different rDNA amounts in UAF30 and *uaf30Δ* strains (typically 1:1.5). Different symbols highlight changes in MNase accessibility as described in the legend to Fig. 3-4B. A cartoon of the genomic region including important features as described in the legend of Fig. 1-2 is indicated below the graphs.

The alterations in promoter accessibility extended over the coding region probably as a consequence of a more regular arrangement of histone molecules. Thus, the reorganization of structural constituents of rDNA chromatin in the UAF30 deletion strain correlates well with the changes in MNase sensitivity of the 35S rDNA.

3.3.2 Hmo1 binding to the rDNA is abolished in UAF and CF mutant strains

The high-mobility group (HMG) protein Hmo1 is another important structural rDNA component. Hmo1 associates throughout the 35S rRNA gene locus in a Pol I-dependent manner and binds to the promoters of most ribosomal protein genes (Kasahara et al., 2007; Hall et al., 2006). To analyze the association of the Hmo1 protein with the rDNA locus ChEC analysis was performed with wild-type and mutant strains carrying deletions in the UAF

subunits UAF30 or RRN5, or in the CF subunit RRN7 and expressing Hmo1-MNase. In addition to hybridization of the blots with probe rDNp, Hmo1 binding to the promoter of the RPS23A gene was analyzed with probe NUP57 as a control (Fig. 3-12).

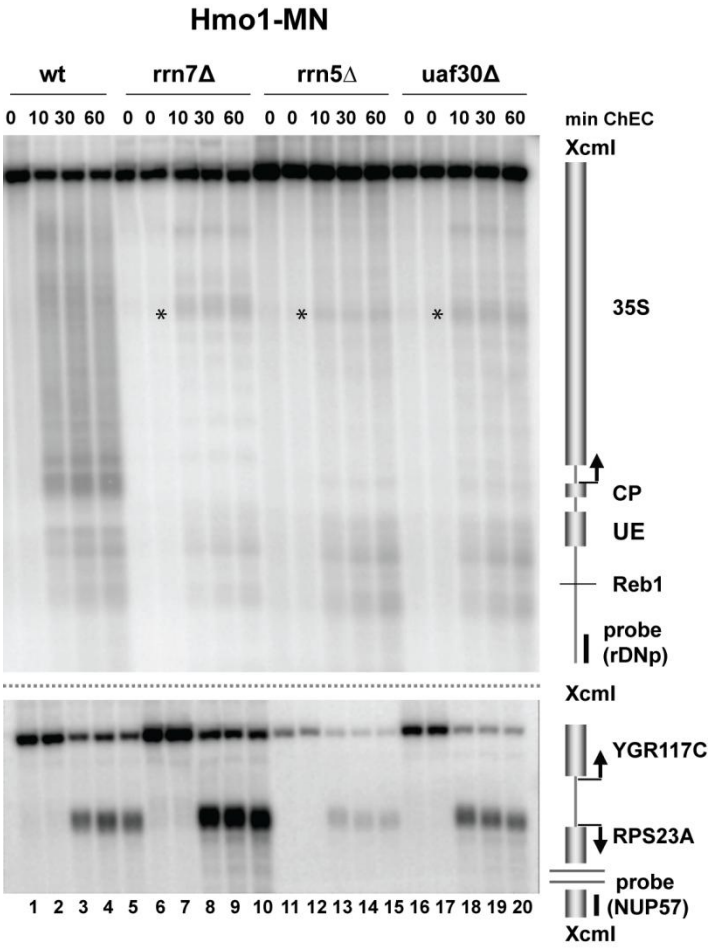

Fig. 3-12
Hmo1 association is disrupted in UAF and RRN7 deletion strains
Wild-type yeast (y621), or mutant (y890, y1171, y1676) strains deleted in the genes indicated above the respective lanes and expressing HMO1 as fusion proteins with a C-terminal MNase were cultured to exponential phase in YPD at 30°C. After formaldehyde crosslinking, isolated nuclei were subjected to ChEC for the times indicated above each lane. DNA was isolated and analyzed as described in the legend to Figure 3-4A. In addition to Southern blot hybridization with probe rDNp (upper panel) the same membrane was also hybridized with probe NUP57 detecting a 4.2-k fragment encompassing the *RPS23A* gene locus (lower panel). Asterisks marks signals that are still detected on the blot due to previous labeling with the NUP57 probe.

In the wild-type strain Hmo1-MNase mediated cleavage was detected at the rDNA promoter, spreading along the 35S transcribed region (Fig. 3-12, upper panel, lanes 1-5). This association was severly compromised in the *uaf30Δ* mutant (Fig. 3-12, upper panel, lanes 16-20). This is consistent with recent data showing that only few rRNA genes in the *uaf30Δ* strain are transcribed by Pol I (Hontz et al., 2009) and with the observation that Hmo1 associates with 35S rDNA in a Pol I-dependent manner (Kasahara et al., 2007). Consistent with this the binding of Hmo1 to the rDNA was also impaired in the PSW strain *rrn5Δ* and in the Pol I-defective mutant *rrn7Δ* (Fig. 3-12, upper panel, lanes 6-15). In contrast, Hmo1-MNase mediated cleavage within the control locus at the promoter region of the Hmo1 target gene RPS23A was not affected in any of the strains analyzed (Fig. 3-12, lower panel, lanes 1-20).

3.4 Analysis of histone density at the rDNA locus in UAF30 deletion strains

rDNA chromatin structure is altered in the UAF deletion strains. This is supported by the observed reorganization of several structural rDNA components in the UAF30 deletion mutant according to the changes in MNase digestion profiles for the 35S rDNA. The regular MNase cleavage pattern observed in *uaf30Δ* strains indicates that the 35S coding region is assembled in nucleosomes in this genetic background.

3.4.1 Psoralen analysis of deletion strains suggests a nucleosomal arrangement of rDNA chromatin

The altered chromatin structure in the different mutant strains was confirmed by psoralen crosslinking analysis. This method allows the distinction between the actively transcribed, nucleosome-free (*s-band*) and the inactive (*f-band*) rDNA genes (Dammann et al., 1993). Nuclei were subjected to psoralen crosslinking analysis. The DNA was isolated, digested with XcmI and SacII, separated in a 1% agarose gel and analyzed in a Southern blot with probe ETS1 detecting promoter and 35S coding regions of the rRNA gene (Fig. 3-13).
For the psoralen analysis the NOY505 wild-type strain and the mutant strains were grown in YPG. As a control the analysis was performed with wild-type strain y1671 cultured in YPD. The amount of psoralen incorporation into rDNA may differ depending on strain background and growth conditions. For y1671 the *s-band* population was overrepresented (Figure 3-13, lane 2, see graph on the right for quantitation of the relative signal intensities). The strain y1671 is a derivative of NOY505, expressing a MNase fusion protein of Cdc14. This protein phosphatase is a subunit of the RENT complex and involved in the regulation of mitotic exit (Shou et al., 1999). Therefore it cannot be excluded that the expression of the fusion protein influences the number of actively transcribed rDNA repeats.

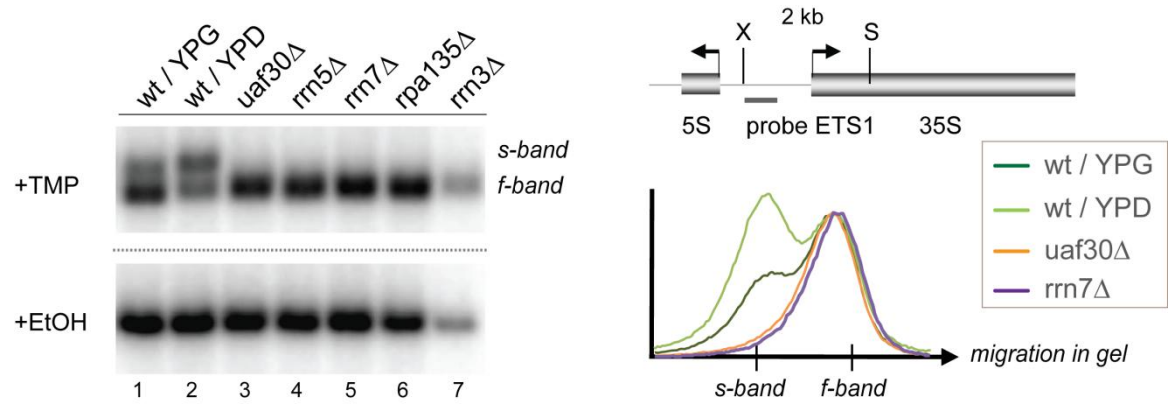

Fig. 3-13 Reduced psoralen accessibility at the rDNA locus suggests a nucleosomal rDNA chromatin structure in the mutant strains

Wild-type yeast (NOY505, y1671), or mutant strains (NOY408-1a, NOY558, NOY604, NOY699, y1120) deleted in the genes indicated above the respective lanes were cultured to exponential phase in YPD (y1671), or YPG (NOY505, NOY408-1a, NOY558, NOY604, NOY699) at 30°C. After formaldehyde crosslinking, isolated nuclei were subjected to psoralen crosslinking analysis. DNA was isolated, digested with XcmI and SacII, separated in a 1% agarose gel and analyzed in a Southern blot with probe ETS1 detecting a 2 kb fragment encompassing promoter and 35S coding regions of the rRNA gene. Data were collected using a FLA-5000 imaging system (FujiFilm). A cartoon of the genomic region including important features, as well as the positions of the XcmI (X) and SacII (S) restriction sites and the probe used for indirect end-labeling is depicted on the right. Graphs on the right depict s- and f-band profiles for samples indicated in the legend. Signal intensities in each lane were derived from the FLA-5000 data, normalized on the respective peak value and plotted against the distance of migration in the gel.

In the strain NOY505 grown in YPG the ratio of *s-band* and *f-band* was substantially lower (Figure 3-13, lane 1, see graph on the right for quantitation of the relative signal intensities). In contrast, rDNA fragments derived from the mutant strains migrated exclusively with *f-band* mobility (Figure 3-13, lanes 3-7, see graph on the right for quantitation of the relative signal intensities). This result demonstrates that in the mutant strains psoralen incorporation into 35S rDNA is strongly reduced. These analyses nicely confirm previous results obtained by psoralen crosslinking with *uaf* deletion mutants (Hontz et al., 2008, PhD thesis Katharina Merz). The observed decrease in psoralen incorporation suggests a nucleosomal arrangement of rDNA repeats. This interpretation is underlined by psoralen analysis of a 3.1-kb fragment derived from a plasmid containing a yeast rRNA gene under the control of the GAL7 promoter. The Pol II-transcribed plasmid also revealed only slightly crosslinked DNA, confirming that DNA sequences transcribed by RNA polymerase II are packaged in nucleosomes (Dammann et al., 1995).

3.4.2 Histone density at the rDNA locus is comparable to Pol II-transcribed genes in the UAF30 deletion mutant

To investigate, whether the diminished psoralen crosslinking efficiency in the UAF deletion mutants is caused by a nucleosomal chromatin structure histone association at the yeast rDNA locus was analyzed in the *uaf30Δ* mutant.

To measure histone density quantitatively, ChEC analysis was performed using nuclei from UAF30 wild-type and *uaf30Δ* strains expressing histone H4 as a fusion protein with a C-terminal MNase. After ChEC, the DNA was isolated and digested with EcoRI yielding three characteristic fragments derived from the rDNA locus (Fig. 3-14A).

As rDNA makes up around 10% of the yeast genome, the three EcoRI fragments could be already detected by SYBR Safe staining after agarose gel electrophoresis of the genomic DNA (Fig. 3-14B and C, SYBR panel, lane 1). In the UAF30 wild-type strain the 2.4 kb fragment encompassing the intergenic spacer region was digested rapidly in the ChEC with H4-MNase, whereas the 18S and 25S containing fragments (1.9 kb; 2.8 kb) were more resistant to degradation (Fig. 3-14B, SYBR panel, lanes 2-5). These analyses confirmed previous findings, that the histone density within the coding region of the 35S rRNA genes is lower than the histone density within the intergenic spacer region in a UAF30 wild-type yeast strain (Merz et al., 2008).

In contrast, in the *uaf30Δ* strain all three fragments were digested with similar and overall slower kinetics (Fig. 3-14C, SYBR panel, lanes 2-5). This indicates that histone densities within the intergenic spacer region and the 35S rRNA coding region are comparable in the *uaf30Δ* strain. Also the bulk genomic DNA represented by a smear above the EcoRI fragments was digested with slower kinetics when compared to the digestion kinetics of this DNA in the wild-type strain. This could be due to the overall reduction in histone exrpession levels observed in the *uaf30Δ* strain (see above).

This observation complicated a direct comparison of rDNA degradation by H4-MNase between the wild-type and the *uaf30Δ* strain. Therefore the degradation of the 1.9 kb fragment encompassing the 18S rDNA was internally compared to degradation of the Pol II-transcribed GAL gene locus for both strains in Southern blot analysis (Fig. 3-14B and C).

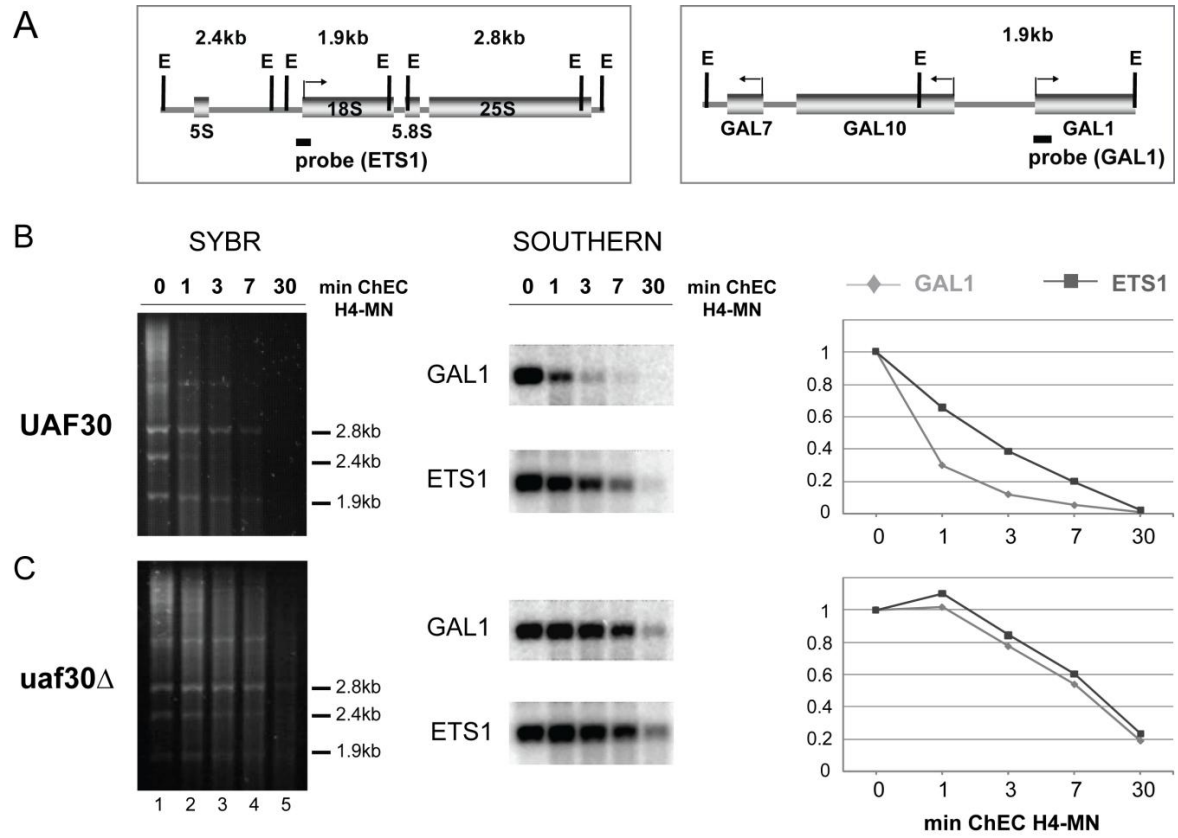

Fig. 3-14 Reduced histone density at the rDNA locus suggests a nucleosomal rDNA chromatin structure in the UAF30 deletion mutant

(A) Cartoons of the genomic regions investigated in B-C including important features, as well as the positions of the EcoRI (E) restriction sites and the probes used for indirect end-labeling. (B-C) Yeast strains (y879, y1175) expressing histone H4 as a fusion protein with a C-terminal MNase and carrying a wild-type UAF30 locus (B), or a complete deletion of the gene (C) were cultured to exponential phase in YPD at 30°C. After formaldehyde crosslinking, isolated nuclei were subjected to ChEC for the times indicated above each lane. DNA was isolated, digested with EcoRI, separated in a 1% agarose gel, visualized by staining with SYBR Safe (left panels), and analyzed in a Southern blot by sequential hybridization with probe GAL1 detecting either a 1.9 kb fragment encompassing parts of the GAL1-10 gene locus, or probe ETS1 detecting a 1.9 kb fragment encompassing the 18S rRNA coding sequence (middle panels). Data were collected using a FLA-5000 imaging system (FujiFilm). FLA-5000 data presented in the middle panels were analyzed with the MultiGauge software (FujiFilm). The signal intensity obtained for the full length EcoRI fragment after hybridization with the two different probes was plotted against the time of ChEC (graphs on the right).

For quantitative Southern blot analysis, the DNA in the gel was transferred to a membrane and sequentially hybridized with probes GAL1 and ETS1 specifically detecting a 1.9 kb EcoRI fragment originating from the single copy GAL1 locus, and a 1.9 kb EcoRI fragment encompassing the external transcribed spacer 1 (ETS1) and 18S rRNA coding region, respectively (Fig. 3-14A).

In the UAF30 wild-type strain the GAL1 fragment was digested with faster kinetics than the ETS1 fragment (Fig. 3-14B, compare panels GAL1 and ETS1; see the graph on the right for quantitation of the relative signal intensities). This is consistent with a reduced histone

density at the 35S rRNA genes when compared to the histone density at other genomic loci that are transcribed by Pol II (Merz et al., 2008). In the *uaf30Δ* strain instead degradation of both fragments followed the same kinetics (Fig. 3-14C, compare panels GAL1 and ETS1; see the graph on the right for quantitation of the relative signal intensities). Similar results were obtained with a strain expressing H2B as MNase-fusion protein (Fig. 3-15).

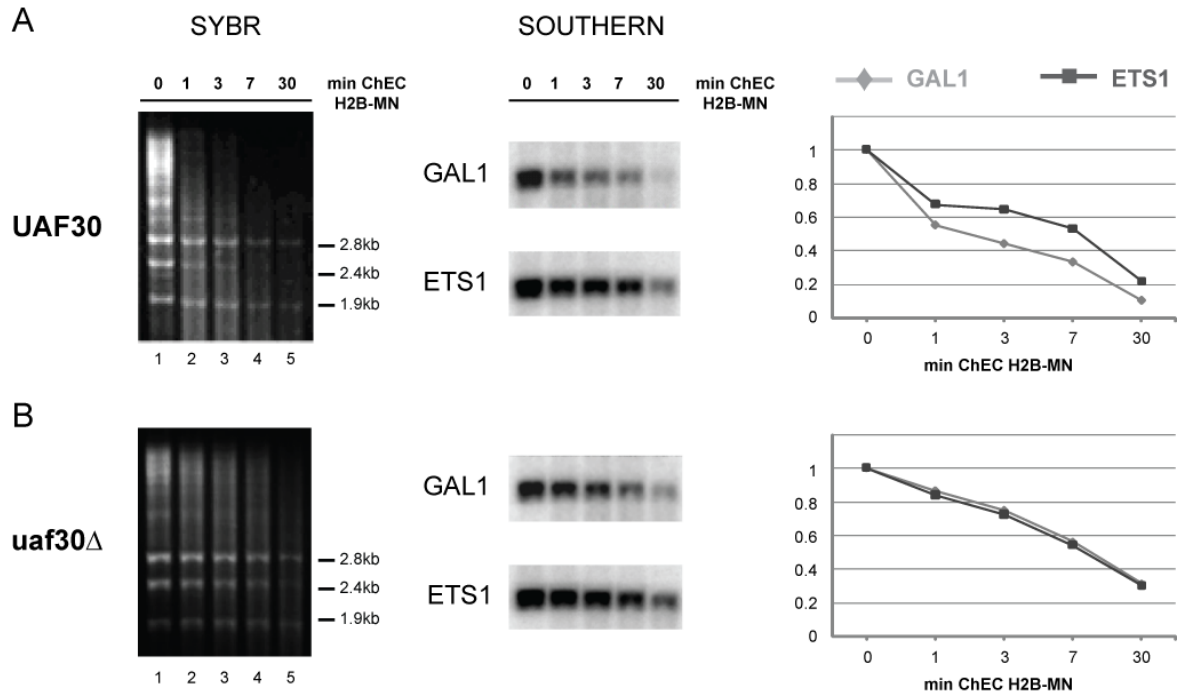

Fig. 3-15 H2B association in wild-type and uaf30Δ strains
(A-B) Yeast strains (y617, y1171) expressing histone H2B as a fusion protein with a C-terminal MNase and carrying a wild-type UAF30 locus (A), or a complete deletion of the gene (B) were cultured to exponential phase in YPD at 30°C. After formaldehyde crosslinking, isolated nuclei were subjected to ChEC for the times indicated above each lane. DNA was isolated and analyzed as described in the legend to Fig. 3-14.

Again in the UAF30 wild-type strain the GAL1 fragment was digested with faster kinetics than the ETS1 fragment (Fig. 3-15A, compare panels GAL1 and ETS1; see the graph on the right for quantitation of the relative signal intensities) whereas in the *uaf30Δ* strain degradation of both fragments followed very similar kinetics (Fig. 3-15B, compare panels GAL1 and ETS1; see the graph on the right for quantitation of the relative signal intensities). Thus, in the UAF30 deletion mutant degradation of the rDNA fragment (ETS1) is comparable to degradation of a Pol II-transcribed gene locus. This result supports the idea of a nucleosomal arrangement of rRNA genes in the *uaf30Δ* strain.

3.5. Deletion of UAF30 leads to compositional and structural changes within 35S rDNA promoter chromatin

The MNase accessibility assays demonstrated that the presence of UAF at the UE is important for organizing chromatin structure at the rDNA promoter. These results were confirmed by the observed change in association of several structural rDNA components with this region. Therefore UAF seems to mediate a specific chromatin structure at the promoter that is important for efficient initiation of Pol I transcription. To gain more insight into the composition of rDNA promoter chromatin in the absence of UAF, the association of promoter-bound factors was analyzed in the UAF30 deletion mutant.

In addition, the role of UAF in the formation of pre-initiation complexes (PICs) at the rDNA promoter region was investigated. The ability of UAF to stabilize TBP and CF at the rDNA promoter region in the absence of an active Pol I-Rrn3 complex has been discussed controversially in the literature (Keys et al., 1996; Aprikian et al., 2001; Bordi et al., 2001). To examine the function of UAF in PIC formation at the rDNA promoter, the association of UAF and CF was analyzed after shutdown of Pol I transcription and in mutant strains carrying deletions in RRN3 or RPA135 coding for a Pol I subunit.

3.5.1 Uaf30 is required for the specific association of Pol I transcription factors with the rDNA promoter

To analyze the interaction of Pol I transcription factors with the rDNA promoter depending on the presence of Uaf30 in more detail ChEC experiments with strains expressing MNase fusion proteins of UAF subunit Rrn9, CF subunit Rrn7 and TATA-binding protein Spt15 (TBP) were carried out in both wild-type and *uaf30Δ* strains. The results are demonstrated in Fig. 3-16.

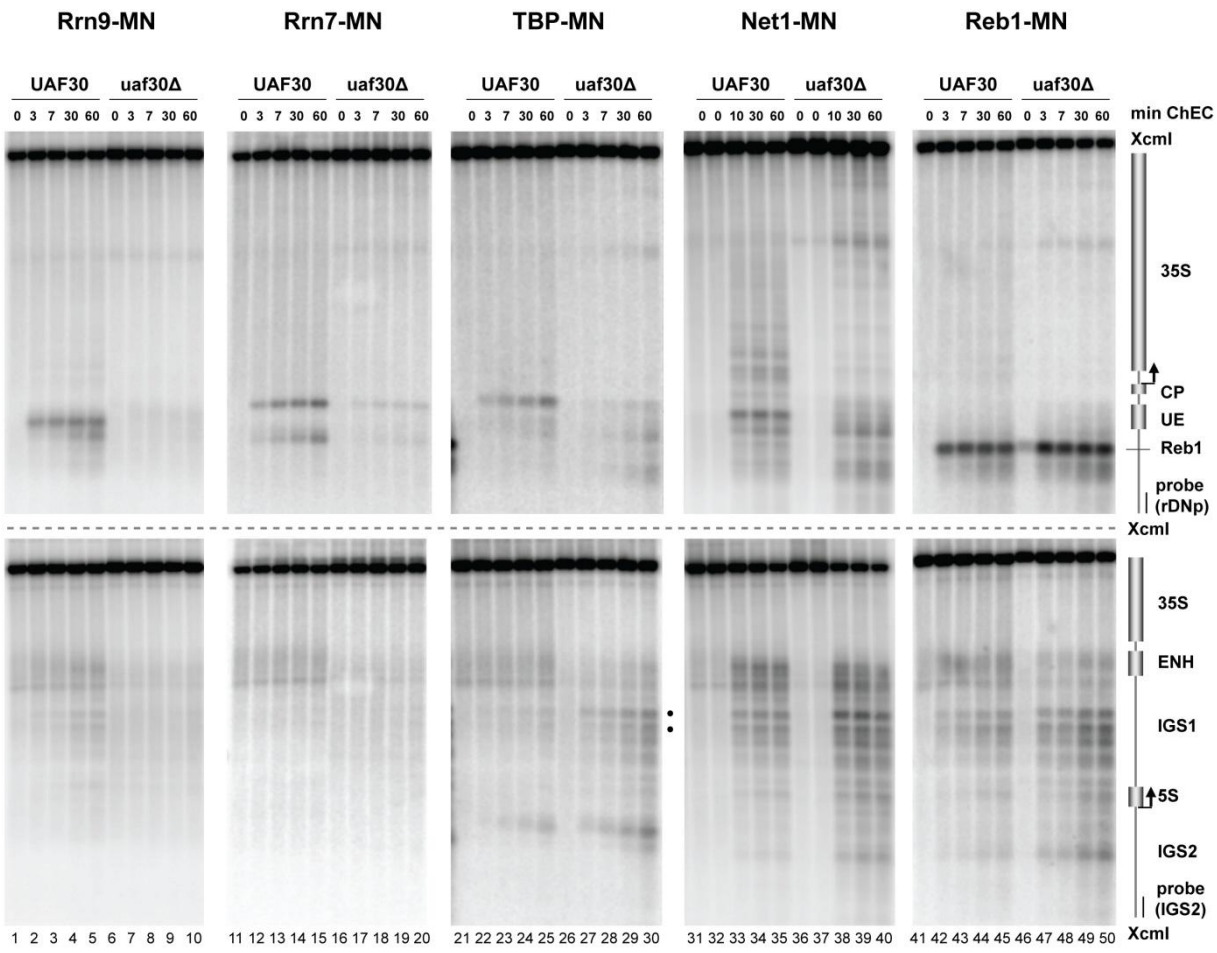

Fig. 3-16 Uaf30 is required for the specific association of Pol I transcription factors with the rDNA promoter

(A) Yeast strains (y881, y1121, y1151, y1184, y1185, y1328, y1329, y1453, y1689, y1692) expressing the genes indicated above each panel as fusion proteins with a C-terminal MNase and carrying a wild-type UAF30 locus, or a complete deletion of the gene were cultured to exponential phase in YPD at 30°C. After formaldehyde crosslinking, isolated nuclei were subjected to ChEC for the times indicated above each lane. DNA was isolated and analyzed as described in the legend to Figure 3-4A. In addition to Southern blot hybridization with probe rDNp (upper panels) this analysis was also performed with probe IGS2 (lower panels).

Cleavage by UAF and CF components fused to MNase in the wild-type strain occurred at their known binding sites within the UE and the CP, whereas association of these factors with the promoter region was reduced (Rrn7) or even completely abolished (Rrn9) in the *uaf30Δ* mutant (Fig. 3-16, upper panels, lanes 1-20). This is in accordance with previous ChIP experiments, showing that Uaf30 is required for the association of UAF with the UE *in vivo* (Hontz et al., 2009). The TBP-MNase produced a strong cut between the UE and the CP in the wild-type strain. In the *UAF30* deletion mutant, cleavage at this site was diminished and additional cuts occurred at regions within the UE and upstream of the Reb1 binding site (Fig. 3-16, upper panels, lanes 21-30; see Fig. 3-17 for a profile analysis of lanes 25 and 30 in Fig.

3-16). These areas have already been shown to become more accessible in the *uaf30Δ* strain after digestion of rDNA chromatin with exogenously added MNase (Fig. 3-4A, lanes 16-20). TBP is a general transcription factor for all three RNA polymerases. The observed delocalization to regions upstream of its known binding site in the *uaf30Δ* strain might indicate a possible role for this factor in transcription initiation at regions other than the Pol I initiation site.

The Net1-MNase fusion protein induced multiple cuts clustering around the 35S rDNA promoter in the UAF30 wild-type strain (Fig. 3-16, upper panel, lanes 31-35). This cleavage pattern closely resembled those of other RENT components Sir2 and Cdc14 when expressed as MNase fusion-proteins (Figs. 3-24 and 3-27). Similar to the change in cleavage pattern for TBP-MNase in the *uaf30Δ* strain, Net1-MNase cleavages were observed to cluster around the Reb1 binding site in this genetic background (Fig. 3-16, upper panel, lanes 36-40; see Fig. 3-17 for a profile analysis of lanes 35 and 40 in Fig. 3-16).

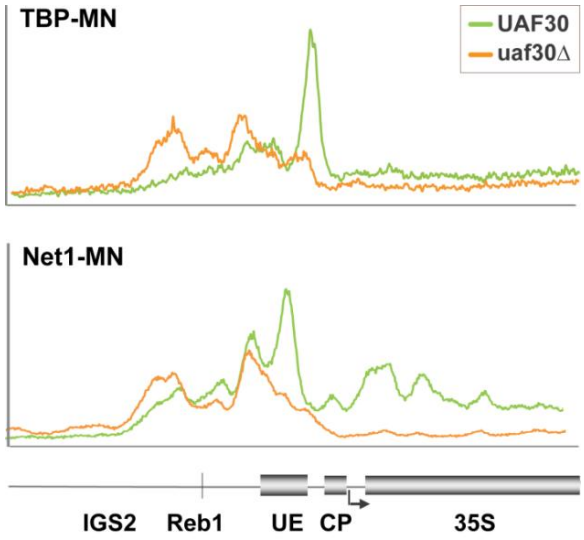

Fig. 3-17 Profile analysis of TBP and Net1 association in Fig. 3-16
Profiles of DNA-fragment patterns obtained after 60 minutes ChEC of the fusion protein indicated in the legend of each graph. FLA-5000 data presented in Fig. 3-16 were analyzed with the MultiGauge software (FujiFilm). The signal intensity in the respective lanes was plotted against the distance of migration in the gel. Signal intensities of MNase profiles compared in one graph were normalized to the different rDNA amounts in UAF30 and uaf30Δ strains (typically 1:1.5). A cartoon of the genomic region including important features as described in the legend of Fig. 1-2 is indicated below the graphs.

The identical membranes were hybridized with a probe detecting the 3´end of the 35S rDNA, the 5S rDNA, and parts of the noncoding intergenic spacer regions. Rrn9-MNase produced weak cuts within IGS1 and the ENH region in a strain expressing a UAF30 wild-type allele.

This has already been observed for multiple rDNA promoter-bound factors (Merz et al., 2008). These cleavage events were not observed in the *uaf30Δ* strain (Fig. 3-16, lower panel, compare lanes 1-5 with lanes 6-10). This could be an indication for structural rearrangements within the rDNA locus upon deletion of UAF30.

The TBP-MNase induced a distinct cut at the 5'-end of the 5S rRNA gene in both UAF30 wild-type and *uaf30Δ* strains (Fig. 3-16, lower panel, lanes 21-30). This is consistent with its function as a subunit of the Pol III transcription factor TFIIIB. Furthermore, the cleavage by TBP-MNase in the *uaf30Δ* strain was enhanced within IGS1 (Fig. 3-16, lower panel, compare lanes 21-25 with 26-30, black dots). This region was previously identified as a bidirectional Pol II promoter (E-pro) (Ganley et al., 2005). As TBP is generally required for transcription by all three nuclear RNA polymerases (Hernandez, 1993), the enhanced TBP recruitment might indicate that Pol II silencing within IGS1 is impaired in the *uaf30Δ* strain. Strong cleavage by Net1-MNase and Reb1-MNase was observed in IGS1 and at the ENH region upstream of the rDNA 3'-end in UAF30 and *uaf30Δ* strains (Fig. 3-16, lower panel, lanes 31-50). The deletion of UAF30 does not seem to influence the association of these factors with IGS1. The cleavage mediated by Reb1-MNase within the ENH region was weak compared to the cleavage at the promoter proximal binding site (Fig. 3-16, lanes 41-50). This observation is consistent with recent ChIP data (Jones et al., 2007).

Taken together, these data confirm that Uaf30 is required for efficient recruitment of other UAF components and CF to the rDNA promoter. In the absence of Uaf30 the association of TBP and Net1 with the rDNA promoter changes qualitatively and quantitatively, whereas Reb1 binding is unaltered. Intiguingly the deletion of UAF30 also influences the interaction of TBP with the downstream region of the 35S rRNA-gene.

3.5.2 Inhibition of Pol I transcription does not affect the association of transcription factors with the 35S rDNA promoter region

To ascertain, that the observed changes in transcription factor binding were not caused by the strong reduction of Pol I transcription in the *UAF30* deletion mutant, ChEC analyses were performed in the *RRN3* wild-type and the *rrn3-ts* strains expressing either the CF subunit Rrn11, TBP, or Net1 as MNase fusion proteins. The results are shown in Fig. 3-18A and profiles for TBP- and Net1-MNase are displayed in Fig. 3-18B.

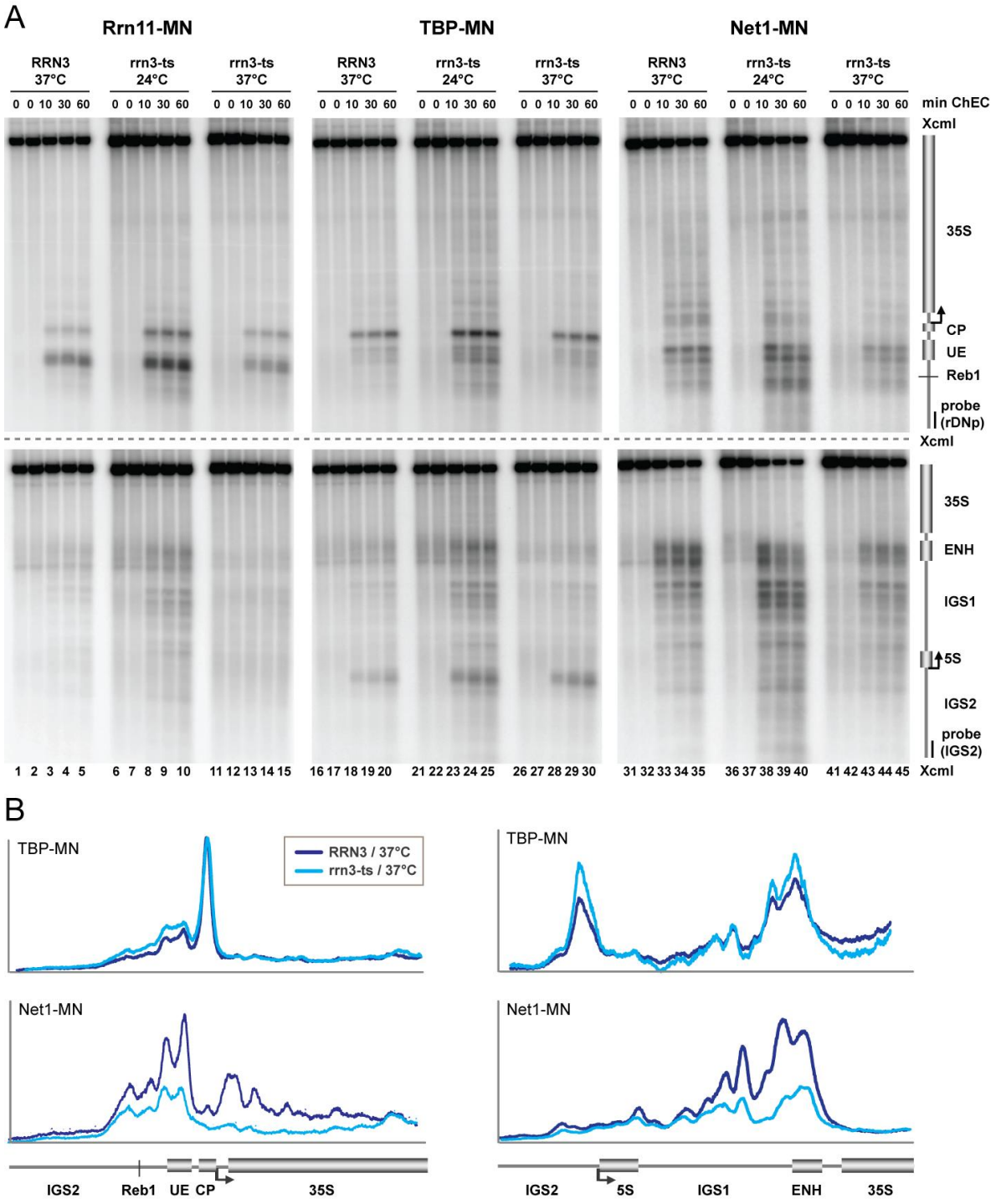

Fig. 3-18 Transcriptional shutdown does not affect the association of transcription factors

(A) Yeast strains (1143, 1144, 1148, 1149, 1707, 1712) expressing the genes indicated above each panel as fusion proteins with a C-terminal MNase and carrying a wild-type RRN3 locus, or a temperature sensitive rrn3-ts allele were cultured to exponential phase in YPD at 24°C. Cells were split and either fixed with formaldehyde or further incubated in YPD at 37°C for another 120 minutes before formaldehyde crosslinking. Isolated nuclei were subjected to ChEC for the times indicated above each lane. DNA was isolated and analyzed as described in the legend of Fig. 3-16. (B) Profiles of DNA-fragment patterns obtained after 60 minutes ChEC of the fusion protein indicated in the legend of each graph. FLA-5000 data presented in (A) were analyzed with the MultiGauge software (FujiFilm). The signal intensity in the respective lanes was plotted against the distance of migration in the gel. Signal intensities of MNase profiles compared in one graph were normalized to the different rDNA amounts in RRN3 and rrn3-ts strains. A cartoon of the genomic region including important features as described in the legend of Fig. 1-2 is indicated below the graphs.

Cutting mediated by the respective MNase fusion proteins did not reveal qualitative differences in transcription factor association after shutdown of Pol I transcription at 37°C in the *rrn3-ts* strain. The observed shift of TBP- and Net1-mediated cleavage to regions more upstream of the rDNA promoter around the Reb1 binding site observed for the *uaf30Δ* strain (Fig. 3-16) was not detected for the *rrn3-ts* strain (Fig. 3-18A, upper panels, lanes 16-45; see Fig. 3-18B, left panels, for a profile analysis of lanes 20, 30, 35 and 34 in Fig. 3-18A). However, the profile analysis for TBP and Net1 revealed a reduced association of Net1 with both rDNA promoter and enhancer regions after disruption of Pol I transcription, whereas TBP association was not decreased under these conditions (Fig. 3-18A, lanes 16-45; see Fig. 3-18B, for a profile analysis of Fig. 3-18A, lanes 20, 30, 35 and 45). This is consistent with the observation, that Net1 stimulates Pol I transcription both *in vivo* and *in vitro* (Shou et al., 2001). Furthermore, Net1 has been shown to preferentially associate with actively transcribed rDNA repeats in ChEC-psoralen experiments (Manuel Wittner, data not shown).

Cleavage within the IGS1 was enhanced in the *rrn3-ts* strain at the permissive temperature (Fig. 3-18A, lower panels, lanes 6-10, 21-25 and 36-40). This effect is probably generated by the lower formaldehyde crosslinking efficiency at 24°C, resulting in an increased random degradation of DNA.

Thus, shutdown of Pol I transcription does not impair the stability of the promoter bound UAF-TBP-CF complex. The altered cleavage observed for the Pol I transcription factors and for Net1 in the *uaf30Δ* strains is a direct consequence of the absence of Uaf30. Therefore UAF seems to be required for the specific recruitment of TBP and CF to the rDNA promoter and sufficient for maintaining these associations, even after shutting off Pol I transcription.

3.5.3 UAF and CF form a stable complex at the rDNA promoter in the absence of Pol I or Rrn3 *in vivo*

So far it has not been determined whether the presence of UAF is sufficient to stabilize initiation complexes at the rDNA promoter region in the absence of an active Pol I-Rrn3 complex. Earlier *in vivo* footprinting experiments followed by *in vitro* studies using an immobilized rDNA template suggested, that stable initiation complexes at the rDNA promoter can only be obtained in the presence of both Pol I and Rrn3 (Aprikian et al., 2001; Bordi et al., 2001). These data lead to the model of a Pol I transcription cycle, where CF is recruited by Pol I and Rrn3 to promoter bound UAF and displaced after each productive initiation event (Aprikian et al., 2001). On the other hand, a stepwise model for Pol I pre-initiation complex formation had been proposed, where UAF recruits TBP and CF forming a stable complex which serves as a platform for the initiation competent Pol I-Rrn3 complex (Keys et al., 1996). In ChEC experiments with *rrn3-ts* strains expressing Rrn11- (Fig. 3-18A) or Uaf30-MNase (PhD thesis Katharina Merz) stable association of UAF and CF with the rDNA promoter region was observed even after shutting off Pol I transcription. These results support the second model, as it suggests that CF does not leave the promoter together with Rrn3-Pol I.

To address the question of whether UAF is sufficient for the formation of a stable pre-initiation complex, even in the complete absence of Pol I and Rrn3 ChEC experiments were performed in an *rrn7Δ* mutant expressing the UAF subunit Uaf30 as MNase fusion protein and in *rpa135Δ* and *rrn3Δ* strains expressing Uaf30 or the CF subunit Rrn7 as MNase fusion proteins. The results are shown in Fig. 3-19.

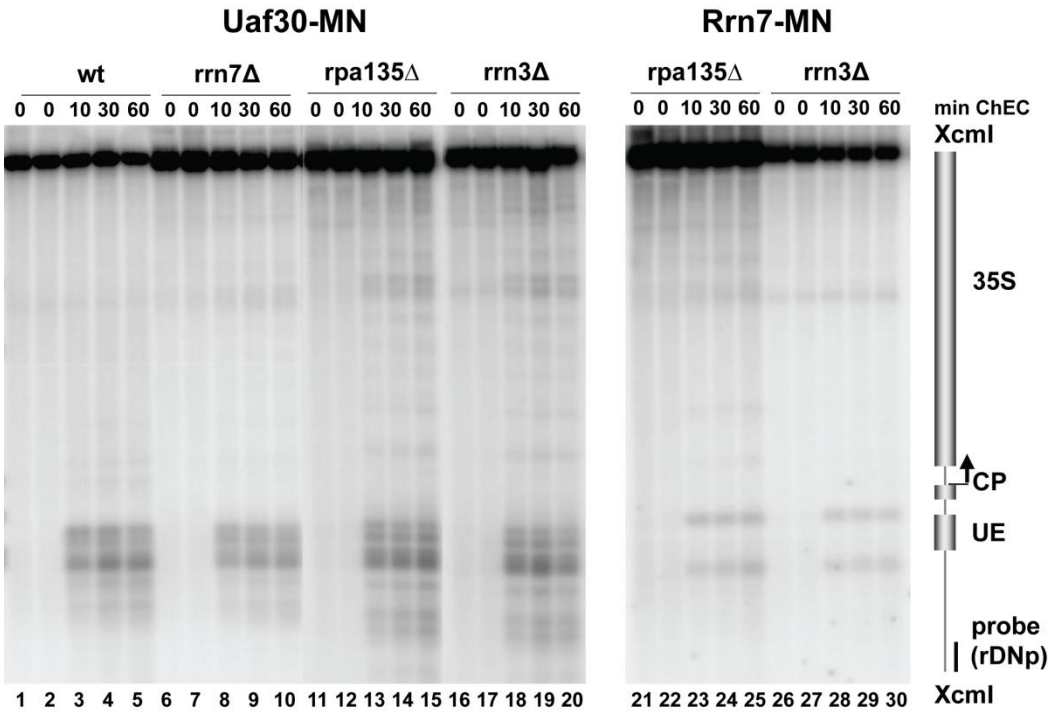

Fig. 3-19 UAF is sufficient to stabilize CF binding to the CP
Yeast strains (y618, y1109, y1926, y1927, y1928, y1929) expressing the genes indicated above each panel as fusion proteins with a C-terminal MNase and being either wild-type (wt) or deleted in the genes indicated were cultured to exponential phase in YPG at 30°C. After formaldehyde crosslinking, isolated nuclei were subjected to ChEC for the times indicated above each lane. DNA was isolated and analyzed as described in the legend to Figure 3-4A.

Cleavage for Uaf30-MNase was observed at the rDNA promoter region in the wild-type strain and in all three mutant strains (Fig. 3-19, lanes 1-20). This is consistent with previous *in vivo* footprinting analysis showing that UAF remains bound to the promoter region in the absence of RRN7, RRN3 or of the Pol I subunit RPA43 (Bordi et al., 2001). In addition the typical cleavage pattern for the CF subunit Rrn7 around the UE was detected in *rpa135Δ* and *rrn3Δ* strains (Fig. 3-19, lanes 21-30). This is in contrast to the *in vivo* data that could not detect the CF footprint in the absence of RRN3 or Pol I (Bordi et al., 2001). Bordi *et al*. inferred the absence of CF indirectly from DNA protection patterns while in the ChEC analysis the physical association of this factor with the CP was determined.

Taken together the above results lead to the conclusion that the association of UAF with its respective binding site does not require CF, Pol I or Rrn3. Furthermore, UAF and CF form a stable complex at the rDNA promoter region, even in the absence of a Pol I-Rrn3 complex. Modification of the yeast SPT15 locus for expression of TBP-MNase in the mutant strains failed in spite of repeated attempts. Therefore it was not possible to analyze TBP association in the absence of Pol I or Rrn3.

3.5.4 RNA polymerases II and III gain access to the promoter region in the UAF30 deletion mutant

Primer extension analyses revealed that the UAF30 deletion strain uses both RNA polymerases I and II for rRNA transcription, with most of the transcripts derived by Pol I and ~10% of transcription carried out by Pol II (Siddiqi et al., 2001). Interestingly, in these experiments the sites for Pol II initiation were localized upstream of the Pol I initiation site (+1), ranging from position -9 to -95 with a major start site at approximately position -29 (Vu et al., 1999). Initiation of Pol II transcription requires the transcription factor TFIID, which is composed of TBP and several TBP-associated factors (Lee and Young, 2000). As shown in Fig. 3-16, binding of TBP in the *uaf30Δ* strain was observed upstream of the 35S rDNA promoter. This suggests an involvement of TBP in initiation of Pol II transcription upstream of the Pol I promoter.

To investigate the association of Pol I, Pol II and, as a control, Pol III with the rDNA promoter region, ChEC experiments were carried out with both wild-type and *uaf30Δ* strains expressing MNase fusion proteins of Pol I subunit Rpa190, Pol II subunit Rpb3 and Pol III subunit Rpo31. As a further control, Brf1 was included in the analysis. This protein is together with TBP and Bdp1 part of the RNA polymerase III transcription initiation factor TFIIIB. The results for the Southern blot analyses are depicted in Fig. 3-20. Profiles of MNase cuts within the promoter region are illustrated in Fig. 3-21.

As observed earlier (Merz et al., 2008) Rpa190-MNase produced a distinct cleavage pattern spreading along the entire transcribed 35S rDNA region in the UAF30 wild-type strain (Fig. 3-20, lanes 1-5). In contrast, in the *uaf30Δ* strain Pol I association with the transcribed region was strongly reduced (Fig. 3-20, lanes 6-10). This is consistent with recent ChIP data, showing a reduction in overall association of Pol I with the rDNA tandem array in the absence of UAF30 (Hontz et al., 2009). As outlined above the association of Hmo1 with the 35SrDNA region, which is Pol I-dependent and clearly detected in the wild-type strain, was also disrupted in the *uaf30Δ* mutant (Fig. 3-12). Additionally a shift of Rpa190-MNase mediated cleavage events to upstream promoter regions was observed (see Fig. 3-21 for a profile analysis of lanes 5 and 10 in Fig. 3-20, upper panel).

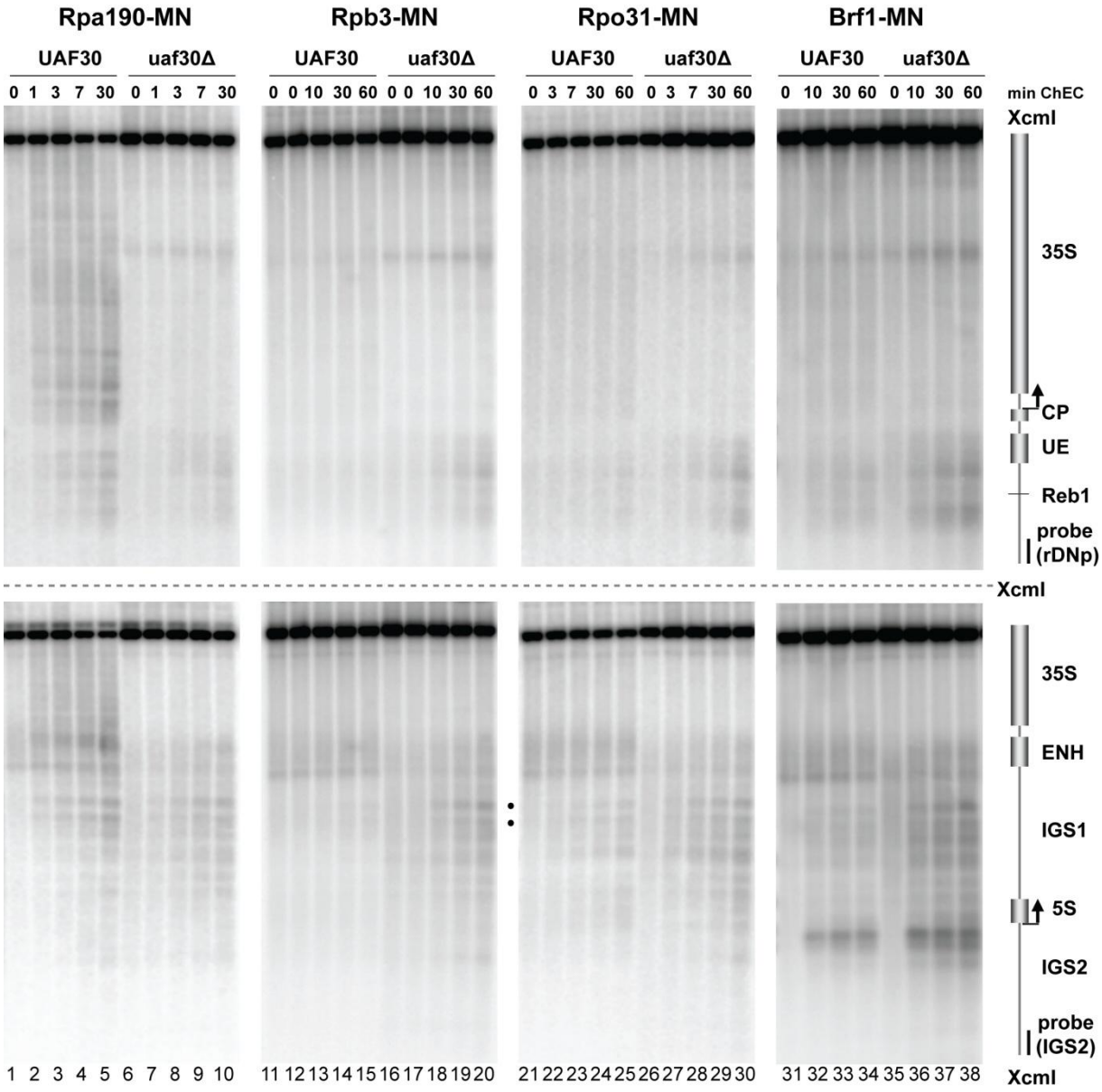

Fig. 3-20 RNA Polymerases II and III gain access to the promoter region in the UAF30 deletion mutant

Yeast strains (y624, y1174, y1273, y1294, y1330, y1681, y1688, y1694) expressing the genes indicated above each panel as fusion proteins with a C-terminal MNase and carrying a wild-type UAF30 locus, or a complete deletion of the gene were cultured to exponential phase in YPD at 30°C. After formaldehyde crosslinking, isolated nuclei were subjected to ChEC for the times indicated above each lane. DNA was isolated and analyzed as described in the legend to Figure 3-16.

For UAF30 wild-type strains expressing MNase fusion proteins of Rpb3, Rpo31 and Brf1 no cleavage was detected within the 35S coding region (Fig. 3-20, lanes 11-15, 21-25 and 31-34). The Rpb3 fusion protein produced weak cuts within the 35S rDNA promoter region in the *uaf30Δ* strain (Fig. 3-20, upper panel, lanes 16-20), coinciding with the cleavage sites of TBP-MNase in this genetic background (see Fig. 3-21 for a profile analysis of lanes 15 and 20

in Fig. 3-20, upper panel and compare with profile analysis in Fig. 3-17, upper panel). Unexpectedly also Rpo31 and the Pol III transcription factor Brf1 cut the rDNA at these sites in the UAF30 deletion mutant (Fig. 3-20, lanes 26-30 and 35-38, see Fig. 3-21 for a profile analysis of lanes 25, 30, 34 and 38 in Fig. 3-20, upper panels).

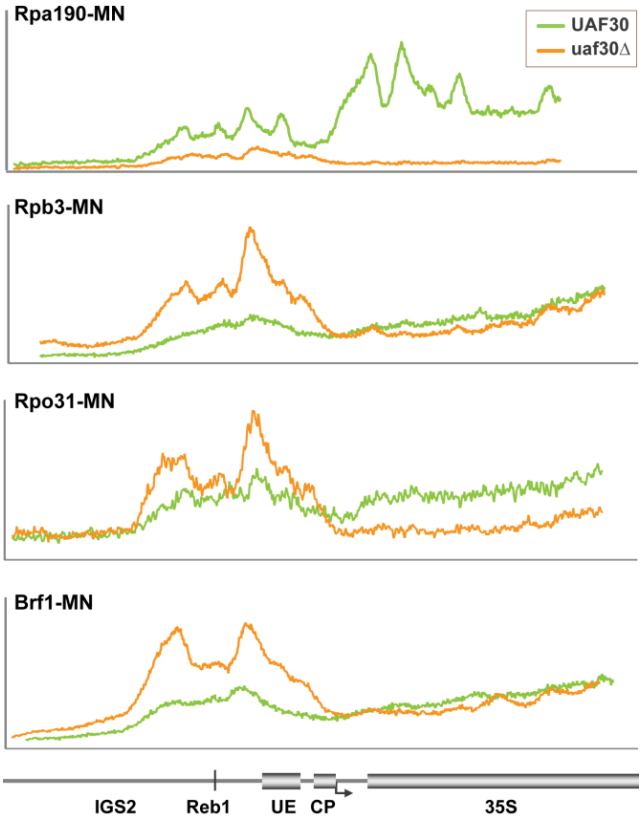

Fig. 3-21 Profile analysis of Fig. 3-20
Profiles of DNA-fragment patterns obtained after 30 minutes (Rpa190-MNase expressing strains) or 60 minutes (all other strains) ChEC of the fusion protein indicated in the legend of each graph. FLA-5000 data presented in Fig. 3-20 were analyzed with the MultiGauge software (FujiFilm). The signal intensity in the respective lanes was plotted against the distance of migration in the gel. Signal intensities of MNase profiles compared in one graph were normalized to the different rDNA amounts in UAF30 and uaf30Δ strains (typically 1:1.5). A cartoon of the genomic region including important features as described in the legend of Fig. 1-2 is indicated below the graphs.

The profile analysis shows that the cleavage mediated by Rpb3, Rpo31 and Brf1 fusion proteins match exactly the cuts mediated by TBP-MNase in this genetic background (compare profile analysis in Fig. 3-21 with Fig. 3-17).

The above results suggest that transcription initiation at regions upstream of the Pol I promoter might be achieved not only by Pol II but also by Pol III initiation complexes in the UAF30 deletion mutant. The coherence of TBP colocalization with these complexes supposes

a possible role for this general transcription factor in initiation of 35S rDNA transcription by RNA polymerases other than Pol I.

The membranes in Fig. 3-20 were also hybridized with a probe detecting the 3´end of the 35S rDNA, the 5S rDNA, and parts of the intergenic spacer regions (Fig. 3-20, lower panels). As expected, Rpo31- and Brf1-MNase mediated cleavage at the 5S rRNA gene in the wild-type and the *uaf30Δ* strains (Fig. 3-20, lower panels; lanes 21-38). Rpo31-MNase mediated cleavage within 5S rDNA was rather weak, but similar results were obtained for several other Pol III subunits (Diploma thesis Manuel Wittner). Interestingly, enhanced cleavage by Rpb3-MNase in the *uaf30Δ* strain was detected at the bidirectional Pol II promoter within IGS1 (Fig. 3-20, lower panel; lanes 11-20, black dots). This correlates with the increased cleavage by TBP-MNase in this genetic background (Fig. 3-16, lower panel, lanes 21-30, black dots). These results suggest that UAF30 deletion decreases rDNA silencing of Pol II transcription within this region.

Transcription from this site is regulated by the silent information regulator Sir2 and drives repeat expansion (Kobayashi et al., 2005). As mentioned before, the increase in cleavage mediated by Pol II and TBP as a potential Pol II transcription factor within the IGS1 might represent an upregulation of E-pro transcription in the *uaf30Δ* strain. The enhanced E-pro transcription is likely the reason for the expansion of rDNA repeats observed in this genetic background.

3.5.5 Inhibition of Pol I transcription does not allow the access of Pol II and Pol III to the rDNA promoter region

To investigate whether the binding of Pol II and Pol III at the rDNA promoter region is induced by the absence of UAF30 or occurrs as a consequence of impaired Pol I transcription, ChEC experiments were carried out in the *RRN3* and *rrn3-ts* strains, expressing Rpa190-, Rpb3-, or Rpo31-MNase (Fig. 3-22).

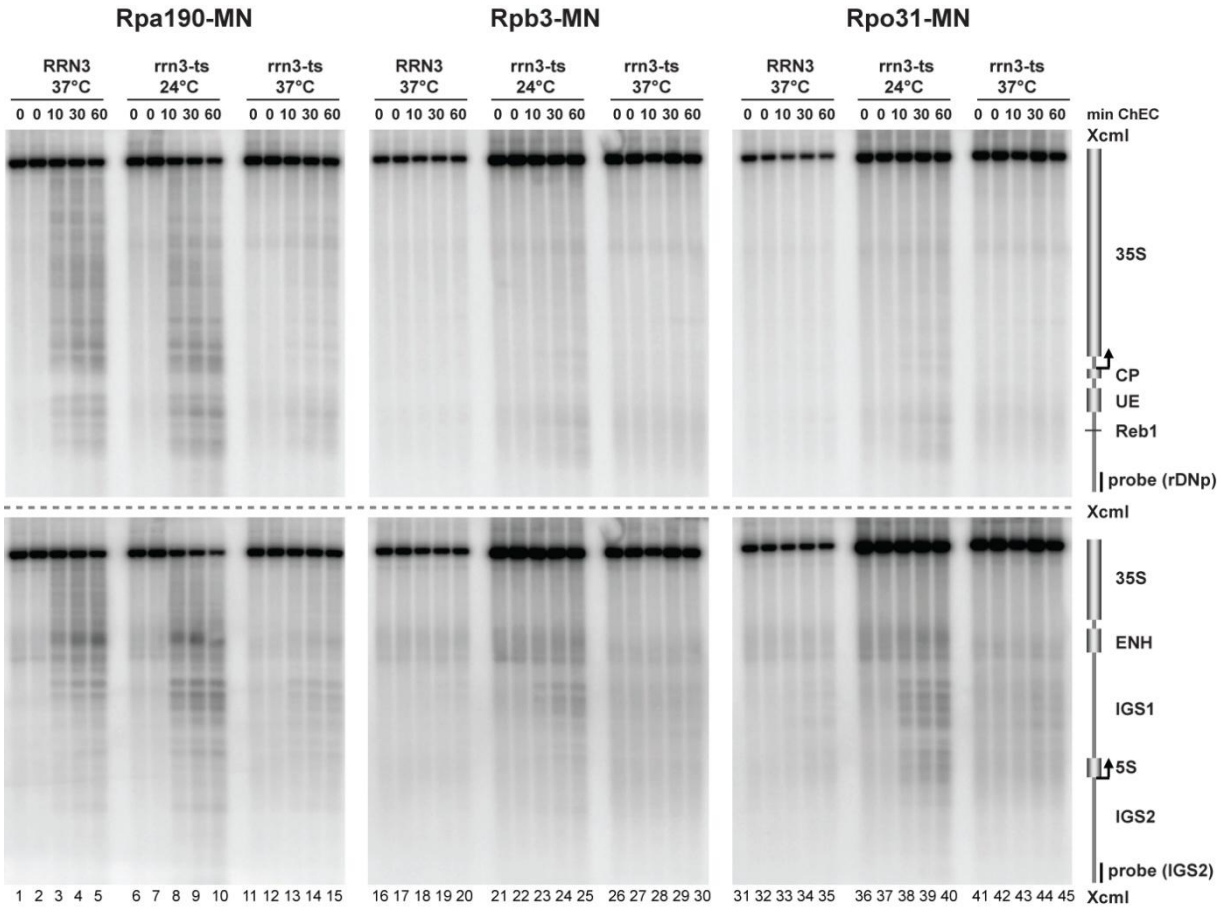

Fig. 3-22 Disruption of Pol I transcription does not allow access of Pol II and Pol III to the rDNA
(A) Yeast strains (y938, y945, y1560, y1566, y1708, y1713) expressing the genes indicated above each panel as fusion proteins with a C-terminal MNase and carrying a wild-type RRN3 locus, or a temperature sensitive rrn3-ts allele were cultured to exponential phase in YPD at 24°C. Cells were split and either fixed with formaldehyde or further incubated in YPD at 37°C for another 120 minutes before formaldehyde crosslinking. Isolated nuclei were subjected to ChEC for the times indicated above each lane. DNA was isolated and analyzed as described in the legend to Fig. 3-16.

As expected, Rpa190-MNase cleavage in the rrn3-ts strain could no longer be detected at the 35S rDNA at 37°C (Fig. 3-22, lanes 11-15). In addition, Rpb3- and Rpo31-MNase fusion proteins did not cleave at the 35S rDNA promoter in this condition (Fig. 3-22, lanes 26-30 and 41-45). These results demonstrate, that shutting off Pol I transcription does not allow for association of other polymerases with the rDNA promoter region. Therefore, the presence of UAF seems to prevent binding of alternative initiation complexes to this region. Hybridization of the membranes with probe IGS2 again revealed as already observed above that Rpo31-MNase mediated cleavage within 5S rDNA was rather weak (see also Fig. 3-20).

3.5.6 Chromatin immunoprecipitation assay (ChIP) to confirm the interaction of factors with the rDNA promoter in the UAF30 deletion mutant

The above results suggest a possible interaction of Pol II and Pol III initiation complexes with the rDNA promoter region in the *uaf30Δ* strain. This is consistent with the emergence of Pol II transcripts upon deletion of Uaf30 (Siddiqi et al., 2001). To corroborate these results Chromatin immunoprecipitation (ChIP) experiments were performed. With this method the direct physical interaction of proteins with rDNA can be investigated *in vivo*. Therefore the ChIP assay is the appropriate method to confirm the results obtained in the ChEC experiments.

ChIP was performed with formaldehyde-fixed cells using the triple HA-tag present at the C-terminus of each MNase fusion protein. After cell lysis the DNA was sonicated to obtain small fragments with a size of 500-1000 bp. A fraction of the lysates served as an input control. The residual chromatin extracts were incubated with an antibody against the HA-Tag and with Protein G sepharose to enrich the MNase-HA_3-tagged proteins bound by the antibody. Thereby the proteins together with the associated DNA fragments were precipitated. ChIP was performed in three independent experiments for each protein. The relative DNA amounts present in input and precipitated (IP) DNA were determined by quantitative PCR. All samples were run in triplicate to ensure accuracy of the data. The average values of IP normalized to the input from the three independent experiments for each protein and standard deviations were calculated.

The percentage from three different rDNA regions co-precipitating with either Rpa190, Rpb3, Rpo31, TBP, Brf1 and, as a control, Reb1 in wild-type and *uaf30Δ* strains was determined (Fig. 3-23). The rDNA promoter, 25S and 5S rRNA coding regions were amplified in qPCR analysis using specific primer pairs that are depicted in Fig. 3-23.

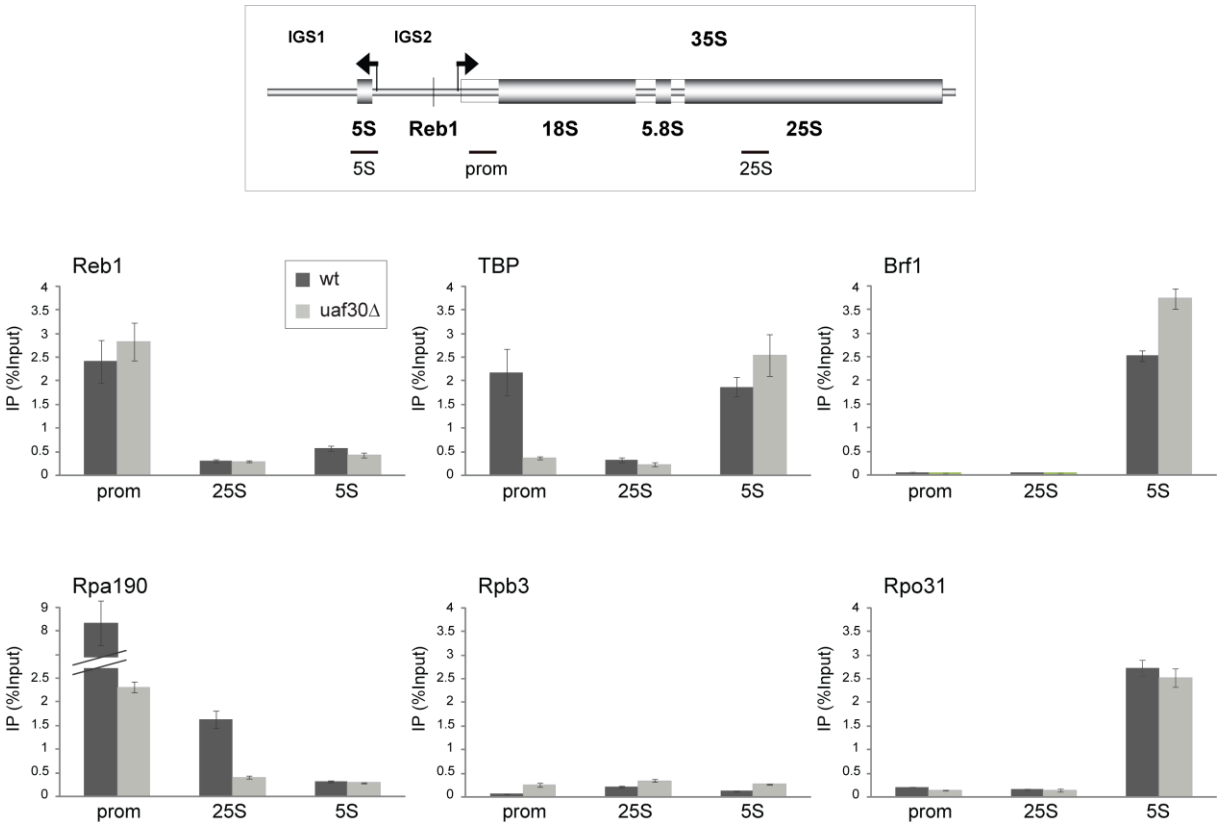

Fig. 3-23 ChIP assay in the UAF30 deletion mutant

A cartoon of the genomic rDNA locus including important features as described in the legend of Fig. 1-2 and the regions amplified by specific primer pairs in the quantitative PCR (qPCR) analysis of the ChIP experiments (prom, 5S, 25S) is depicted above. Yeast strains (y624, y1174, y1184, y1185, y1273, y1294, y1328, y1329, y1330, y1681, y1688, y1694) expressing the genes indicated above each panel as fusion proteins with a C-terminal triple HA-tag and carrying a wild-type UAF30 locus, or a complete deletion of the gene were cultured to exponential phase in YPD at 30°C. After formaldehyde crosslinking, crude extracts were prepared and subjected to ChIP experiments as described in Materials and Methods. Specific rDNA regions present in the input and retained on the beads (IP) were quantified by qPCR with primer pairs 969/970, 710/711, and 920/921 amplifying the promoter region (prom), the end of the 25S rRNA coding sequence (25S) and the 5S rRNA coding sequence (5S), respectively. The bar graphs depict percent of total input DNA retained after precipitation (IP) of the HA-tagged proteins indicated. Error bars represent the standard deviation of three independent ChIP experiments, each of which was analyzed in triplicate qPCR reactions.

The ChIP data reflected well most of the results obtained in the ChEC analyses. Strong enrichment of rDNA promoter DNA in both wild-type and *uaf30Δ* strains was observed in precipitations with Reb1 protein. For the Pol I subunit Rpa190 an about 4-fold reduction in association with promoter and 25S regions in the UAF30 deletion strain was detected. This is consistent with recent ChIP data, also showing a reduced Pol I association with the rDNA locus in the absence of Uaf30 (Hontz et al., 2009) and with the ChEC data shown above (Fig. 3-20). Accordingly, the amount of rDNA promoter co-precipitating with TBP decreased in the *uaf30Δ* strain as already visualized in the Southern blot (Fig. 3-16). These results confirm, that only few genes are actively transcribed in the *uaf30Δ* strain (Hontz et al., 2009).

However, a specific enrichment of Rpb3, Rpo31 or Brf1 at the 35S rDNA promoter in the *uaf30Δ* strain could not be detected with this method. The ChIP data for the HA-tagged Rpb3 protein show that Pol II association at the rDNA promoter and coding regions in the *uaf30Δ* mutant seems to be slightly enriched to an IP percentage of 0.2%, but this is still in the range of background detection. Similar results could not be obtained for Rpo31 or Brf1. As the ChEC signals for these proteins were even lower than observed for Rpb3, the interaction of these factors with the rDNA promoter is presumably only transient and very weak. Therefore the detection of these interactions might be difficult using the ChIP method.

3.6. Silencing of ribosomal DNA in the UAF30 deletion mutant

In the UAF30 deletion mutant, the function of UAF to suppress Pol II transcription of the 35S rDNA is impaired (Siddiqi et al., 2001). Different from silencing of rRNA gene transcription by Pol II, silencing of Pol II reporter genes inserted into the rDNA locus is also dependent on UAF (Cioci et al., 2003). The above results demonstrate that in addition silencing of the bidirectional Pol II promoter E-pro within the IGS1 might be impaired in the *uaf30Δ* mutant.
In *S. cerevisiae* the Sir2 protein is required for efficient silencing of Pol II-dependent reporter genes inserted at the rDNA locus (Bryk et al., 1997; Fritze et al., 1997; Smith et al., 1997) and for silencing of E-pro transcription within IGS1 (Kobayashi and Ganley, 2005). The Sir2 protein is together with Net1 and Cdc14 a subunit of the nucleolar RENT complex and is associated with both promoter and enhancer regions of the rDNA locus (Huang et al., 2003).
Apart from its role in rDNA silencing the SIR2 gene is important for silencing of the cryptic mating type genes at the HML and HMR loci and at the telomeric regions in S. *cerevisiae* (S Loo and J Rine, 2003).

3.6.1 Deletion of UAF30 leads to loss of Sir2 from the rDNA locus

The Sir2 gene is required for efficient silencing of Pol II-dependent reporter genes inserted at the rDNA locus (Bryk et al., 1997; Fritze et al., 1997; Smith et al., 1997). Recent studies revealed that silencing of reporter genes was strongly decreased in mutants with defects in UAF (Cioci et al., 2003). Therefore the association of Sir2 with rDNA was analyzed in UAF

deletion strains. ChEC experiments were carried out with UAF wild-type and the UAF mutant strains *rrn5Δ* and *uaf30Δ* expressing Sir2-MNase.

As mentioned before, Sir2 is involved in silencing at the HML and HMR loci in S. *cerevisiae* (S Loo et al., 2003). Therefore Southern blot analysis for Sir2-MNase was performed with probes rDNp and IGS2 detecting promoter and enhancer regions of the 35S rDNA (Fig. 3-24A) and in addition as an internal control with probe GIT1 detecting the HMR locus (Fig. 3-24B).

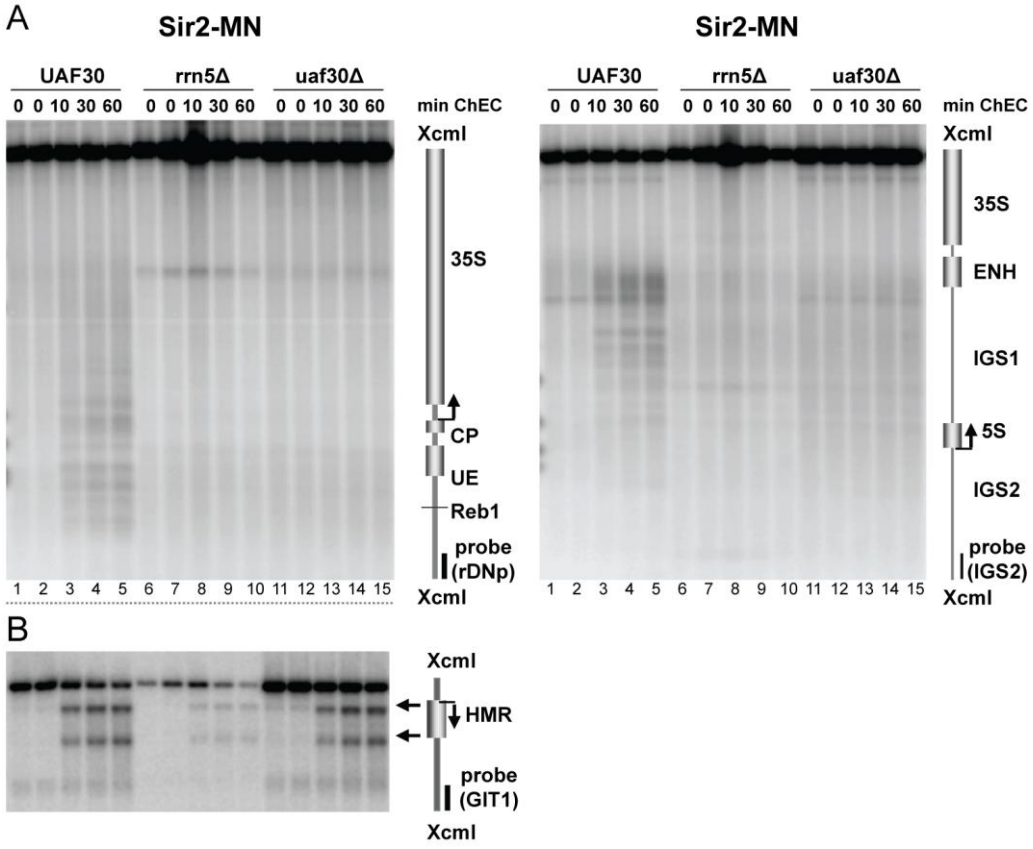

Fig. 3-24 Sir2 association with the 35S rDNA is disrupted upon deletion of UAF30
(A) Yeast strains (y1450, y1674, y1691) expressing SIR2 as fusion protein with a C-terminal MNase and carrying a wild-type UAF30 or RRN5 locus, or a complete deletion of one of the genes were cultured to exponential phase in YPD at 30°C. After formaldehyde crosslinking, isolated nuclei were subjected to ChEC for the times indicated above each lane. DNA was isolated and analyzed as described in the legend to Figure 3-16. (B) The same membranes as in (A) were additionally hybridized withIn with probe GIT1 detecting the HMR locus.

In the UAF30 wild-type strain Sir2-MNase cut at the Pol I promoter, extending into the 35S rRNA coding region and within the IGS1 and ENH region (Fig. 3-24A, lanes 1-5). This is consistent with previous ChIP data localizing the protein to both promoter and enhancer regions of rDNA (Huang et al., 2003). The overall cleavage pattern closely resembled the Net1- and Cdc14-MNase cleavage pattern (Fig. 3-16, lanes 31-35 and Fig. 3-27A, lanes 1-5).

In both UAF mutant strains, association of Sir2 with rDNA promoter and IGS1/ENH regions was completely abolished (Fig. 3-24A, lanes 6-15). In contrast, association of the RENT subunit Net1 could still be detected in the UAF30 deletion strain (Fig. 3-16, lanes 36-40). Cleavage of Sir2-MNase at the HMR locus was not affected, indicating that Sir2 levels were not limiting in the UAF30 deletion strain and that the association with the rDNA locus was specifically affected (Fig 3-24B).

The loss of Sir2 from the rDNA locus in the UAF deletion strains gives an explanation for the impaired silencing of Pol II reporter genes in PSW strains (Cioci, 2003). Consistently, we find that Sir2 is absent from the rDNA locus in the RRN5 deletion strain. Furthermore it has been shown that SIR2 overexpression cannot rescue the Pol II silencing defect in rDNA of PSW strains which might indicate that UAF is required to recruite Sir2 to the rDNA.

3.6.2 TBP association with the IGS1 is enhanced in the absence of SIR2

The above data demonstrate, that Sir2 binding to the rDNA is abolished in the *uaf30Δ* strain. Since Sir2 has been shown to silence the bidirectional Pol II promoter within IGS1 (Kobayashi et al., 2005), loss of this protein might be the cause for an increased cleavage of TBP- and Pol II-MNase within this region observed upon UAF30 deletion (Figs. 3-16 and 3-20). To investigate whether TBP association with this region is also enhanced in the absence of Sir2 ChEC experiments were performed in a SIR2 wild-type and *sir2Δ* strain, expressing TBP-MNase (Fig. 3-25).

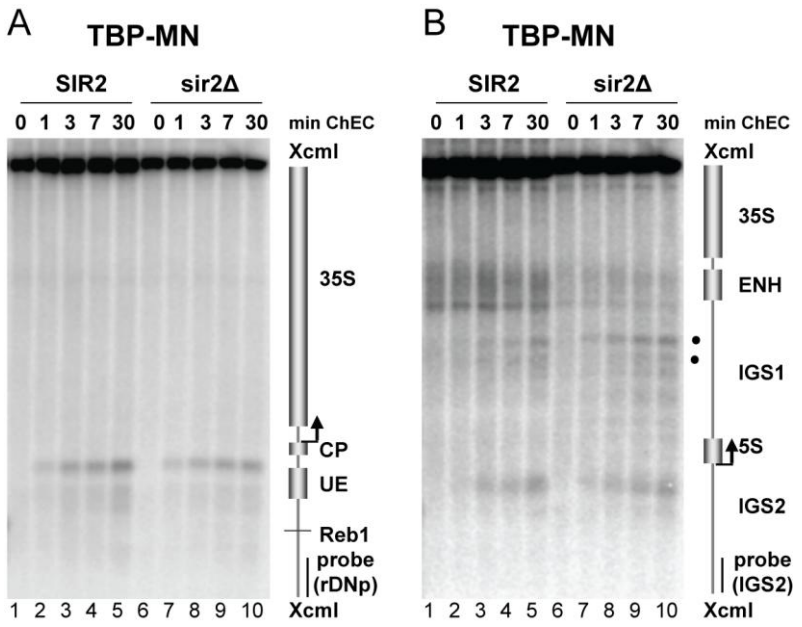

Fig. 3-25 TBP association in a SIR2 deletion mutant
(A) Yeast strains (y1185, y1346) expressing TBP as fusion protein with a C-terminal MNase and carrying a wild-type SIR2 locus, or a complete deletion of the gene were cultured to exponential phase in YPD at 30°C. After formaldehyde crosslinking, isolated nuclei were subjected to ChEC for the times indicated above each lane. DNA was isolated and analyzed with probe rDNp. (B) The identical membranes in (A) were analyzed with probe IGS2.

Cleavage by TBP-MNase in the wild-type strain occurred as already shown in Fig. 3-16 between the UE and the CP. In the SIR2 deletion strain identical cutting was observed within the rDNA promoter region (Fig. 3-25A, lanes 1-10). Whereas TBP-MNase mediated cleavage at the 35S rDNA promoter was unaltered in the *sir2*Δ strain, an increased cleavage within IGS1 compared to the cleavage occurring in the wild-type strain was observed (Fig. 3-25B, lanes 1-10, black dots). The observed pattern were very similar to the TBP-MNase mediated cleavage in the IGS1 in the *uaf30Δ* strain (Fig. 3-25B, compare lanes 6-10 with Fig. 3-16, lower panel, lanes 26-30, black dots). This can be visualized even more clearly in a profile analysis shown in Fig. 3-26 for TBP-MNase in the *uaf30Δ* and in the *sir2*Δ strains compared to the respective wild-type strains.

Thus, the loss of Sir2 from the rDNA in the UAF30 deletion strain can well account for the observed increase in association of Pol II and TBP with the IGS1. Whether this leads to an increased transcription of the bidirectional Pol II promoter in the absence of UAF still remains to be determined. We also investigated association of the Pol I transcription machinery and of other RNA polymerases with the rDNA promoter in SIR2 deletion strains, but could not detect any differences when compared to the associaton of these factors in the corresponding wild-type strains (data not shown). This in good accordance with the observation that SIR2 deletion affects silencing of Pol II reporter genes in rDNA but does not influence Pol I transcription of 35S rRNA genes (Oakes et al., 1999).

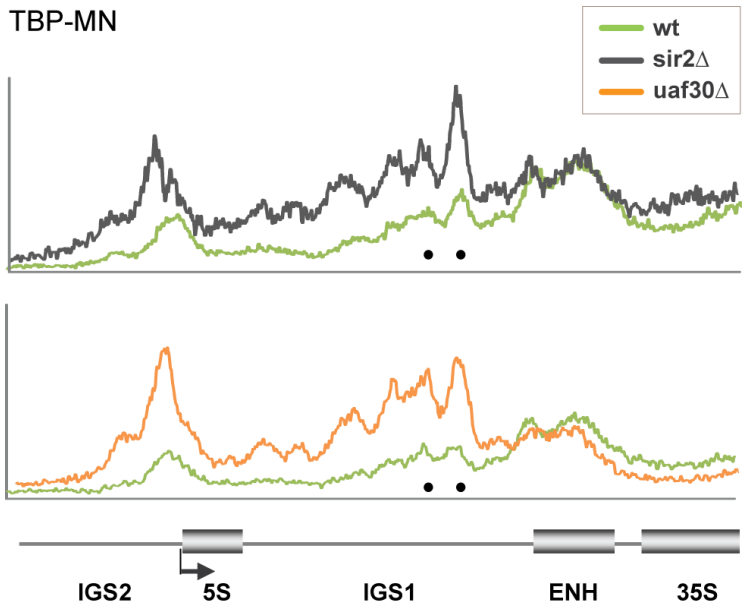

Fig. 3-26 Profile analysis of TBP association at the rDNA enhancer in mutant strains
Profiles of DNA-fragment patterns obtained after 60 minutes ChEC of the fusion protein indicated in the legend of ach graph. FLA-5000 data presented in Figs. 3-16 and 3-25 were analyzed with the MultiGauge software (FujiFilm). The signal intensity in the respective lanes was plotted against the distance of migration in the gel. Signal intensities of MNase profiles compared in one graph were normalized to the different rDNA amounts in UAF30 and uaf30Δ strains (typically 1:1.5) and SIR2 and sir2Δ strains (typically 1:0.5). A cartoon of the genomic region including important features as described in the legend of Fig. 1-2 is indicated below the graphs.

3.6.3 Association of RENT subunit Cdc14 is reduced upon deletion of UAF30

The proteins Sir2 and Net1 are subunits of the nucleolar RENT complex. As Net1 and Sir2 behaved different in the ChEC analysis in the Uaf30 deletion strain, the association of the third RENT subunit Cdc14 was also analyzed in this genetic background. The RENT complex is recruited to the rDNA enhancer via Fob1. To complete the analysis of the association of the RENT complex with respect to UAF deletion, ChEC analysis was performed in UAF30 wild-type and *uaf30Δ* strains expressing Cdc14 or Fob1 as MNase fusion proteins. The results are shown in Fig. 3-27.

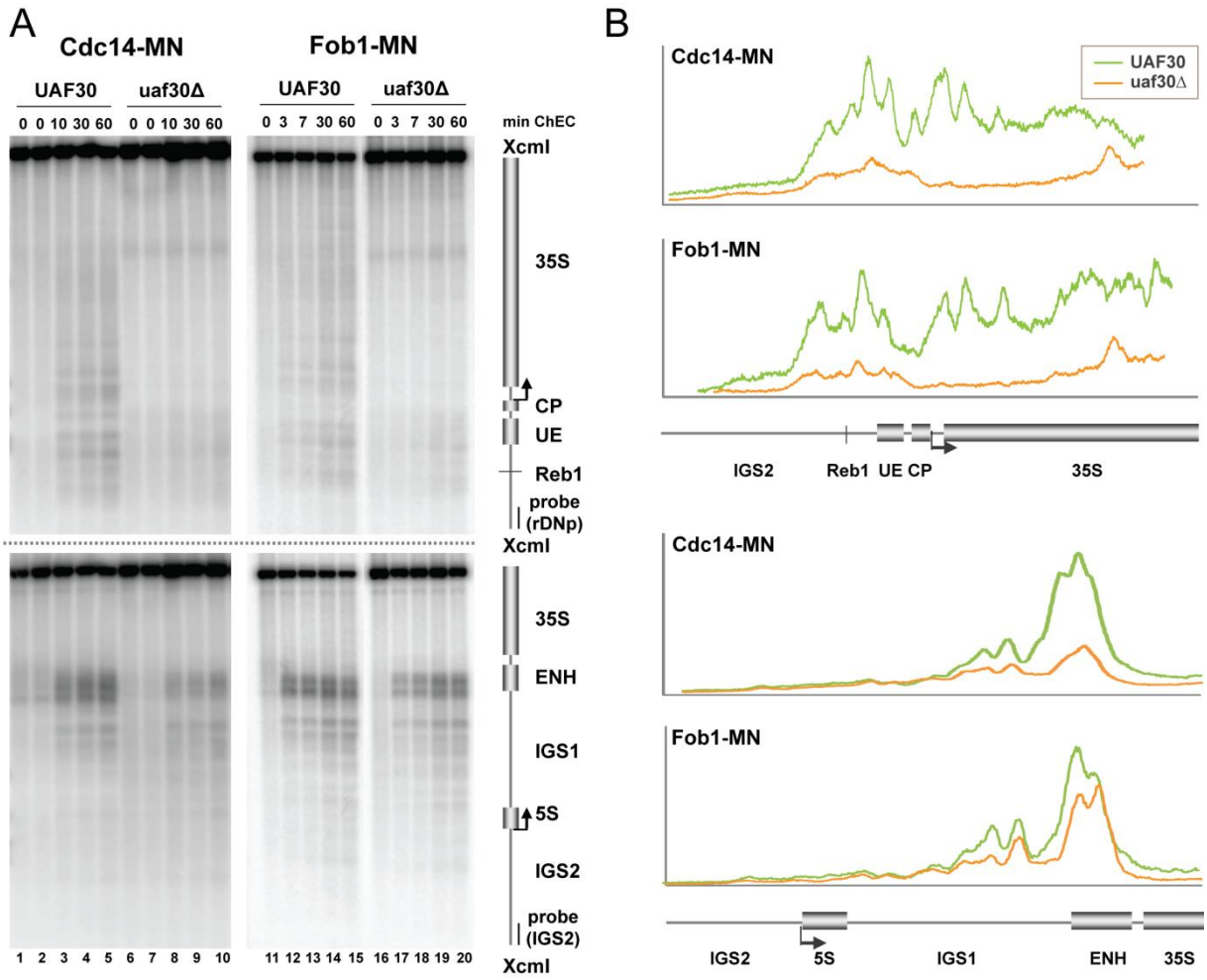

Fig. 3-27 Association of Cdc14 and Fob1 with the rDNA locus in the UAF30 deletion strain
(A) Yeast strains (y624, y1174, y1273, y1294, y1330, y1681, y1688, y1694) expressing the genes indicated above each panel as fusion proteins with a C-terminal MNase and carrying a wild-type UAF30 locus, or a complete deletion of the gene were cultured to exponential phase in YPD at 30°C. After formaldehyde cross-linking, isolated nuclei were subjected to ChEC for the times indicated above each lane. DNA was isolated and analyzed as described in the legend to Figure 3-16. (B) Profiles of DNA-fragment patterns obtained after 60 minutes ChEC of the fusion protein indicated in the legend of each graph. FLA-5000 data presented in (A) were analyzed with the MultiGauge software (FujiFilm). The signal intensity in the respective lanes was plotted against the distance of migration in the gel. Signal intensities of MNase profiles compared in one graph were normalized to the different rDNA amounts in UAF30 and uaf30Δ strains (typically 1:1.5). A cartoon of the genomic region including important features as described in the legend of Fig. 1-2 is indicated below the graphs.

In the wild-type strain the Cdc14 mediated cleavage was identical to the cleavage pattern produced by the other RENT subunits Sir2 and Net1 (Fig. 3-27A, compare lanes 1-5 to Fig. 3-16, lanes 31-35 and Fig. 3-24A, lanes 1-5). In the UAF30 deletion mutant the interaction of Cdc14 with both promoter and enhancer regions was sustantially reduced (Fig. 3-27A, lanes 6-10, see Fig 3-27B for a profile analysis of lanes 5 and 10 in Fig. 3-27A). The expression of the Fob1-MNase fusion protein in wild-type cells revealed strong cleavage events within the

rDNA enhancer region. In addition, cleavage at the rDNA promoter and the 5´end of the 35S coding region resembling the pattern observed for the RENT subunits was detectable (Fig. 3-27A, lanes 11-15). This is consistent with ChIP data localizing Fob1 to both the enhancer and to a lower extent at the promoter region of the rDNA (Huang et al., 2003). In the *uaf30Δ* mutant, binding of Fob1 to the RFB was nearly unaffected, whereas association with the promoter region was strongly reduced (Fig. 3-27A, lanes 16-20; see Fig. 3-27B for a profile analysis of lanes 15 and 20 in Fig. 3-27A).

Thus, RENT subunits behave differently in their association with the rDNA locus upon UAF30 deletion. Whereas Sir2 dissociates from the rDNA locus (Fig. 3-24A), Cdc14 remains partially bound to both promoter and enhancer regions (Fig. 3-27). Net1 is still fully associated with the ENH region of the rDNA locus but specific recruitment to its binding sites at the rDNA promoter region seems to be impaired in the UAF30 deletion mutant (Fig. 3-16). The association of Fob1 with rDNA enhancer regions remains unaffected whereas binding to the promoter is almost completely abolished (Fig. 3-27). Thus, Net1 and to a lesser extent Cdc14 can still be recruited to the rDNA enhancer region via Fob1 in the UAF30 deletion strain. However, the presence of Fob1 is not sufficient to recruit Sir2 to this region in the *uaf30Δ* strain.

4 Discussion

4.1 UAF determines chromatin structure at the rDNA locus in *S. cerevisiae*

The Pol I transcription factor UAF has been demonstrated to be crucial for both, polymerase specificity and silencing of Pol II transcription at the rDNA locus. Since chromatin provides a mean to control access of protein factors to DNA a model has been proposed in which UAF is an important determinant for chromatin structure at the rDNA locus (Cioci et al., 2003). However, the exact nature of rDNA chromatin established by UAF remained to be characterized. The aim of this study was to provide a detailed analysis of the UAF-dependent rDNA chromatin state thus providing for the first time the molecular basis for the observed phenomena.

4.1.1. UAF organizes promoter and long-range chromatin structure at the 35S rRNA gene

Chromatin structure at the rDNA locus was analyzed by exogenous MNase digestion, revealing drastic structural changes in the chromatin domain encompassing the 35S rRNA gene upon deletion of components of the UAF complex (Fig. 3-4). Although UAF binds site-specific to a DNA element in the 35S rDNA promoter chromatin alterations extend over the 35S coding region, whereas the IGS regions are hardly affected (Figs. 3-4 and 3-5). The observed changes are even more pronounced in the PSW strain compared to the UAF30 deletion mutant. Accordingly in the PSW strain Pol I transcription is completely abolished whereas in the *uaf30Δ* strain a heterogenous population of Pol I and Pol II transcribe the rRNA genes. This indicates that the respective transcriptional state of rDNA may determine chromatin structure of the locus.

Another alternative chromatin state displaying MNase accessibility pattern compatible with the presence of regularily phased nucleosomes was detected at the 35S coding region of several Pol I-defective mutant strains (Fig. 3-4). UAF is still bound to the UE in these mutants (Fig. 3-19). Interestingly, when analyzing a mutant strain in which both CF subunit RRN7 and UAF subunit RRN9 have been deleted rDNA chromatin structure is identical to that observed in the UAF deletion mutants (PhD thesis Katharina Merz). Thus, the presence of UAF is

required to establish the specific chromatin state observed in the *rrn7Δ* strain. This is consistent with the observation, that a PSW phenotype in a core factor deletion strain can only be established upon deletion of UAF subunit genes (Oakes et al., 1999) and argues for a role of UAF in organizing rDNA chromatin structure downstream of its binding site (Cioci et al., 2003).

The absence of UAF subunits strongly reduces or even completely abolishes Pol I transcription of 35S rRNA genes (Vu et al., 1999; Siddiqi et al., 2001). It is thus conceivable, that the changes in chromatin structure within the transcribed 35S rDNA region are a consequence of transcription by different RNA polymerase systems. However, conditional shut-down of Pol I transcription in a RRN3 temperature sensitive strain does not allow for the establishment of an alternative chromatin state as observed in the absence of UAF subunits (Fig. 3-6). Thus, 35S rDNA chromatin is at least transiently stable. This is in agreement with recent data from our group demonstrating that while Pol I leaves the 35S rDNA upon RRN3 inactivation, Hmo1 – a specific chromatin component of actively transcribed rRNA genes - still remains associated with this locus (Merz et al., 2008). The data show that the absence of Pol I transcription (at least in a short-term) is not sufficient to reorganize rDNA chromatin and that additional mechanisms are required for the chromatin transition.

4.1.2. rDNA repeats are assembled into nucleosomes in the absence of UAF

In the UAF30 deletion strain less than 10% of the rRNA genes are transcribed by Pol I whereas the remaining repeats are transcribed by an average of 1.5 Pol II molecules per rRNA gene (Hontz et al., 2008). The rDNA repeats actively transcribed by Pol I have been shown to be nucleosome-free and largely devoid of histone proteins (Dammann et al., 1993; Merz et al., 2008). However, the chromatin composition of the rDNA template transcribed by Pol II, representing the main population in the *uaf30Δ* strain has not been determined yet.

The regular MNase digestion pattern observed for the 35S coding region together with the distinct arrangement of histone proteins within the open reading frame in the UAF30 deletion mutant suggest a nucleosomal organization of rDNA repeats in this genetic background. This is supported by the observation that rDNA has a strongly reduced psoralen

accessibility upon deletion of UAF subunits (Fig. 3-13). Our quantitative analysis of histone occupancies in the UAF30 deletion mutant revealed similar histone densities at the rDNA locus and the transcriptional inactive GAL1-10 gene locus (Figs. 3-14 and 3-15). In contrast histone density at the rDNA locus is lower than histone density at the GAL1-10 locus in a wild-type strain ((Merz et al., 2008)). Taken together the results demonstrate that the main population of rRNA genes in the UAF30 deletion mutant is nucleosomal.

4.1.3. UAF might influence higher-order chromatin structures at the rDNA locus

For the rDNA locus the organization in a higher-order structure called the “ribomotor” has been proposed. In this model each rDNA transcription unit forms a loop bringing the Pol I promoter in the vicinity of the enhancer element (Kempers-Veenstra et al., 1986). As the Reb1 protein binds to both of these regions it was proposed to be a potential candidate in stabilizing such a structure (Kulkens et al., 1992).

ChEC analysis with UAF and CF subunits revealed weak cleavage within IGS1 and the enhancer region for the promoter-bound factors ((Fig. 3-16), and (Merz et al., 2008)). This observation supports the idea of a loop structure at the rDNA locus allowing for a transient association of promoter-bound factors with the rDNA enhancer region. Intriguingly, the weak cleavage of UAF and CF subunits is not detectable in the UAF30 deletion strain, where the promoter association of these factors is strongly impaired. As an alternative explanation the loop structure at the rDNA locus might be affected in the UAF30 deletion strain. This hypothesis is strengthened by the observation that the association of Fob1 with the rDNA promoter region is almost completely abolished in the UAF mutant whereas in the wild-type strain the protein binds to both the enhancer and to a lower extent to promoter regions of the rDNA (Fig. 3-27). Thus, Fob1 might also be implicated in the organization of higher-order structures at the rDNA locus. Consistently, cleavage of UAF and CF subunits within the enhancer region is not detected in *fob1Δ* strains (data not shown).

Taken together the data suggest that in the absence of UAF30 rDNA arrangement in higher-order structures might be at least partially affected, since association of promoter-bound factors with the rDNA enhancer region and vice versa is disrupted in this genetic background. However, binding of Reb1, which has been proposed to play a role in stabilizing such loop structures, is not abolished in the UAF30 deletion mutant (Fig. 3-16).

4.2 UAF is required for proper assembly of the Pol I initiation complex at the rDNA promoter region

In the UAF30 deletion strain binding of other UAF or CF subunits is strongly affected explaining the reduced Pol I transcription (Hontz et al., 2008). However, the specific changes in rDNA promoter chromatin in this genetic background have not been determined yet. Therefore ChEC experiments were performed to elucidate how promoter structure and association of factors with this region are reorganized upon deletion of UAF30.

4.2.1. UAF is required for the specific association of Pol I transcription factors with the rDNA promoter region

The ChEC experiments performed in this study allowed a detailed analysis of binding characteristics for promoter-bound factors in the absence of UAF30 (Fig. 3-16). Consistent with recent ChIP data (Hontz et al., 2008), the association of the UAF subunit Rrn9 with the UE is abolished in this genetic background. Importantly, the Rrn9-MNase fusion protein is properly expressed in the *uaf30Δ* background (Fig. 3-9). Consequently, binding of the CF subunit Rrn7 to the CP is barely detectable in the UAF30 deletion mutant. In a PSW strain deleted in RRN5 Pol I transcription is completely abolished. Accordingly, Rrn7 binding to the CP is not detectable in this genetic background (data not shown).

The association of TBP to the rDNA promoter is decreased in the UAF30 deletion strain. Furthermore, TBP translocates to regions upstream of its typical binding-site within the Pol I promoter. The Net1 protein is similarily delocalized in the mutant background associating with regions flanking the promoter proximal Reb1 binding site. This indicates severe changes in rDNA promoter chromatin architecture in the absence of UAF. This reorganization of transcription factor association is not observed after shut-down of Pol I transcription. Thus, UAF is required for the specific targeting of these factors to their respective binding sites at the rDNA promoter region.

4.2.2. UAF is sufficient for the stable assembly of pre-initiation complexes at the rDNA promoter region

Controverse results have led to two different models for the assembly and maintenance of pre-initiation complexes at the rDNA promoter (Bordi et al., 2001; Aprikian et al., 2001; Steffan et al., 1996) (Fig. 1-5). In contrast to earlier *in vitro* studies the ChEC data obtained in this study argue against the release of CF from the Pol I promoter after each initiation cycle (Aprikian et al., 2001). CF remains associated with the CP after Pol I has left the locus and also in the complete absence of Pol I or Rrn3 (Figs. 3-18 and 3-19). Footprinting analyses suggested that CF binding is dependent on the binding of Rrn3 and Pol I *in vivo* (Bordi et al., 2001). However, while the footprinting method only allows the indirect analysis of DNA protection pattern, the ChEC data provide evidence for the direct physical association of factors at the DNA. Finally, the above study concluded that UAF binds the UE in the absence of CF, Rrn3 or Pol I, which is consistent with the ChEC data (Fig. 3-19). In summary the results support a model of Nomura and co-workers with UAF recruiting CF and TBP to the 35S rDNA promoter, which serves as a platform for transcription initiation by the Pol I-Rrn3 complex (Keys et al., 1996). Accordingly the presence of UAF at the UE is sufficient for stabilizing at least partial PIC assembly at the rDNA promoter region.

4.2.3. UAF limits the access of alternative transcription initiation complexes to the Pol I promoter

Pol II transcription in the UAF deletion strains initiates at a cryptic Pol II promoter which is located upstream of the Pol I transcription start site (Vu et al., 1999). Consistent with this, Pol II is detected upstream of the Pol I promoter flanking a promoter proximal Reb1 recognition sequence in the *uaf30Δ* strain (Fig. 3-20). Interestingly, the TATA-binding protein TBP colocalizes with Pol II in this genetic background, suggesting a role for this general transcription factor in transcription initiation at the cryptic Pol II promoter. Whether other Pol II transcription factors also associate with this region in the UAF30 deletion mutant still needs to be determined in ChEC experiments. Intriguingly, Pol III and the Pol III transcription factor Brf1 also bound to the cryptic promoter region upstream of the Pol I promoter in the *uaf30Δ* strain (Fig. 3-20). However, the Pol III transcription factor TFIIIC subunit Tfc6 could

not be detected at this region in the *uaf30Δ* strain (data not shown). Since transcription of certain Pol III-dependent genes does not require TFIIIC (Dieci et al., 2000), it is possible that the TFIIIB complex alone is involved in Pol III transcription initiation at this region. However, since Pol III terminates within stretches of more than 5 consecutive thymidine(T)-residues in the coding strand (Allison and Hall, 1985) it is unlikely that the enzyme is capable of producing a full-length 35S rRNA containing multiple of potential termination signals. Nevertheless, as the shut-down of Pol II transcription in the strains only leads to an about 3-fold decrease in rRNA synthesis (Vu et al., 1999), Pol III could be responsible for the synthesis of the residual (perhaps prematurely terminated) 35S rRNA transcripts still detected in these strains.

4.2.4 Reb1 might allow binding of transcription factors to a cryptic promoter region in the absence of UAF

While the association of promoter-bound factors is impaired or altered in the *uaf30Δ* strain Reb1 binding remains unaffected. Furthermore, the region around the Reb1 binding site not only becomes more accessible to exogenous MNase digestion but also to binding of other factors such as TBP, Net1 or polymerase complexes. Reb1 has been suggested to play a role in influencing chromatin structure by creating nucleosome-free regions (NFRs) (Fedor and Kornberg, 1989; Chasman et al., 1990). Thus, in the absence of UAF Reb1 binding to its promoter proximal recognition site might create NFRs being accessible for diverse transcription factors promoting transcription initiation at cryptic promoters. It is conceivable, that UAF prevents the establishment of these NFRs in the wild-type strain thereby restricting the access of other polymerase complexes to this region. Consistent with this model, two potential TATA box motifs are located just upstream and downstream of the Reb1 binding site.

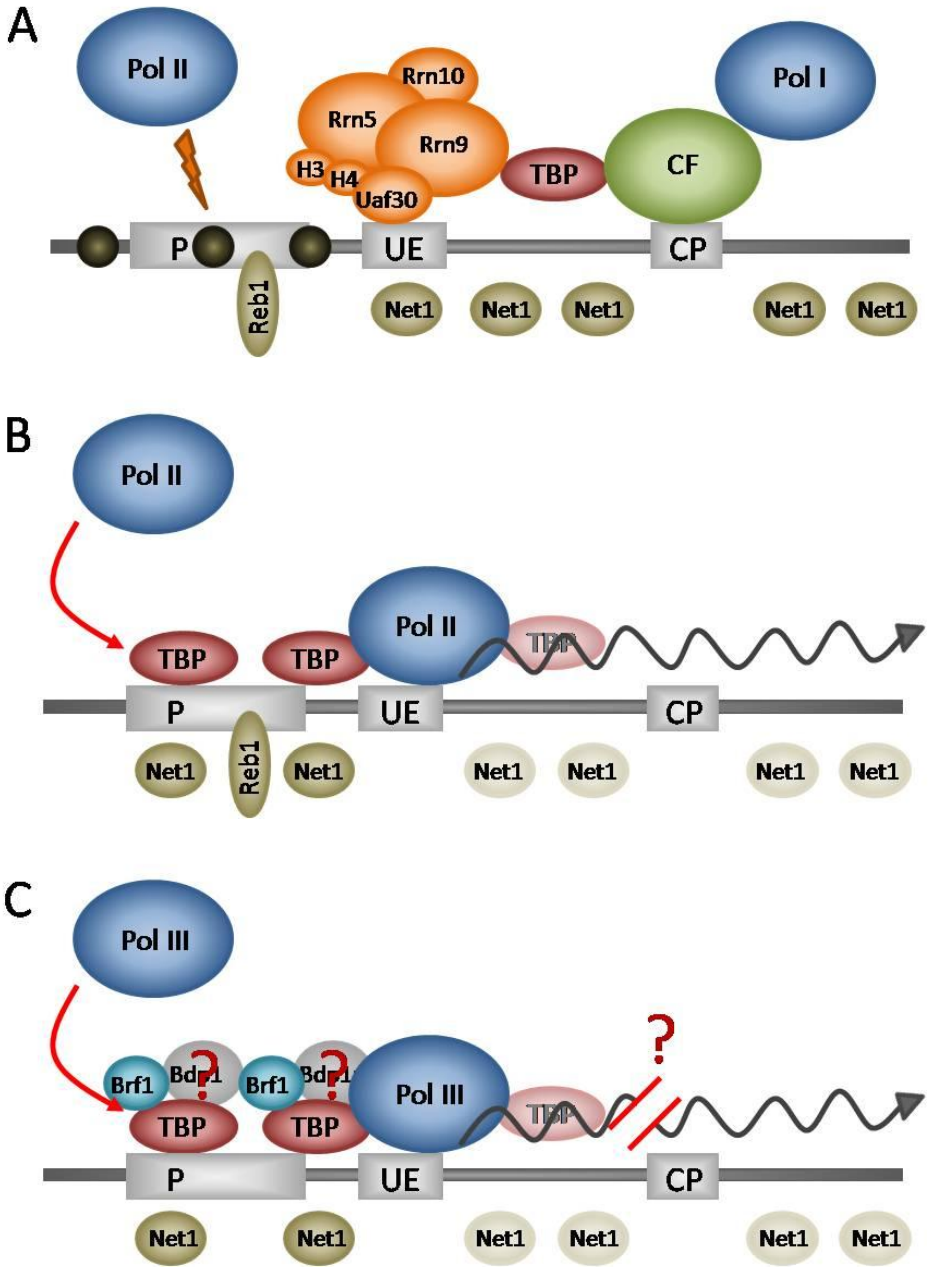

Fig. 4-1 Model for the function of Reb1 in Pol II / Pol III transcription initiation
(A) In a wild-type yeast cell UAF prevents access to nucleosome-free regions (NFRs, black balls). Thus, the access of other polymerases to the cryptic promoter (P) upstream of the Pol I initiation site is restricted. Instead, UAF recruits CF via TBP and activates Pol I transcription. Note, that the exact position and size of the cryptic promoter is unknown. (B) In the absence of Uaf30 UAF complex binding to the UE is impaired. Net1 and TBP association with regions downstream of the Pol I promoter is decreased (represented by lighter colors of the balls). Instead, TBP and Net1 cluster around the Reb1 binding site. In the absence of UAF NFRs become accessible for several DNA-binding proteins. Thus, Pol II transcription factors as TBP can bind to these regions and recruit Pol II initiation complexes that are capable to transcribe the 35S rRNA gene. (C) TBP recruits together with Brf1 (and presumably also with Bdp1 forming TFIIIB) Pol III to the cryptic promoter region. Whether Pol III is capable to transcribe the fulllength 35S transcript still remains to be determined.

4.3 UAF influences silencing at the rDNA locus

Interestingly, the ChEC data obtained in this study demonstrate that also the association of Pol II and TBP with the IGS1 region is strongly increased in the *uaf30Δ* strain. This indicates a defect in silencing of Pol II transcription within IGS1 in this genetic background. Accordingly, silencing of reporter genes integrated within the IGS2 region has been described to be abolished in a UAF deletion strain (Cioci et al., 2003).

4.3.1 UAF is required for recruitment of Sir2 to the rDNA locus

A model has been proposed for silencing of Pol II reporter genes in which UAF nucleates a specific chromatin structure at the Pol I promoter region which is then spread with the help of other factors, e. g. Sir2 to regions further downstream at the rDNA locus (Cioci et al., 2003) (Fig. 1-6). The ChEC experiments in this study demonstrate that the association of Sir2 with promoter and enhancer regions of the rDNA locus is lost upon deletion of UAF30 or in the PSW background (Fig. 3-24). Importantly, Sir2 levels are not limiting in UAF deletion strains, because the protein still binds to other genomic target sites. Furthermore, SIR2 over-expression cannot rescue the Pol II silencing defect in rDNA of PSW strains indicating that the disruption of silencing is independent of Sir2 concentration (Cioci et al., 2003). Thus, the absence of Sir2 provides the molecular explanation for the observed silencing defect in PSW strains (Fig. 1-6C). In addition, the occurrence of elevated Pol II and TBP levels at the site of the bidirectional Pol II promoter can be explained by the absence of Sir2 from this region since transcription of E-pro is negatively regulated by the silencing protein. Activation of E-pro transcription drives repeat expansion which is consistent with the increase of rDNA copy number in the *uaf30Δ* strain. Nevertheless, the data cannot explain why a deletion of SIR2 increases the rate of switching to PSW (Oakes et al., 1999), as it does not seem to be associated with the rDNA locus at all in the PSW background. Thus, UAF seems to be required for the association of Sir2 with the rDNA locus and it is possible that the complex is directly involved in Sir2 recruitment to rDNA.

4.3.2 RENT complex assembly is disrupted upon deletion of UAF30

Sir2 is a component of the RENT complex (Shou et al., 1999; Straight et al., 1999). Whereas Sir2 is displaced from the 35S rDNA in UAF deletion strains (Figs. 3-24) the two other known RENT subunits Net1 and Cdc14 remain fully or partially associated with this locus (Figs. 3-16 and 3-27). Therefore RENT complex composition is substantially altered in the UAF30 deletion mutant. In addition, the association of Net1 and Cdc14 with the rDNA requires ongoing Pol I transcription (data not shown). Interestingly, the interaction of Net1 with the IGS1 and enhancer region in *uaf30*Δ strains is less affected than its association with the 35S rDNA promoter. This is in agreement with different requirements for RENT binding to its rDNA interaction sites (Huang et al., 2003). RENT association with the ENH region of the rDNA depends on Fob1 binding to its respective recognition site at the RFB which is unaltered upon UAF30 deletion (Fig. 3-27). However, the presence of Fob1 and Net1 is not sufficient to recruit Sir2 to this region in the *uaf30*Δ strain. Therefore, another yet unknown mechanism, which requires UAF is important for RENT integrity.

5 Summary

Chromatin is the template of all processes involved in DNA metabolism in the eukaryotic cell. Accordingly, chromatin is a dynamic structure which changes in its composition and posttranslational modification correlating with the functional state of a genomic locus. An excellent example to study the correlation between transcription and chromatin structure is the ribosomal DNA (rDNA) locus in *Saccharomyces cerevisiae*. This multicopy gene locus harbors the 35S ribosomal RNA (rRNA) genes which are transcribed by the specialized RNA polymerase I (Pol I). 35S rDNA coexists in two different chromatin states correlating with the transcriptional activity of the genes. Interestingly, RNA polymerase II (Pol II) cannot access the rDNA locus and transcription of Pol II-dependent reporter genes within the rDNA is silenced. The upstream activating factor, UAF, plays an important role in determining polymerase specificity and Pol II silencing. A model has been proposed in which UAF nucleates a specific chromatin structure at its binding site within the rDNA promoter region which is then propagated over the entire Pol I-transcribed region. However, an in depth molecular characterization of the UAF-dependent rDNA chromatin structure was missing so far.

The aim of this study was to analyze the role of UAF in the establishment of rDNA chromatin structure to test the predictions made by the above model. Therefore rDNA chromatin was analyzed in different mutant strains by three independent methods investigating DNA accessibility and protein composition. The data demonstrate that UAF is an important determinant of 35S rDNA chromatin structure. Deletion of UAF subunits leads to a drastic reorganization of rDNA promoter chromatin. In the absence of UAF flanking regions of the promoter proximal binding site for the Reb1 protein become accessible for binding of Pol II and III and associated transcription factors, and may be sites of transcription initiation in these strains. The observed chromatin alterations extend throughout the 35S rRNA coding sequence. Importantly, none of the above changes can be provoked by short term inactivation of Pol I transcription demonstrating that the alterations are not a consequence of the reduced Pol I transcription levels in the mutant strains. Furthermore, it was demonstrated that the integrity of the UAF complex is required for the association of the silent information regulator Sir2 with the rDNA locus,

which can explain defective Pol II reporter gene silencing upon deletion of UAF components.

Taken together the analyses shed light on how UAF organizes rDNA chromatin determining RNA polymerase specificity at the 35S rDNA promoter and rDNA silencing of Pol II transcription. The obtained results provide a solid molecular basis for earlier observations suggesting that a single factor like UAF can be a mediator between transcriptional activity and chromatin structure of a genomic locus.

6 Literature

Aalfs, J. D., and Kingston, R. E. (2000). What does 'chromatin remodeling' mean? Trends Biochem. Sci *25*, 548-555.

Adams, C. C., and Workman, J. L. (1993). Nucleosome displacement in transcription. Cell *72*, 305-308.

Allison, D. S., and Hall, B. D. (1985). Effects of alterations in the 3' flanking sequence on in vivo and in vitro expression of the yeast SUP4-o tRNATyr gene. EMBO J *4*, 2657-2664.

Aprikian, P., Moorefield, B., and Reeder, R. H. (2001). New model for the yeast RNA polymerase I transcription cycle. Mol. Cell. Biol *21*, 4847-4855.

Ausió, J. (2000). Are linker histones (histone H1) dispensable for survival? Bioessays *22*, 873-877.

Bash, R., and Lohr, D. (2001). Yeast chromatin structure and regulation of GAL gene expression. Prog. Nucleic Acid Res. Mol. Biol *65*, 197-259.

Bassett, A., Cooper, S., Wu, C., and Travers, A. (2009). The folding and unfolding of eukaryotic chromatin. Current Opinion in Genetics & Development *19*, 159-165.

Bier, M., Fath, S., and Tschochner, H. (2004). The composition of the RNA polymerase I transcription machinery switches from initiation to elongation mode. FEBS Lett *564*, 41-46.

Bordi, L., Cioci, F., and Camilloni, G. (2001). In vivo binding and hierarchy of assembly of the yeast RNA polymerase I transcription factors. Mol. Biol. Cell *12*, 753-760.

Brewer, B. J., and Fangman, W. L. (1988). A replication fork barrier at the 3' end of yeast ribosomal RNA genes. Cell *55*, 637-643.

Brewer, B. J., Lockshon, D., and Fangman, W. L. (1992). The arrest of replication forks in the rDNA of yeast occurs independently of transcription. Cell *71*, 267-276.

Brinkley, B. R., Tousson, A., and Valdivia, M. M. (1985). The kinetochore of mammalian chromosomes: structure and function in normal mitosis and aneuploidy. Basic Life Sci *36*, 243-267.

Bryk, M., Banerjee, M., Murphy, M., Knudsen, K. E., Garfinkel, D. J., and Curcio, M. J. (1997). Transcriptional silencing of Ty1 elements in the RDN1 locus of yeast. Genes Dev *11*, 255-269.

Bryk, M., Briggs, S. D., Strahl, B. D., Curcio, M. J., Allis, C. D., and Winston, F. (2002). Evidence that Set1, a factor required for methylation of histone H3, regulates rDNA silencing in S. cerevisiae by a Sir2-independent mechanism. Curr. Biol *12*, 165-170.

Buck, S. W., Sandmeier, J. J., and Smith, J. S. (2002). RNA polymerase I propagates unidirectional spreading of rDNA silent chromatin. Cell *111*, 1003-1014.

Burkhalter, M. D., and Sogo, J. M. (2004). rDNA enhancer affects replication initiation and mitotic recombination: Fob1 mediates nucleolytic processing independently of replication. Mol. Cell *15*, 409-421.

Buttinelli, M., Di Mauro, E., and Negri, R. (1993). Multiple nucleosome positioning with unique rotational setting for the Saccharomyces cerevisiae 5S rRNA gene in vitro and in vivo. Proc. Natl. Acad. Sci. U.S.A *90*, 9315-9319.

Cadwell, C., Yoon, H. J., Zebarjadian, Y., and Carbon, J. (1997). The yeast nucleolar protein Cbf5p is involved in rRNA biosynthesis and interacts genetically with the RNA polymerase I transcription factor RRN3. Mol. Cell. Biol *17*, 6175-6183.

Camerini-Otero, R. D., Sollner-Webb, B., and Felsenfeld, G. (1976). The organization of histones and DNA in chromatin: evidence for an arginine-rich histone kernel. Cell *8*, 333-347.

Carmen, A. A., Milne, L., and Grunstein, M. (2002). Acetylation of the yeast histone H4 N terminus regulates its binding to heterochromatin protein SIR3. J. Biol. Chem *277*, 4778-4781.

Chasman, D. I., Lue, N. F., Buchman, A. R., LaPointe, J. W., Lorch, Y., and Kornberg, R. D. (1990). A yeast protein that influences the chromatin structure of UASG and functions as a powerful auxiliary gene activator. Genes Dev *4*, 503-514.

Cheung, P., Allis, C. D., and Sassone-Corsi, P. (2000). Signaling to Chromatin through Histone Modifications. Cell *103*, 263-271.

Cioci, F., Vu, L., Eliason, K., Oakes, M., Siddiqi, I. N., and Nomura, M. (2003). Silencing in yeast rDNA chromatin: reciprocal relationship in gene expression between RNA polymerase I and II. Mol. Cell *12*, 135-145.

Clapier, C. R., and Cairns, B. R. (2009). The biology of chromatin remodeling complexes. Annu. Rev. Biochem *78*, 273-304.

Conconi, A. (1987). Correlation between gene activity and chromatin structure in mouse erythroleukemia cells.

Conconi, A., Widmer, R. M., Koller, T., and Sogo, J. (1989). Two different chromatin structures coexist in ribosomal RNA genes throughout the cell cycle. Cell *57*, 753-761.

Conrad-Webb, H., and Butow, R. A. (1995). A polymerase switch in the synthesis of rRNA in Saccharomyces cerevisiae. Mol. Cell. Biol *15*, 2420-2428.

Dammann, R., Lucchini, R., Koller, T., and Sogo, J. M. (1993). Chromatin structures and transcription of rDNA in yeast Saccharomyces cerevisiae. Nucleic Acids Res *21*, 2331-2338.

Dammann, R., Lucchini, R., Koller, T., and Sogo, J. M. (1995). Transcription in the yeast rRNA gene locus: distribution of the active gene copies and chromatin structure of their flanking regulatory sequences. Mol. Cell. Biol *15*, 5294-5303.

Defossez, P. A., Prusty, R., Kaeberlein, M., Lin, S. J., Ferrigno, P., Silver, P. A., Keil, R. L., and Guarente, L. (1999). Elimination of replication block protein Fob1 extends the life span of yeast mother cells. Mol. Cell *3*, 447-455.

Dieci, G., Percudani, R., Giuliodori, S., Bottarelli, L., and Ottonello, S. (2000). TFIIIC-independent in vitro transcription of yeast tRNA genes. J. Mol. Biol *299*, 601-613.

Dragon, F., Gallagher, J. E. G., Compagnone-Post, P. A., Mitchell, B. M., Porwancher, K. A., Wehner, K. A., Wormsley, S., Settlage, R. E., Shabanowitz, J., Osheim, Y., et al. (2002). A large nucleolar U3 ribonucleoprotein required for 18S ribosomal RNA biogenesis. Nature *417*, 967-970.

Dror, V., and Winston, F. (2004). The Swi/Snf chromatin remodeling complex is required for ribosomal DNA and telomeric silencing in Saccharomyces cerevisiae. Mol. Cell. Biol *24*, 8227-8235.

Drouin, G., and de Sá, M. M. (1995). The concerted evolution of 5S ribosomal genes linked to the repeat units of other multigene families. Mol. Biol. Evol *12*, 481-493.

Dutnall, R. N., and Pillus, L. (2001). Deciphering NAD-dependent deacetylases. Cell *105*, 161-164.

Elgin, S. C. (1990). Chromatin structure and gene activity. Curr. Opin. Cell Biol *2*, 437-445.

Elgin, S. C., and Weintraub, H. (1975). Chromosomal proteins and chromatin structure. Annu. Rev. Biochem *44*, 725-774.

Elion, E. A., and Warner, J. R. (1986). An RNA polymerase I enhancer in Saccharomyces cerevisiae. Mol. Cell. Biol *6*, 2089-2097.

Elion, E. A., and Warner, J. R. (1984). The major promoter element of rRNA transcription in yeast lies 2 kb upstream. Cell *39*, 663-673.

Fangman, W. L., and Brewer, B. J. (1992). A question of time: replication origins of eukaryotic chromosomes. Cell *71*, 363-366.

Fatica, A., and Tollervey, D. (2002). Making ribosomes. Curr. Opin. Cell Biol *14*, 313-318.

Fedor, M. J., and Kornberg, R. D. (1989). Upstream activation sequence-dependent alteration of chromatin structure and transcription activation of the yeast GAL1-GAL10 genes. Mol. Cell. Biol *9*, 1721-1732.

Freidkin, I., and Katcoff, D. J. (2001). Specific distribution of the Saccharomyces cerevisiae linker histone homolog HHO1p in the chromatin. Nucleic Acids Res *29*, 4043-4051.

French, S. L., Osheim, Y. N., Cioci, F., Nomura, M., and Beyer, A. L. (2003). In exponentially growing Saccharomyces cerevisiae cells, rRNA synthesis is determined by the summed RNA polymerase I loading rate rather than by the number of active genes. Mol. Cell. Biol *23*, 1558-1568.

French, S. L., Osheim, Y. N., Schneider, D. A., Sikes, M. L., Fernandez, C. F., Copela, L. A., Misra, V. A., Nomura, M., Wolin, S. L., and Beyer, A. L. (2008). Visual analysis of the yeast 5S rRNA gene transcriptome: regulation and role of La protein. Mol. Cell. Biol *28*, 4576-4587.

Fritze, C. E., Verschueren, K., Strich, R., and Easton Esposito, R. (1997). Direct evidence for SIR2 modulation of chromatin structure in yeast rDNA. EMBO J *16*, 6495-6509.

Fry, C. J., and Peterson, C. L. (2001). Chromatin remodeling enzymes: who's on first? Curr. Biol *11*, R185-197.

Gadal, O., Labarre, S., Boschiero, C., and Thuriaux, P. (2002). Hmo1, an HMG-box protein, belongs to the yeast ribosomal DNA transcription system. EMBO J *21*, 5498-5507.

Ganley, A. R. D., Hayashi, K., Horiuchi, T., and Kobayashi, T. (2005). Identifying gene-independent noncoding functional elements in the yeast ribosomal DNA by phylogenetic footprinting. Proc. Natl. Acad. Sci. U.S.A *102*, 11787-11792.

Gartenberg, M. (2009). Heterochromatin and the cohesion of sister chromatids. Chromosome Res *17*, 229-238.

Gasser, S. M., and Cockell, M. M. (2001). The molecular biology of the SIR proteins. Gene *279*, 1-16.

Geiduschek, E. P., and Kassavetis, G. A. (2001). The RNA polymerase III transcription apparatus. J. Mol. Biol *310*, 1-26.

Gottlieb, S., and Esposito, R. E. (1989). A new role for a yeast transcriptional silencer gene, SIR2, in regulation of recombination in ribosomal DNA. Cell *56*, 771-776.

Grewal, S. I. S., and Moazed, D. (2003). Heterochromatin and epigenetic control of gene expression. Science *301*, 798-802.

Grewal, S. I. S., and Elgin, S. C. R. (2002). Heterochromatin: new possibilities for the inheritance of structure. Current Opinion in Genetics & Development *12*, 178-187.

Grewal, S. I. S., and Jia, S. (2007). Heterochromatin revisited. Nat Rev Genet *8*, 35-46.

Hall, D. B., Wade, J. T., and Struhl, K. (2006). An HMG protein, Hmo1, associates with promoters of many ribosomal protein genes and throughout the rRNA gene locus in Saccharomyces cerevisiae. Mol. Cell. Biol *26*, 3672-3679.

Hanson, C. V., Shen, C. K., and Hearst, J. E. (1976). Cross-linking of DNA in situ as a probe for chromatin structure. Science *193*, 62-64.

Hawkins, T., Mirigian, M., Selcuk Yasar, M., and Ross, J. L. (2009). Mechanics of microtubules. J Biomech. Available at: http://www.ncbi.nlm.nih.gov/pubmed/19815217 [Accessed November 10, 2009].

Hayes, J. J., Clark, D. J., and Wolffe, A. P. (1991). Histone contributions to the structure of DNA in the nucleosome. Proc. Natl. Acad. Sci. U.S.A *88*, 6829-6833.

Hecht, A., and Grunstein, M. (1999). Mapping DNA interaction sites of chromosomal proteins using immunoprecipitation and polymerase chain reaction. Meth. Enzymol *304*, 399-414.

Hennig, W. (1999). Heterochromatin. Chromosoma *108*, 1-9.

Hernandez, N. (1993). TBP, a universal eukaryotic transcription factor? Genes Dev *7*, 1291-1308.

Hontz, R. D., French, S. L., Oakes, M. L., Tongaonkar, P., Nomura, M., Beyer, A. L., and Smith, J. S. (2008). Transcription of multiple yeast ribosomal DNA genes requires targeting of UAF to the promoter by Uaf30. Mol. Cell. Biol *28*, 6709-6719.

Hontz, R. D., Niederer, R. O., Johnson, J. M., and Smith, J. S. (2009). Genetic identification of factors that modulate ribosomal DNA transcription in Saccharomyces cerevisiae. Genetics *182*, 105-119.

Hoppe, G. J., Tanny, J. C., Rudner, A. D., Gerber, S. A., Danaie, S., Gygi, S. P., and Moazed, D. (2002). Steps in assembly of silent chromatin in yeast: Sir3-independent binding of a Sir2/Sir4 complex to silencers and role for Sir2-dependent deacetylation. Mol. Cell. Biol *22*, 4167-4180.

Huang, J., and Moazed, D. (2003). Association of the RENT complex with nontranscribed and coding regions of rDNA and a regional requirement for the replication fork block protein Fob1 in rDNA silencing. Genes Dev *17*, 2162-2176.

Imai, S., Armstrong, C. M., Kaeberlein, M., and Guarente, L. (2000). Transcriptional silencing and longevity protein Sir2 is an NAD-dependent histone deacetylase. Nature *403*, 795-800.

Jones, H. S., Kawauchi, J., Braglia, P., Alen, C. M., Kent, N. A., and Proudfoot, N. J. (2007). RNA polymerase I in yeast transcribes dynamic nucleosomal rDNA. Nat. Struct. Mol. Biol *14*, 123-130.

Kaeberlein, M., McVey, M., and Guarente, L. (1999). The SIR2/3/4 complex and SIR2 alone promote longevity in Saccharomyces cerevisiae by two different mechanisms. Genes Dev *13*, 2570-2580.

Kasahara, K., Ohtsuki, K., Ki, S., Aoyama, K., Takahashi, H., Kobayashi, T., Shirahige, K., and Kokubo, T. (2007). Assembly of regulatory factors on rRNA and ribosomal protein genes in Saccharomyces cerevisiae. Mol. Cell. Biol *27*, 6686-6705.

Kasinsky, H. E., Lewis, J. D., Dacks, J. B., and Ausió, J. (2001). Origin of H1 linker histones. FASEB J *15*, 34-42.

Keener, J., Dodd, J. A., Lalo, D., and Nomura, M. (1997). Histones H3 and H4 are components of upstream activation factor required for the high-level transcription of yeast rDNA by RNA polymerase I. Proc. Natl. Acad. Sci. U.S.A *94*, 13458-13462.

Keener, J., Josaitis, C. A., Dodd, J. A., and Nomura, M. (1998). Reconstitution of yeast RNA polymerase I transcription in vitro from purified components. TATA-binding protein is not required for basal transcription. J. Biol. Chem *273*, 33795-33802.

Kempers-Veenstra, A. E., Oliemans, J., Offenberg, H., Dekker, A. F., Piper, P. W., Planta, R. J., and Klootwijk, J. (1986). 3'-End formation of transcripts from the yeast rRNA operon. EMBO J *5*, 2703-2710.

Keys, D. A., Lee, B. S., Dodd, J. A., Nguyen, T. T., Vu, L., Fantino, E., Burson, L. M., Nogi, Y., and Nomura, M. (1996). Multiprotein transcription factor UAF interacts with the upstream element of the yeast RNA polymerase I promoter and forms a stable preinitiation complex. Genes Dev *10*, 887-903.

Keys, D. A., Vu, L., Steffan, J. S., Dodd, J. A., Yamamoto, R. T., Nogi, Y., and Nomura, M. (1994). RRN6 and RRN7 encode subunits of a multiprotein complex essential for the initiation of rDNA transcription by RNA polymerase I in Saccharomyces cerevisiae. Genes Dev *8*, 2349-2362.

Kobayashi, T., Heck, D. J., Nomura, M., and Horiuchi, T. (1998). Expansion and contraction of ribosomal DNA repeats in Saccharomyces cerevisiae: requirement of replication fork blocking (Fob1) protein and the role of RNA polymerase I. Genes Dev *12*, 3821-3830.

Kobayashi, T., Hidaka, M., Nishizawa, M., and Horiuchi, T. (1992). Identification of a site required for DNA replication fork blocking activity in the rRNA gene cluster in Saccharomyces cerevisiae. Mol. Gen. Genet *233*, 355-362.

Kobayashi, T., and Horiuchi, T. (1996). A yeast gene product, Fob1 protein, required for both replication fork blocking and recombinational hotspot activities. Genes Cells *1*, 465-474.

Kobayashi, T., Nomura, M., and Horiuchi, T. (2001). Identification of DNA cis elements essential for expansion of ribosomal DNA repeats in Saccharomyces cerevisiae. Mol. Cell. Biol *21*, 136-147.

Kobayashi, T., and Ganley, A. R. D. (2005). Recombination regulation by transcription-induced cohesin dissociation in rDNA repeats. Science *309*, 1581-1584.

Kobayashi, T., Horiuchi, T., Tongaonkar, P., Vu, L., and Nomura, M. (2004). SIR2 regulates recombination between different rDNA repeats, but not recombination within individual rRNA genes in yeast. Cell *117*, 441-453.

Kornberg, R. D., and Lorch, Y. (1999a). Chromatin-modifying and -remodeling complexes. Curr. Opin. Genet. Dev *9*, 148-151.

Kornberg, R. D., and Lorch, Y. (1999b). Twenty-five years of the nucleosome, fundamental particle of the eukaryote chromosome. Cell *98*, 285-294.

Kressler, D., Linder, P., and de La Cruz, J. (1999). Protein trans-acting factors involved in ribosome biogenesis in Saccharomyces cerevisiae. Mol. Cell. Biol *19*, 7897-7912.

Kulkens, T., Riggs, D. L., Heck, J. D., Planta, R. J., and Nomura, M. (1991). The yeast RNA polymerase I promoter: ribosomal DNA sequences involved in transcription initiation and complex formation in vitro. Nucleic Acids Res *19*, 5363-5370.

Kulkens, T., van der Sande, C. A., Dekker, A. F., van Heerikhuizen, H., and Planta, R. J. (1992). A system to study transcription by yeast RNA polymerase I within the chromosomal context: functional analysis of the ribosomal DNA enhancer and the RBP1/REB1 binding sites. EMBO J *11*, 4665-4674.

Labrador, M., and Corces, V. G. (2002). Setting the boundaries of chromatin domains and nuclear organization. Cell *111*, 151-154.

Lalo, D., Steffan, J. S., Dodd, J. A., and Nomura, M. (1996). RRN11 encodes the third subunit of the complex containing Rrn6p and Rrn7p that is essential for the initiation of rDNA transcription by yeast RNA polymerase I. J. Biol. Chem *271*, 21062-21067.

Landry, J., Sutton, A., Tafrov, S. T., Heller, R. C., Stebbins, J., Pillus, L., and Sternglanz, R. (2000). The silencing protein SIR2 and its homologs are NAD-dependent protein deacetylases. Proc. Natl. Acad. Sci. U.S.A *97*, 5807-5811.

Lee, T. I., and Young, R. A. (2000). Transcription of eukaryotic protein-coding genes. Annu. Rev. Genet *34*, 77-137.

Léger-Silvestre, I., Trumtel, S., Noaillac-Depeyre, J., and Gas, N. (1999). Functional compartmentalization of the nucleus in the budding yeast Saccharomyces cerevisiae. Chromosoma *108*, 103-113.

Li, B., Carey, M., and Workman, J. L. (2007). The Role of Chromatin during Transcription. Cell *128*, 707-719.

Lin, C. W., Moorefield, B., Payne, J., Aprikian, P., Mitomo, K., and Reeder, R. H. (1996). A novel 66-kilodalton protein complexes with Rrn6, Rrn7, and TATA-binding protein to promote polymerase I transcription initiation in Saccharomyces cerevisiae. Mol. Cell. Biol *16*, 6436-6443.

Linskens, M. H., and Huberman, J. A. (1988). Organization of replication of ribosomal DNA in Saccharomyces cerevisiae. Mol. Cell. Biol *8*, 4927-4935.

Lohr, D. (1983). Chromatin structure differs between coding and upstream flanking sequences of the yeast 35S ribosomal genes. Biochemistry *22*, 927-934.

Lohr, D. (1984). Organization of the GAL1-GAL10 intergenic control region chromatin. Nucleic Acids Res *12*, 8457-8474.

Lohr, D., and Hopper, J. E. (1985). The relationship of regulatory proteins and DNase I hypersensitive sites in the yeast GAL1-10 genes. Nucleic Acids Res *13*, 8409-8423.

Lorch, Y., LaPointe, J. W., and Kornberg, R. D. (1992). Initiation on chromatin templates in a yeast RNA polymerase II transcription system. Genes Dev *6*, 2282-2287.

Luger, K. (2003). Structure and dynamic behavior of nucleosomes. Curr. Opin. Genet. Dev *13*, 127-135.

Meneghini, M. D., Wu, M., and Madhani, H. D. (2003). Conserved histone variant H2A.Z protects euchromatin from the ectopic spread of silent heterochromatin. Cell *112*, 725-736.

Merz, K. (2007). In vivo Analyse der Chromatinstruktur ribosomaler DNA in S. cerevisiae.

Merz, K., Hondele, M., Goetze, H., Gmelch, K., Stoeckl, U., and Griesenbeck, J. (2008). Actively transcribed rRNA genes in S. cerevisiae are organized in a specialized chromatin associated with the high-mobility group protein Hmo1 and are largely devoid of histone molecules. Genes Dev *22*, 1190-1204.

Miller, O. L., and Beatty, B. R. (1969). Visualization of nucleolar genes. Science *164*, 955-957.

Moazed, D. (2001). Common themes in mechanisms of gene silencing. Mol. Cell *8*, 489-498.

Morrow, B. E., Johnson, S. P., and Warner, J. R. (1989). Proteins that bind to the yeast rDNA enhancer. J. Biol. Chem *264*, 9061-9068.

Moss, T., Langlois, F., Gagnon-Kugler, T., and Stefanovsky, V. (2007). A housekeeper with power of attorney: the rRNA genes in ribosome biogenesis. Cell. Mol. Life Sci *64*, 29-49.

Mougey, E. B., O'Reilly, M., Osheim, Y., Miller, O. L., Beyer, A., and Sollner-Webb, B. (1993). The terminal balls characteristic of eukaryotic rRNA transcription units in chromatin spreads are rRNA processing complexes. Genes Dev *7*, 1609-1619.

Muller, M., Lucchini, R., and Sogo, J. M. (2000). Replication of yeast rDNA initiates downstream of transcriptionally active genes. Mol. Cell *5*, 767-777.

Musters, W., Knol, J., Maas, P., Dekker, A. F., van Heerikhuizen, H., and Planta, R. J. (1989). Linker scanning of the yeast RNA polymerase I promoter. Nucleic Acids Res *17*, 9661-9678.

Nislow, C., Ray, E., and Pillus, L. (1997). SET1, a yeast member of the trithorax family, functions in transcriptional silencing and diverse cellular processes. Mol. Biol. Cell *8*, 2421-2436.

Nogi, Y., Vu, L., and Nomura, M. (1991). An approach for isolation of mutants defective in 35S ribosomal RNA synthesis in Saccharomyces cerevisiae. Proc. Natl. Acad. Sci. U.S.A *88*, 7026-7030.

Noma K, Allis, C. D., and Grewal, S. I. (2001). Transitions in distinct histone H3 methylation patterns at the heterochromatin domain boundaries. Science *293*, 1150-1155.

Nomura, M. (2001). Ribosomal RNA genes, RNA polymerases, nucleolar structures, and synthesis of rRNA in the yeast Saccharomyces cerevisiae. Cold Spring Harb. Symp. Quant. Biol *66*, 555-565.

Oakes, M., Siddiqi, I., Vu, L., Aris, J., and Nomura, M. (1999). Transcription factor UAF, expansion and contraction of ribosomal DNA (rDNA) repeats, and RNA polymerase switch in transcription of yeast rDNA. Mol. Cell. Biol *19*, 8559-8569.

Oakes, M. L., Siddiqi, I., French, S. L., Vu, L., Sato, M., Aris, J. P., Beyer, A. L., and Nomura, M. (2006). Role of histone deacetylase Rpd3 in regulating rRNA gene transcription and nucleolar structure in yeast. Mol. Cell. Biol *26*, 3889-3901.

Olins, A. L., and Olins, D. E. (1974). Spheroid chromatin units (v bodies). Science *183*, 330-332.

Orphanides, G., LeRoy, G., Chang, C. H., Luse, D. S., and Reinberg, D. (1998). FACT, a factor that facilitates transcript elongation through nucleosomes. Cell *92*, 105-116.

Orphanides, G., and Reinberg, D. (2000). RNA polymerase II elongation through chromatin. Nature *407*, 471-475.

Orphanides, G., Wu, W. H., Lane, W. S., Hampsey, M., and Reinberg, D. (1999). The chromatin-specific transcription elongation factor FACT comprises human SPT16 and SSRP1 proteins. Nature *400*, 284-288.

Osheim, Y. N., French, S. L., Keck, K. M., Champion, E. A., Spasov, K., Dragon, F., Baserga, S. J., and Beyer, A. L. (2004). Pre-18S ribosomal RNA is structurally compacted into the SSU processome prior to being cleaved from nascent transcripts in Saccharomyces cerevisiae. Mol. Cell *16*, 943-954.

Palladino, F., Laroche, T., Gilson, E., Axelrod, A., Pillus, L., and Gasser, S. M. (1993). SIR3 and SIR4 proteins are required for the positioning and integrity of yeast telomeres. Cell *75*, 543-555.

Patterton, H. G., Landel, C. C., Landsman, D., Peterson, C. L., and Simpson, R. T. (1998). The biochemical and phenotypic characterization of Hho1p, the putative linker histone H1 of Saccharomyces cerevisiae. J. Biol. Chem *273*, 7268-7276.

Pazin, M. J., and Kadonaga, J. T. (1997). What's up and down with histone deacetylation and transcription? Cell *89*, 325-328.

Petes, T. D. (1979). Yeast ribosomal DNA genes are located on chromosome XII. Proc. Natl. Acad. Sci. U.S.A *76*, 410-414.

Peyroche, G., Milkereit, P., Bischler, N., Tschochner, H., Schultz, P., Sentenac, A., Carles, C., and Riva, M. (2000). The recruitment of RNA polymerase I on rDNA is mediated by the interaction of the A43 subunit with Rrn3. EMBO J *19*, 5473-5482.

Philippsen, P., Thomas, M., Kramer, R. A., and Davis, R. W. (1978). Unique arrangement of coding sequences for 5 S, 5.8 S, 18 S and 25 S ribosomal RNA in Saccharomyces cerevisiae as determined by R-loop and hybridization analysis. J. Mol. Biol *123*, 387-404.

Prescott, E. M., Osheim, Y. N., Jones, H. S., Alen, C. M., Roan, J. G., Reeder, R. H., Beyer, A. L., and Proudfoot, N. J. (2004). Transcriptional termination by RNA polymerase I requires the small subunit Rpa12p. Proc. Natl. Acad. Sci. U.S.A *101*, 6068-6073.

Puig, O., Caspary, F., Rigaut, G., Rutz, B., Bouveret, E., Bragado-Nilsson, E., Wilm, M., and Séraphin, B. (2001). The tandem affinity purification (TAP) method: a general procedure of protein complex purification. Methods *24*, 218-229.

Reeder, R. H., Guevara, P., and Roan, J. G. (1999). Saccharomyces cerevisiae RNA polymerase I terminates transcription at the Reb1 terminator in vivo. Mol. Cell. Biol *19*, 7369-7376.

Reeder, R. H., and Lang, W. H. (1997). Terminating transcription in eukaryotes: lessons learned from RNA polymerase I. Trends Biochem. Sci *22*, 473-477.

Rice, J. C., and Allis, C. D. (2001). Histone methylation versus histone acetylation: new insights into epigenetic regulation. Curr. Opin. Cell Biol *13*, 263-273.

Richards, E. J., and Elgin, S. C. R. (2002). Epigenetic codes for heterochromatin formation and silencing: rounding up the usual suspects. Cell *108*, 489-500.

Rine, J., and Herskowitz, I. (1987). Four genes responsible for a position effect on expression from HML and HMR in Saccharomyces cerevisiae. Genetics *116*, 9-22.

S Loo, A., and J Rine (2003). Silencing and Heritable Domains of Gene Expression.

Scheer, U., and Hock, R. (1999). Structure and function of the nucleolus. Curr. Opin. Cell Biol *11*, 385-390.

Schmid, M., Durussel, T., and Laemmli, U. K. (2004). ChIC and ChEC; genomic mapping of chromatin proteins. Mol. Cell *16*, 147-157.

Schneider, D. A., French, S. L., Osheim, Y. N., Bailey, A. O., Vu, L., Dodd, J., Yates, J. R., Beyer, A. L., and Nomura, M. (2006). RNA polymerase II elongation factors Spt4p and Spt5p play roles in transcription elongation by RNA polymerase I and rRNA processing. Proc. Natl. Acad. Sci. U.S.A *103*, 12707-12712.

Shou, W., Sakamoto, K. M., Keener, J., Morimoto, K. W., Traverso, E. E., Azzam, R., Hoppe, G. J., Feldman, R. M., DeModena, J., Moazed, D., et al. (2001). Net1 stimulates RNA polymerase I transcription and regulates nucleolar structure independently of controlling mitotic exit. Mol. Cell *8*, 45-55.

Shou, W., Seol, J. H., Shevchenko, A., Baskerville, C., Moazed, D., Chen, Z. W., Jang, J., Shevchenko, A., Charbonneau, H., and Deshaies, R. J. (1999). Exit from mitosis is triggered by Tem1-dependent release of the protein phosphatase Cdc14 from nucleolar RENT complex. Cell *97*, 233-244.

Siddiqi, I. N., Dodd, J. A., Vu, L., Eliason, K., Oakes, M. L., Keener, J., Moore, R., Young, M. K., and Nomura, M. (2001). Transcription of chromosomal rRNA genes by both RNA polymerase I and II in yeast uaf30 mutants lacking the 30 kDa subunit of transcription factor UAF. EMBO J *20*, 4512-4521.

Sinclair, D. A., and Guarente, L. (1997). Extrachromosomal rDNA circles--a cause of aging in yeast. Cell *91*, 1033-1042.

Smith, J. S., and Boeke, J. D. (1997). An unusual form of transcriptional silencing in yeast ribosomal DNA. Genes Dev *11*, 241-254.

Smith, J. S., Brachmann, C. B., Celic, I., Kenna, M. A., Muhammad, S., Starai, V. J., Avalos, J. L., Escalante-Semerena, J. C., Grubmeyer, C., Wolberger, C., et al. (2000). A phylogenetically conserved NAD+-dependent protein deacetylase activity in the Sir2 protein family. Proc. Natl. Acad. Sci. U.S.A *97*, 6658-6663.

Smith, J. S., Caputo, E., and Boeke, J. D. (1999). A genetic screen for ribosomal DNA silencing defects identifies multiple DNA replication and chromatin-modulating factors. Mol. Cell. Biol *19*, 3184-3197.

Sogo, J. M., Stahl, H., Koller, T., and Knippers, R. (1986). Structure of replicating simian virus 40 minichromosomes. The replication fork, core histone segregation and terminal structures. J. Mol. Biol *189*, 189-204.

Sperling, A. S., and Grunstein, M. (2009). Histone H3 N-terminus regulates higher order structure of yeast heterochromatin. Proceedings of the National Academy of Sciences *106*, 13153-13159.

Steffan, J. S., Keys, D. A., Dodd, J. A., and Nomura, M. (1996). The role of TBP in rDNA transcription by RNA polymerase I in Saccharomyces cerevisiae: TBP is required for upstream activation factor-dependent recruitment of core factor. Genes Dev *10*, 2551-2563.

Steffan, J. S., Keys, D. A., Vu, L., and Nomura, M. (1998). Interaction of TATA-binding protein with upstream activation factor is required for activated transcription of ribosomal DNA by RNA polymerase I in Saccharomyces cerevisiae in vivo. Mol. Cell. Biol *18*, 3752-3761.

Straight, A. F., Shou, W., Dowd, G. J., Turck, C. W., Deshaies, R. J., Johnson, A. D., and Moazed, D. (1999). Net1, a Sir2-associated nucleolar protein required for rDNA silencing and nucleolar integrity. Cell *97*, 245-256.

Sun, Z. W., and Hampsey, M. (1999). A general requirement for the Sin3-Rpd3 histone deacetylase complex in regulating silencing in Saccharomyces cerevisiae. Genetics *152*, 921-932.

Tanny, J. C., Dowd, G. J., Huang, J., Hilz, H., and Moazed, D. (1999). An Enzymatic Activity in the Yeast Sir2 Protein that Is Essential for Gene Silencing. Cell *99*, 735-745.

Telford, D. J., and Stewart, B. W. (1989). Micrococcal nuclease: its specificity and use for chromatin analysis. Int. J. Biochem *21*, 127-137.

Ushinsky, S. C., Bussey, H., Ahmed, A. A., Wang, Y., Friesen, J., Williams, B. A., and Storms, R. K. (1997). Histone H1 in Saccharomyces cerevisiae. Yeast *13*, 151-161.

Venema, J., and Tollervey, D. (1999). Ribosome synthesis in Saccharomyces cerevisiae. Annu. Rev. Genet *33*, 261-311.

Visintin, R., Hwang, E. S., and Amon, A. (1999). Cfi1 prevents premature exit from mitosis by anchoring Cdc14 phosphatase in the nucleolus. Nature *398*, 818-823.

Vogelauer, M., Cioci, F., and Camilloni, G. (1998). DNA protein-interactions at the Saccharomyces cerevisiae 35 S rRNA promoter and in its surrounding region. Journal of Molecular Biology *275*, 197-209.

Vu, L., Siddiqi, I., Lee, B. S., Josaitis, C. A., and Nomura, M. (1999). RNA polymerase switch in transcription of yeast rDNA: role of transcription factor UAF (upstream activation factor) in silencing rDNA transcription by RNA polymerase II. Proc. Natl. Acad. Sci. U.S.A *96*, 4390-4395.

Wai, H., Johzuka, K., Vu, L., Eliason, K., Kobayashi, T., Horiuchi, T., and Nomura, M. (2001). Yeast RNA polymerase I enhancer is dispensable for transcription of the chromosomal rRNA gene and cell growth, and its apparent transcription enhancement from ectopic promoters requires Fob1 protein. Mol. Cell. Biol *21*, 5541-5553.

Warner, J. R. (1989). Synthesis of ribosomes in Saccharomyces cerevisiae. Microbiol. Rev *53*, 256-271.

West, A. G., Gaszner, M., and Felsenfeld, G. (2002). Insulators: many functions, many mechanisms. Genes Dev *16*, 271-288.

Workman, J. L. (2006). Nucleosome displacement in transcription. Genes Dev *20*, 2009-2017.

Yamamoto, R. T., Nogi, Y., Dodd, J. A., and Nomura, M. (1996). RRN3 gene of Saccharomyces cerevisiae encodes an essential RNA polymerase I transcription factor which interacts with the polymerase independently of DNA template. EMBO J *15*, 3964-3973.

7 Abbreviations

Amp	ampicilline
APS	ammonium persulfate
ATP	adenosine triphosphate
ARS	autonomous replication sequence
bp	base pair(s)
CEN	centromere
CF	core factor
ChEC	chromatin endogenous cleavage
ChIP	chromain immunoprecipitation
CP	core promoter
C-terminal	carboxy-terminal
Da	Dalton
DNA	desoxyribonucleic acid
dNTP	2-desoxyribonucleotide 5' triphosphate
E. coli	*Escherichia coli*
EDTA	ethylene diamine tetra acetate
EGTA	ethylene glycol tetraacetic acid
ENH	enhancer
E-pro	bidirectional Pol II promoter
f-band	fast migrating band
g	gram(s)
h	hour(s)
IFM	immunofluorescence microscopy
k	kilo
kb	kilo base pair(s)
l	liter(s)
LB	lysogeny broth
mg	milligram(s)
min	minute(s)
ml	milliliter(s)
MNase	micrococcal nuclease
mRNA	messenger RNA
MW	molecular weight

M	molar (mol/l)
nm	nanometer(s)
OD	optical density
ORF	open reading frame
P	promoter
PAGE	poly acryl amide electrophoresis
PBS	phophate buffered saline
PCR	polymerase chain reaction
pH	negative decadic logarithm of [H+]
Pol	RNA polymerase
qPCR	quantitative real-time PCR
rDNA	ribosomal DNA
RFB	replication fork barrier
RNA	ribonucleic acid
RP	ribosomal protein
rpm	rotations per minute
rRNA	ribosomal RNA
RT	room temperature
S	sedimentation coefficient
S. cerevisiae	*Saccharomyces cerevisiae*
s-band	slow migrating band
SDS	sodium dodecyl sulfate
sec	second(s)
snoRNA	small nucleolar RNA
Taq	Thermus aquaticus
TBP	TATA-box binding protein
TCA	tri chloro acetic acid
T/E	terminator / enhancer
tel	telomere
TEMED	tetramethylethylenediamine
Tris	tris(hydroxy methyl) amino methane
U	unit(s)
UAF	upstream activating factor
UE	upstream element
WT	wild-type

Acknowledgments

Ich danke allen, die zum Gelingen dieser Arbeit beigetragen haben.

Prof. Dr. Herbert Tschochner danke ich für die interessante Themenstellung, für das große Interesse an meiner Arbeit und seine ständige Unterstützung.

Mein besonderer Dank gilt Dr. Joachim Griesenbeck für seine außerordentliche und großartige Betreuung. Seine ständige Diskussionsbereitschaft und Unterstützung sowie seine fortwährende Motivation haben nicht nur das Gelingen dieser Arbeit ermöglicht, sie haben es zu einer wahren Freude gemacht.

Bei Dr. Philipp Milkereit möchte ich mich für die vielen guten Anregungen und produktiven Ideen für meine Arbeit bedanken.

Bei meiner „Chromatin Crew" Manuel Wittner, Stephan Hamperl, Ulrike Stöckl und Joachim Griesenbeck möchte ich mich für die große Unterstützung und die schöne und effektive Zusammenarbeit in den letzten Jahren bedanken. Auch bei allen anderen Arbeitskollegen möchte ich mich für ihre Hilfsbereitschaft und das nette Arbeitsklima bedanken.

Großer Dank gilt auch Isabelle Léger-Silvestre, die mir durch ihre großartige Arbeit und Motivation einen wundervollen Einblick in die Struktur der Hefezelle ermöglicht hat und die mir ihre Bilder für diese Arbeit zur Verfügung gestellt hat. Danken möchte ich auch Olivier Gadal für seine Unterstützung bei diesem Projekt.

Für Ihre finanzielle aber vor allem ideelle Unterstützung während meines Studiums und während meiner Promotion danke ich der Studienstiftung des Deutschen Volkes recht herzlich.

Ganz besonders möchte ich mich bei meinen Eltern Helena und Norman, meiner Schwester Virginia und meiner Oma Meta für Ihre große Unterstützung, Ihren Rückhalt und Ihre Liebe bedanken. Auch meiner „Schwiegerfamilie" danke ich für Ihre fortwährende Unterstützung.

Mein größter Dank gilt Tobias für seine unerschütterliche Liebe und die große Unterstützung während der gesamten letzten Jahre und für unsere weitere gemeinsame Zukunft.